POLITECNICO DI TORINO

Collegio di Ingegneria Meccanica, Aerospaziale, dell'Autoveicolo e della Produzione

Master's degree programme in
Mechanical Engineering

Master's Degree Thesis

Mechanical design and layout of an alkaline fuel cell for an Autonomous Underwater Vehicle.

Supervisor

prof. Alessandro Hugo Antonio Monteverde

Candidate

Oscar Alejandro Mena Cordoba
Student ID: s275480

December 2021

Contents

1. Abstract

ENDURUNS is a European R&D project that consists in developing and demonstrating a long endurance sea surveying Autonomous Underwater Vehicle (AUV), powered by a hydrogen fuel cell, to perform seabed mapping, geological studies, surveillance, ocean search missions, mineral and mining exploration. The thesis was developed in the framework of this project in the company HYSYTECH. The thesis is focused on the mechanical design of the fuel cell, figuring out challenges such as the design of the stack to fit a limited space, the heating and cooling process of some components in a sealed environment, setting up the system to guarantee neutral buoyancy, and a stable barycenter, and finally, assuring the capability of the system to deal with the high pressures and the demanding seawater environment. Each challenge is solved using an analytical approach and software modeling, obtaining a conceptual power bank of 300W composed of a stack of 15 cells, able to work in ocean depths up to 800 m and neutral buoyancy in seawater. These results demonstrate the feasibility of a powertrain based on hydrogen fuel cells that allow an increased amount of energy stored onboard in comparison with conventional battery-powered AUVs.

2. Introduction

More than two-thirds of our planet is covered by the oceans, this represents the greatest part of natural resources available. Only the equivalent of 15% of the total area covered by the oceans has been explored so far. Mapping the ocean and studying its resources is quite important in terms of economy and human security since can be obtained reliable information about climate change, availability of resources for sustainable exploitation, seafood production, quality, and condition of sea habitats, new offshore energy, and mining resources, etc. (1)

Some ocean mapping studies have been carried out to evaluate the ocean resources and offshore infrastructure state, they have demonstrated the usefulness and efficacy of vehicles such as Remotely Operated Vehicles (ROVs) and Autonomous Underwater Vehicles (AUVs) equipped with appropriate acoustic and imaging systems, to acquire data that allows the characterization of the examined seafloor and critical infrastructures. Commercially available AUVs are powered by Li-ion batteries providing sufficient energy for limited range operations. They also usually require the use of expensive and manned assistance ships. ROVs have the same limitations as AUVs with the additional requirement of a human operator. (2)

The Gliders, which are an AUV sub-class, are effectively slowly moving AUVs that use variable buoyancy propulsion instead of conventional propellers to minimize propulsion consumption during operation. The autonomy of gliders already available in the market can theoretically last up to a few months, but the quality and speed of the measurements are very poor due to their sinusoidal trajectory. (3)

The operational endurance of state-of-the-art AUVs based on this design concept is limited by the available charge stored in the Li-Ion battery bank typically used to power them. Hence, operational endurance is tightly bound to the energy consumption rate, which is directly associated with the power required for the operation of the sensing systems installed onboard, their autonomy is much lower than the gliders. The propulsion and steering systems, although being also responsible for part of the energy consumed during AUV operation, they are not the primary sources of energy drain, which is primarily driven by the operation of the sensors and communication systems installed onboard. (3)

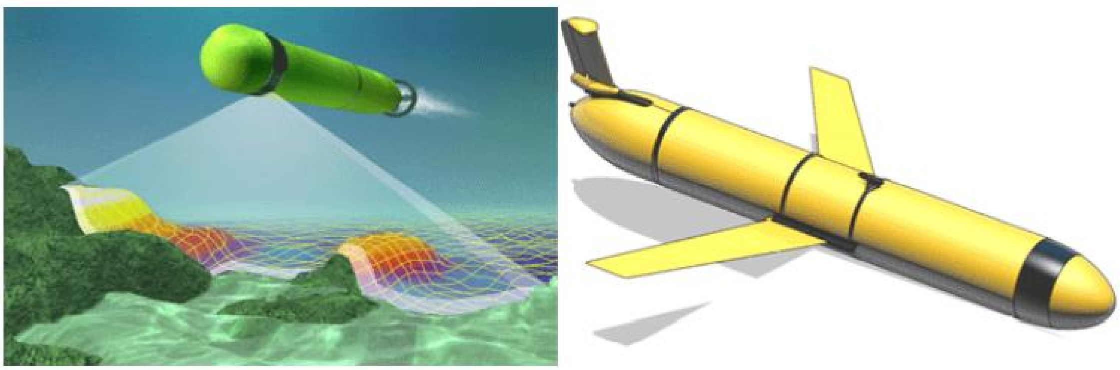

Figure 2.1. AUV and Glider vehicle

Given the necessity of longer missions with a high-quality data collection was born the project ENDURUNS, which is a European consortium project that aims to develop a hybrid AUV capable of operating in propelling and gliding mode, powered by a hydrogen fuel cell. This thesis is developed in the company HYSYTECH under the frame of the project, it has the purpose of designing a power bank system based on a stack of fuel cells, defining the proper elements to guarantee good performance and resistance to the demanding sea conditions, with the final goal of obtaining long autonomy for extended ocean missions.

The type of fuel cell selected for this system is an alkaline fuel cell (AFC), therefore it is described the design, general layout, and the complementary systems needed for its operation, fulfilling the requirements and constraints of adapting such technology to an AUV. Several challenges must be figured out, as it is a vehicle with gliding capabilities, the stability of each component is highly important for the vehicle's optimal performance since it uses buoyancy and gravitational forces to move forward. Therefore, the first challenge is to assure neutral buoyancy and a stable location of the barycenter during operation. This requirement is the base of the design because once fixed the dimensions are also fixed the maximum weight and the desired location of the barycenter.

The vehicle will perform activities at great depths; therefore, it will undergo big pressures, then a lightweight housing must protect the components inside the system. This sealed environment brings a complication to the system, which is the access to a colder source, as the reactions inside the cells generate heat, it is necessary to cool down the stack, then a heat exchanger is needed.

The design of the stack is quite challenging for two reasons, first, the thicknesses of the chambers must be quite small, i.e., the different layers are very close to each other to reduce the electric resistance, but the most critical aspect of a fuel cell are the leakages. It is fundamental to ensure a completely sealed cell because it could bring problems of crossover, short-circuit, or fuel losses.

Analytical methods and simulations will be used to solve each challenge, as there is a high degree of freedom in the design, many hypotheses are taken at the beginning, subsequently some of them are adjusted by following an iterative process and others hypothesis remain pending to verify during the testing phase after construction. The final goal is to obtain a functional and cost-effective power bank with a power output of 300W at 12V using the available resources at the company.

3. Stack design

3.1 Fuel cells

3.1.1 Basic principles

A fuel cell is a device that produces electricity from a chemical reaction where the reactants are Oxygen, Hydrogen, and an electrolyte, while the products are water and an electric current. To have a basic and functional fuel cell are needed two electrodes in two separated spaces, in these elements the reactions take place because it is where the electrolyte and the gas get mixed, also is needed a current collector which closes the circuit and provides the current to the circuit that is intended to feed, and a chamber that can allocate the electrolyte and allow its contact with both electrodes to close the circuit, Figure 3.1 shows the diagram of a very basic fuel cell. (4)

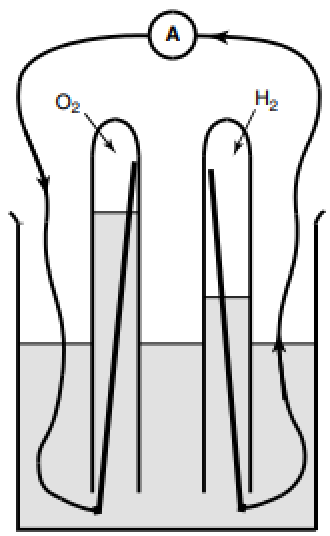

Figure 3.1 Basic fuel cell representation (4).

Even though the process of how and where the electrons resulting from the reaction are obtained may vary for each type of fuel cell, the basic working principle of the fuel cell can be described based on an acid electrolyte. The electrolyte is a substance that releases ions when is combined with water, then an acid electrolyte is a substance with a high presence of hydrogen ions (the difference between acids and bases is that in contact with water acids produce hydrogen ions, while bases capture ions forming OH^- ions, this substance is called an alkaline solution, which is the type of electrolyte used in the alkaline fuel cells). (5)

At the anode which is the electrode through which the electrons enter the circuit, occurs the ionization of hydrogen, i.e. it creates H^+ ions and releases electrons during the process, represented by the half-reaction (*3.2*), the electrons and ions released in this reaction travel to the cathode through the electric circuit and the electrolyte respectively, the cathode is the electrode at the oxygen side, thus the products obtained from the oxidation of hydrogen are consumed at the electrode creating water as a product. (4)

$$2H_2 + O_2 \rightarrow 2H_2O \quad \textit{Global reaction} \tag{3.1}$$

$$2H_2 \rightarrow 4H + 4e^- \textit{ Half reaction at the anode} \tag{3.2}$$

$$O_2 + 4e^- + 4H^+ \rightarrow 2H_2O \textit{ Half reaction at the cathode} \tag{3.3}$$

To obtain a continuous electric current then is necessary to have continuous ions flow through the electrolyte and constant feeding of reactant gasses, and this is the most challenging part to create the setup or the general layout of the fuel cell to make effective the reactions and obtain a performance. Several types of systems are proposed in the literature to reach this, in the following sections this will be expanded.

In the basic fuel cell explained, the electrons released during the hydrogen oxidation at the anode are those that create the usable electric current, the problem is that this basic fuel cell would produce a quite small current, therefore several considerations must be considered to create a basic setup:

1. The current produced depends on the area in which the gas and the electrolyte get in contact with the electrode (4).
2. The distance between the electrodes must be short to reduce as much as possible the

resistance caused by the electrolyte to the electric current (4).

To approach the first aspect, the electrodes must be made flat and aiming to cover as much area as possible, in that way the contact area is increased, but this generates another issue, which is that always there is going to be a space limitation, i.e., the area of the electrode cannot be infinite, thus also the current produced is limited. To increase the contact area were created porous electrodes where the fluids can penetrate the electrode, modern electrodes can increase the contact area up to hundreds of times (4), reaching in this way the maximum achievable contact between the gas, electrode, and electrolyte. The second condition is fulfilled by making the setup such that the electrolyte is stored in a thin layer, as thin as possible, where the thickness of this chamber will be constrained by the manufacturing process and the geometrical parameters of the sealing elements.

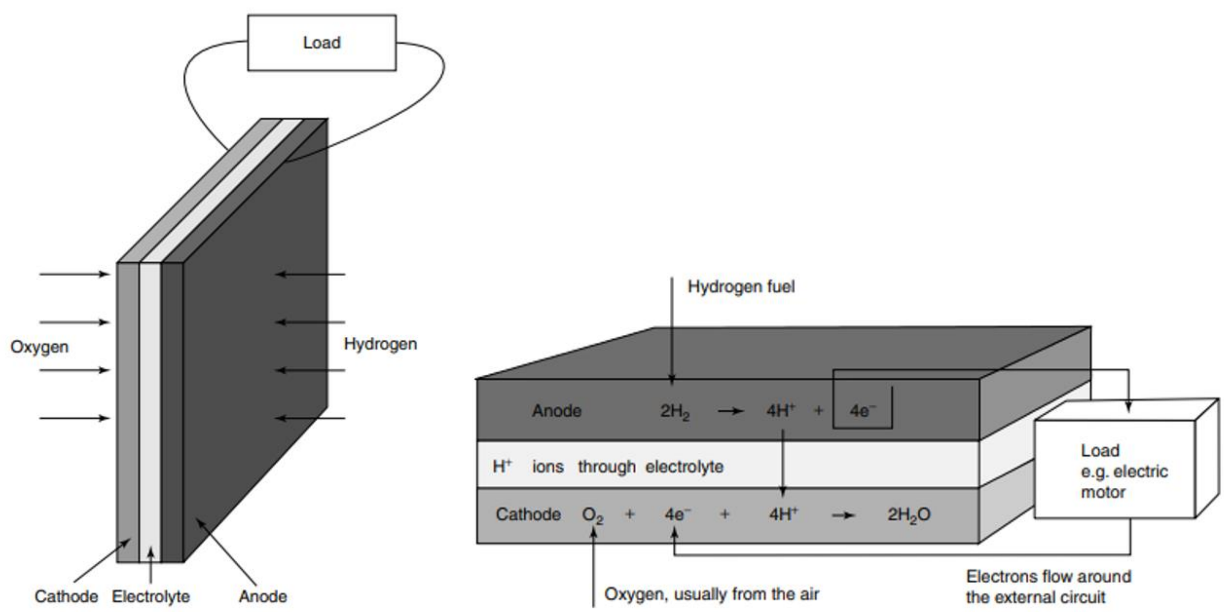

Figure 3.2 - A graphic representation of the setup of a single cell and the reactions at each node in the case of an acid electrolyte (4).

Another aspect to have into account is that these reactions need an activation energy (4), i.e., before the reactions begin, some energy needs to be added in form of heat to notice a little potential difference between the electrodes. This process may be quite slow, thus, to improve the rate of reaction are used catalyzers, a temperature rise, and as was discussed before, an increase in the contact area at the electrodes, where occurs the three-phase contact (reactant gas, solid, or liquid electrolyte and porous electrode).

There are several types of fuel cells, some of the most known are: Polymeric Electrolyte Membrane (PEM), which uses a solid electrolyte (proton exchange membrane), Direct Methanol (DMFC) which are powered by pure methanol, Alkaline Fuel Cells (AFC) where the electrolyte is an alkaline solution, Phosphoric Acid Fuel Cells (PAFC), which was one of the firsts implemented and uses a liquid phosphoric acid as electrolyte (4).

3.1.1.1 Selection of the type of fuel cell to use

As was explained before, in this project the fuel cell aims to feed power to an Autonomous Underwater Vehicle, the considered options were the AFC and PEM fuel cells, they are the two technologies used in vehicles, even though all of them have the same fundamental problems slow reaction rate and the non-availability of hydrogen, Table 3.1 shows some characteristics, differences and operating conditions for each technology.

Table 3.1 – AFC and PEM features (4)

Alkaline Fuel Cells (AFC)	Proton Exchange Membrane (PEM)
• The electrolyte is the Potassium Hydroxide (KOH) a liquid substance where the mobile ions are OH-. • Pure hydrogen and oxygen must be used because the presence of CO_2 degrades the	• It has a solid electrolyte where the protons (Cations of hydrogen) are mobile, thus it could be said that it is relatively simple. (4) • They use a platinum catalyst to address

electrolyte. (4) • Its activation overvoltage is lower in comparison to the other fuel cells (about 0.875 V in each cell). (4) • The cost of the electrolyte is low and there is no need for rare materials for the electrodes, then these are also cheaper than in the other types of cells. • The water production issue is easier to manage with this technology. (4) • As the electrolyte is liquid several challenges present in the PEM cells are avoided, for instance, the humidification of the membrane. (4) • As the operation of the fuel cell goes on, the electrolyte concentration decreases because of the water production, then the electrolyte reservoir must be occasionally refilled. (4)	the problem of low reaction rate, but this catalyst is expensive. (4) • The hydrogen used must be very pure because this technology is very sensitive to impurities. • They have a quick start and a low operating temperature from 30 to 100°C. (4) • A very important aspect is water management, the amount of water cannot be too high because it floods the electrodes but neither too little because the membrane would dry and the conductin would drop. (4) • Pure hydrogen is not the only possible reactant used as a fuel and usually is used in air instead of pure oxygen. (4) • They can be used in a very big range of applications, but it is more widely used in vehicles. (4)

In the end, the Alkaline Fuel Cell was selected for several reasons:

- The application allows access to pure oxygen, as it is an underwater vehicle the reactants must be compressed in tanks anyways, thus whether oxygen or air must be in a tank, then if it is pure oxygen, it will be present in a higher quantity for the same volume.

- The low cost of electrodes and catalysts for the alkaline fuel cell in comparison to PEM fuel cells is another important factor in the selection because as it is a research project the replacing parts are cheaper, then the process of prototyping is easier.
- Also, with this selection is avoided the additional setup needed for the air processing in the case of PEM fuel cells.
- The autonomy of the vehicle is going to depend on the storage capacity and the electrolyte concentration at the reservoir, thus with the proper dimensioning, it may have high autonomy.

3.1.2 Alkaline fuel cells

The alkaline fuel cell uses an aqueous potassium hydroxide electrolyte instead of an acid electrolyte, i.e., the mobile ions are hydroxides OH^-, (4) the basic reactions in an AFC are:

$$2H_2 + O_2 \rightarrow 2H_2O \quad \textit{Global reaction} \tag{3.4}$$

$$2H_2 + 4OH \rightarrow 4H_2O + 4e^- \textit{ Half reaction at the anode} \tag{3.5}$$

$$O_2 + 4e^- + 2H_2O \rightarrow 2OH^- \quad \textit{Half reaction at the cathode} \tag{3.6}$$

Thus, the water is consumed in the cathode and produced double amount at the anode, this excess water can be removed from the system or recirculated by dilution in the KOH tank, by this the performance of the fuel cell decrease with time, while the electrons extracted goes through the circuit from anode to cathode. Figure 2.1 shows the reactions and where it takes place.

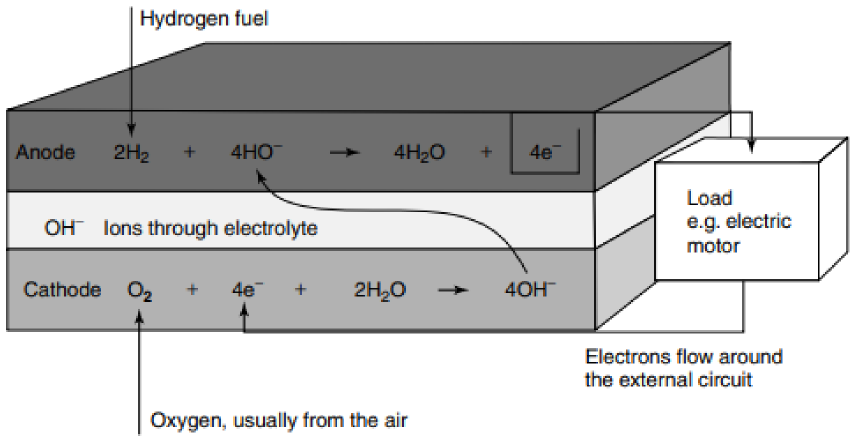

Figure 3.3 – Alkaline fuel cell representation (4).

Additional reactions or different setups may be present according to the type of AFC, there are three types: Mobile Electrolyte AFC, Static Electrolyte AFC, and Dissolved Fuel AFC, the most used are the first two, described briefly as follows.

3.1.2.1 Mobile Electrolyte

It uses a recirculating system for the electrolyte, hydrogen, and in some cases also for the oxygen. In the case of the electrolyte, it is pumped around the system, but special attention must be taken because KOH is a corrosive substance, and also its superficial tension enables it to go through small gaps, then proper sealing elements and corrosive resistant materials are fundamental. One risk aspect is that exists the possibility of the ions conduction through different cells around the stack which may cause a short circuit (4).

As the reaction is exothermic, a heat exchanger must be used to remove the excess heat present in the electrolyte, then this is an important advantage of using a mobile electrolyte, it also may serve as a cooling fluid for the cell.

As it was mentioned before, in these types of cells the water produced at the anode is twice more of what is consumed at the cathode, then here is where the recirculating system for the hydrogen is important, theoretically, the hydrogen will evaporate the water present then utilizing an ejector or a gas pump, the hydrogen is forced to go through a heat exchanger after the reaction, in this device the water gets condensed and separated from the hydrogen and consequently the hydrogen Is reinjected into the circuit (4).

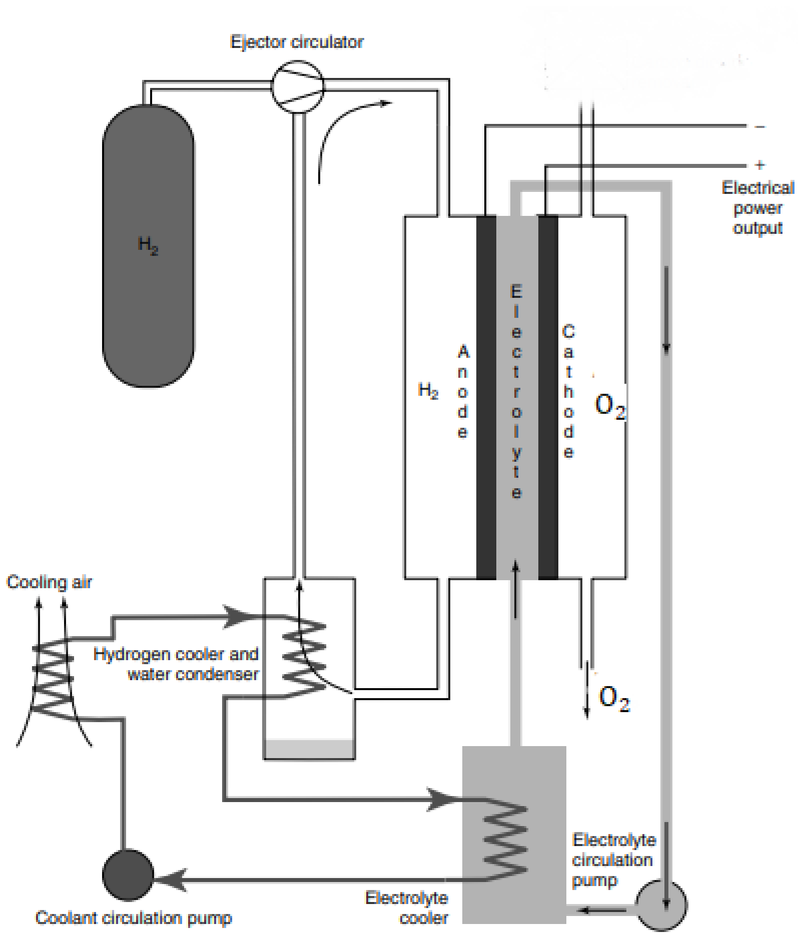

Figure 3.4 - Mobile electrolyte system.

Also, the resulting water after the reaction can be taken out of the cell by mixing it with the electrolyte, this would cause a reduction in concentration, this means that the reactions are going to be less effective in time, in the case of this project is necessary a tank where the maximum capacity will determinate the autonomy of the vehicle, i.e, when this reservoir is full, it means that the mission has finished, also this maximum capacity must be calculated based on the minimum limit of electrolyte concentration to have an acceptable performance of the cell.

Another factor that influences the degradation of the KOH is the presence of Carbon dioxide in the reaction (in the case of using air instead of pure oxygen), thanks to the reaction (*3.19*)

$$2KOH + \mathrm{CO_2} \rightarrow K_2CO_3 + \mathrm{H_2O} \quad (3.7)$$

Where the potassium hydroxide is progressively changed to potassium carbonate, which causes a reduction in hydroxide ions decreasing the performance of the fuel cell. This is not going to be an issue for this fuel cell because will be used pure oxygen to avoid the degradation of the electrolyte. One of the problems of this type of AFC is that as the water is being produced twice more in the anode than in the cathode, it may occur that after some time the concentration of the KOH in the anode is quite bigger than in the cathode, causing the solidification of the electrolyte (4).

Even though this configuration has several drawbacks, and needs additional subsystems to work, it also has several features that are highly beneficial to the performance of the cell and adust appropriately to the characteristics of the project, thus this is the type of configuration that will be used.

3.1.2.1 Static Electrolyte

In this type of AFC, the electrolyte is maintained in the cell using a matrix material, usually asbestos, this material has excellent corrosion resistance and it is highly porous, a feature that is especially important for the cell, the problem is the already known health problems that people that manipulates this kind of materials undergo. The system uses pure oxygen, this is almost a must, because as the electrolyte cannot be renewed the creation of potassium carbonate must be avoided. Also as in the case of the mobile electrolyte, the hydrogen Is recirculated and the water present on it is condensed to consequently reinject it into the system. The main advantage of this configuration is that the electrolyte does not need to be pumped out of the fuel cell, avoiding possible leakages and additional equipment for the process. But as there is no electrolyte recirculation there is a water management problem about how it is going to be taken out from the system (4).

3.1.3 Stack: Cells connected in series

The voltage produced by alkaline fuel cells to obtain a useful current is quite small (around 0.7V) (4), then to increase the voltage to a value that can be suitable, several cells must be connected in series i.e the same current passes for each one of them and the voltage is raised. The number of cells needed depends on several factors but the main ones are the maximum power output needed and the maximum space available (this to account for the contact area), to make a series connection the anode of one cell is connected with the cathode of the following cell with wires or any electrical connection, but the problem by doing so is that as the voltage is extremely low, inefficiencies in this process are important, any loss in this voltage has a big impact, then the cells must be connected cleverly.

To solve this issue a more efficient method of connection has been developed, which is the bipolar plate, this is a crucial component in the layout of the fuel cell, because it is a multifunctional part, in one face it is the anode of one cell and in the other face is the cathode of the next cell, in this way it conducts the electrons from one cell to another, at the same time It works as a distributor of the reactant gases, thanks to the channels that usually are machined on its faces, and finally, it facilitates the holding of thin membranes in their position. The design of the bipolar plate must be optimized for two reasons, the first one is that the contact points must be as large as possible to facilitate the conduction, i.e optimizing the electrical contact, but what this causes is the reduction of the capacity of the mass transport along the electrodes, lower amount of gas would be reaching the desired points, then if the contact points need to be small to do not affect the gas flow, they must be at least recurrent, this fact makes increase remarkably the price of the component (4), (6). (*3.5*) shows different bipolar plates.

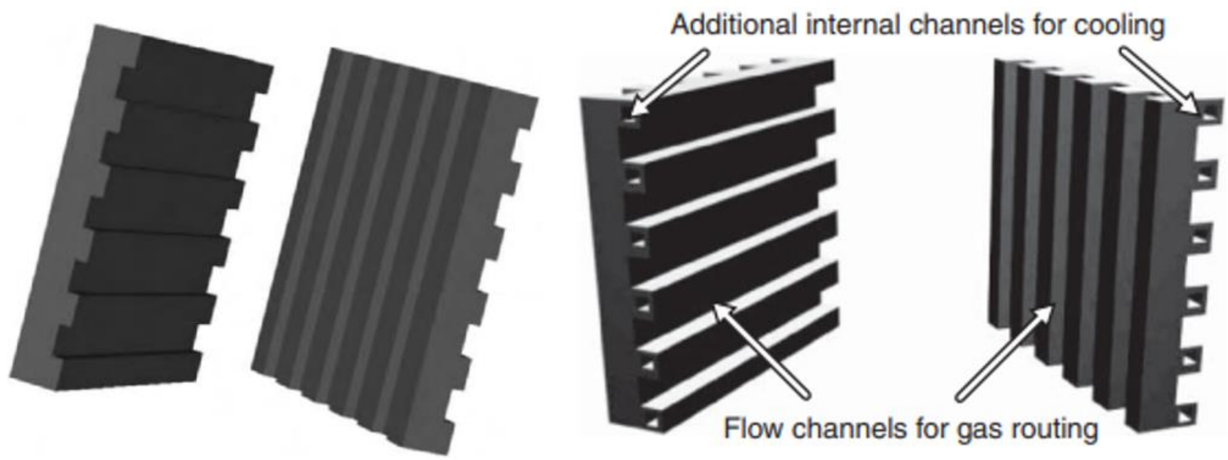

Figure 3.5 - Bipolar plates (4), (6)

After connecting several cells in series, the result is a stack, which is the total group of fuel cells with the desired power output, Figure 3.6 shows a stack of fuel cells.

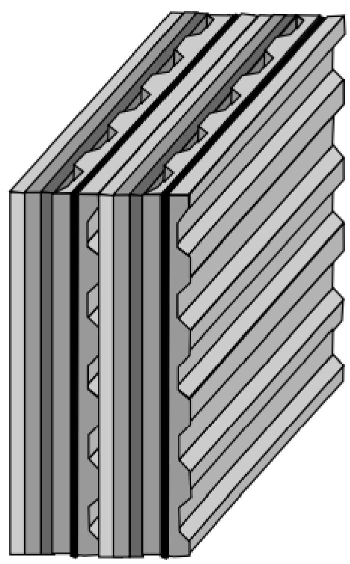

Figure 3.6 – Two cells stack.

3.1.4 Types of gas supply

This is one of the main challenges when designing a fuel cell, to have a continuous current, there must be an uninterrupted supply of reactant gases, which means that is necessary a constant flow of the gases through the electrode. As it was mentioned, the bipolar plates also work as gas distributors such that it is in mechanical contact with the electrode and at the same time there is a flow-through it, but to make this real, a question arises, how can the gases be supplied at the same time without mixing each other during the process? This can be reached by a manifold of channels and several sealing elements to avoid leakages.

In the literature, there are two types of gas supply, Internal manifolds, and External manifolds. In internal manifolds, the gas is fed directly on each channel of the distributor or bipolar plate, such that there is a common channel along the stack to transport the gases to each manifold of channels in the bipolar plates, Figure 3.7 shows an example (4).

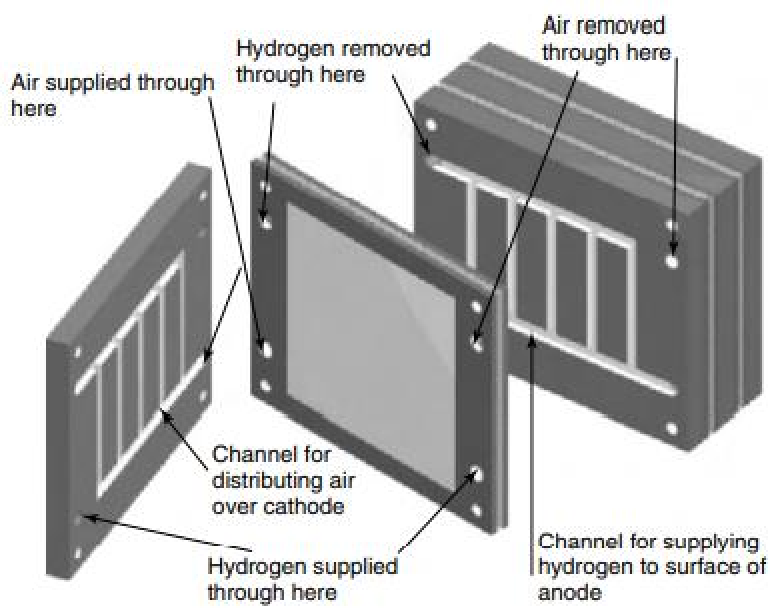

Figure 3.7 - Internal manifold

The external manifolds consist of a group of channels all fed at the same time from a stream of fluid separated each other, i.e. in the top is fed hydrogen, and in the side oxygen, in this project, the selected configuration is the internal manifolds due to the constraints in space, in the layout section, this part will be explained with more detail.

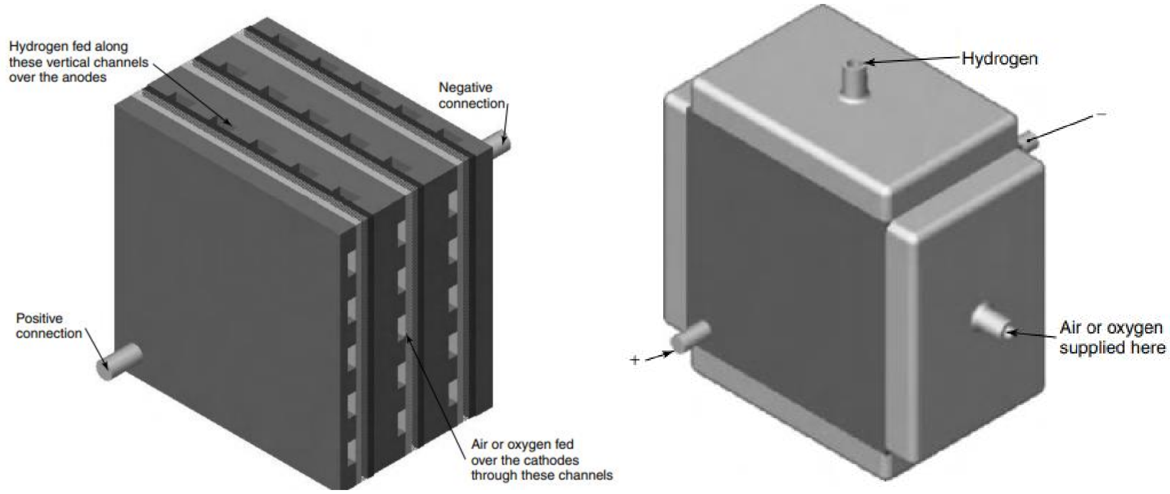

Figure 3.8 - External manifold.

3.1.5 Preliminary design computations

The power bank must be designed such that the power output is 300W at 12V. As a first step, the number of cells needed is chosen based on a typical voltage for a single cell, which is 0.7V, then to obtain 12V is needed approximately 17 cells. Also are defined the operational pressure and temperature. The initial parameters are summarized in Table 3.1.

Table 3.2 - Initial parameters for the fuel cells

Parameter	**Value**
Power output	300W
Operating voltage per cell	0.7V
Number of cells	17
Total voltage	12V
Operation temperature	60-70°C
Operation pressure	1 bar

Note: is important to remark that the energy needed for the components of the system such as pumps and instruments, comes from a battery located outside, thus it is not necessary to compute a higher power output accounting for this energy.

Once that is assumed the operational voltage of a single cell, the current density can be determined from the polarization curve, where a 0.7 voltage corresponds to a current density of 0.47 A/cm². The total current is already known with the power and voltage $I = P/V$ then can be found the total area and the diameter needed.

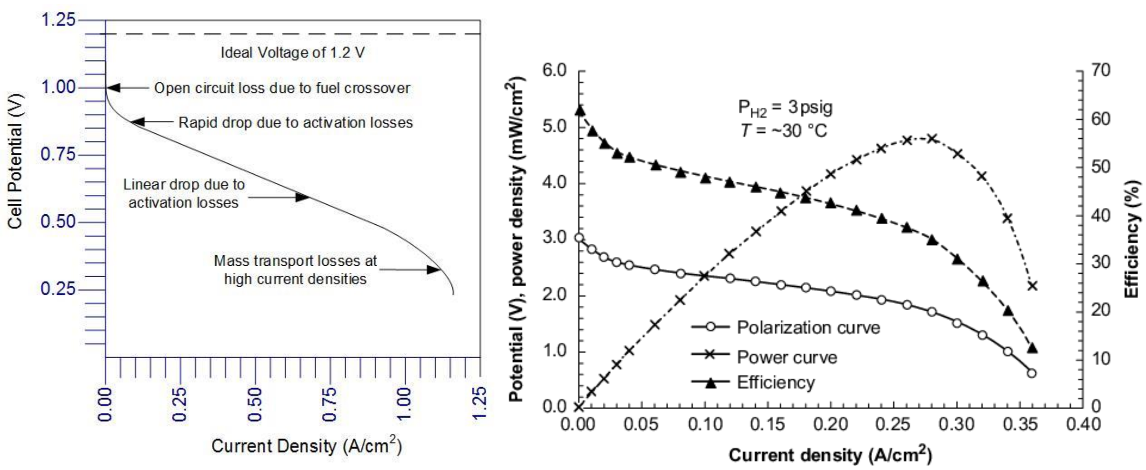

Figure 3.9 – Two examples of polarization curves (7).

$$Current\ density = \frac{P}{AV_c n} \tag{3.8}$$

Where V_c is the voltage per cell, P is the total power, n is the number of cells, and A the area per cell (6). The results are shown in Table 3.3

Table 3.3 - Results from the polarization curve for a single cell

Parameter	Value
Area	53.6 cm²
Diameter	8.26 cm
Total current	25 A

Efficiency	50%

3.1.5.1 Mass balance

The mass balance comes from the needed mass required to obtain a certain amount of charge given by equation (*3.19*), which can be divided by time to obtain current and mass flows.

$$q = z * F * m_{comp} \tag{3.9}$$

Where

q: Obtained charge

z: Number of electrons obtained from each mol of the component.

F: Faraday constant, which says the electric charge of one mol of electrons.

$\mathbf{m_{comp}}$: mass of the component.

Then the current obtained with a flow of a component is given by (*3.19*), (6).

$$I = z * F * \dot{m}_{comp} \tag{3.10}$$

As is already known the power output, voltage, current, the number of cells, and also electrons produced in the reaction, then the mass flows for each component can be found. The electrolyte mass flow is determined just with the volume chamber and a time of filling, the thickness of the electrolyte chamber is 0.05 cm and the area is that one found for the electrode. The filling time was assumed as 15 s. Table 3.4 summarizes the results.

Table 3.4 – Mass flow of reactants and products

Component	Mass flow [g/s]
Hydrogen	0.004
Oxygen	0.031
Water produced	0.035

Electrolyte	0.01

3.1.5.2 Autonomy

The autonomy is given by the capacity of storage in the external tanks. There will be two tanks for oxygen with a load of 2.4 kg/tank and five tanks with hydrogen with 0.125 kg/tank. The autonomy time is computed with the consumed mass flow and the available mass equation (*3.19*). Table 3.5 - parameters to compute the autonomy.Table 3.5 shows the results.

Table 3.5 - parameters to compute the autonomy.

Component	**value**
Oxygen available	4.8 kg
Hydrogen available	0.625 kg
Hydrogen consumed	$4.4\text{x}10^{-6}$ kg/s

$$Autonomy\ time = \frac{m_{H2,consumed}}{\dot{m}_{H2,available}} \tag{3.11}$$

$$\boldsymbol{Autonomy\ time = 38.4\ h = 1.6\ days}$$

3.1.5.3 Electrolyte tank dimensioning

The capacity of the tank is computed by knowing the amount of water produced, the initial volume of electrolyte in the tank, and the molarity limits of the KOH to have an acceptable performance. With the time of operation and the water mass flow found previously is known the volume of water produced. The molarity limits are defined in the range in which the KOH conduction is approximately constant, then are chosen 15M to 7M, where was assumed an initial stored volume of electrolyte of 5L with a molarity of 15M (15 moles/liter). Table 3.6 shows the results.

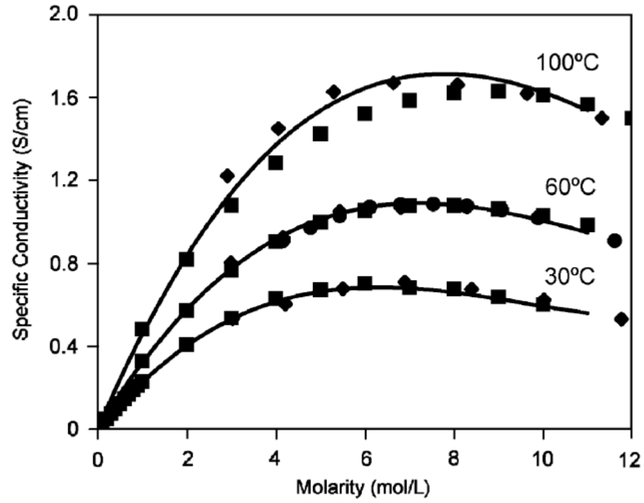

Figure 3.10 – KOH conductivity vs Concentration. Obtained from R.J. Gilliam, J.W. Graydon, D.W. Kirk, S.J. Thorpe, A review of specific conductivities of potassium hydroxide solutions for various concentrations and temperatures, International Journal of Hydrogen Energy,

Table 3.6 - dimensioning of the electrolyte tank

Parameter	**Value**
KOH initial volume	5L
Water produced	4.87 L
Initial molarity	15M
Final molarity	7M
Maximum volume	10.7L

Thus **the volume of the tank** must be **11L**.

3.1.5.4 Thermal balance

In this section are obtained several parameters that help to understand the performance of the cell, for instance, the Open Circuit Voltage (OCV), the efficiency, and the Heat Generation Rate (HGR). The reaction inside the fuel cell is exothermic, then the energy produced in the reaction leaves the cell in three possible types: electricity, ordinary heat, and latent heat (in case of having vapor water as a result), this is important to carry out the thermal analysis of the cell (6).

Open Circuit Voltage (OCV)

It is the theoretically obtained voltage if all the energy in the hydrogen was transformed into electricity, (6).

$$OCV = \frac{|\Delta h}{zF} \tag{3.12}$$

where Δh is the enthañpy of H2O formation

$$\Delta h = \begin{cases} H_2O^l: 286\ kJ/mol \\ H_2O^g: 241.8\ kJ/mol \end{cases}$$

Then OCV is 1.48V in the case of liquid water in the products and 1.28V in the case of vapor products (6). For the preliminary design will be assumed that the water after the reaction is vapor.

$$\boldsymbol{OCV = 1.28V}$$

Utilization coefficient

Not all the fuel injected in the fuel cell reacts, then this factor gives efficiency in the utilization, equation (*3.19*). This value will be assumed as 95%. (6)

$$\mu = \frac{mass\ reacted}{mass\ input} * 100\% \tag{3.13}$$

$$\boldsymbol{\mu = 95\%}$$

Cell efficiency

The efficiency can be computed from the comparison between the maximum obtainable voltage and the actual operating voltage, which is 0.8V, corrected by the utilization coefficient, employing the equation (*3.19*). (6)

$$\eta = \frac{V_c}{1.28} * \mu * 100\% \tag{3.14}$$

$$\boldsymbol{\eta = 58.9\%}$$

Heat generation Rate

It is just how much non-used heat is generated in the cell. OCV minus the power used, described by equation (*3.19*). (6)

$$Q = (OCV - V_{op}) * I_T \tag{3.15}$$

$$\boldsymbol{Q = 12\ W}$$

With this heat can be found the temperature of the streams at the stack's outlet using the thermal balance (eq. 10), assuming that all the fluids enter at the same temperature and leave the stack at the same temperature. (6)

$$Q = \left(\sum C_{pi} * \dot{m}_\imath\right) * (T_{i,out} - Ti_{in}) \tag{3.16}$$

The fluids involved in this process are water, hydrogen, oxygen, and KOH, their specific heat, and mass flow at 60°C are shown in Table 3.7.

Table 3.7 - Specific heat of the fluids at 60°C.

Component	**Cp [kJ/kg*k]**	**$\dot{m}_\imath$ [kg/s]**
H_2	14.38	$4.49*10^{-6}$
O_2	0.924	$3.1*10^{-5}$
H_2O	1.87	$3.5*10^{-5}$
KOH	4.19	0.01

Then for the preliminary conditions, the temperature at the outlet $\boldsymbol{T_{i,out} = 61°C}$, temperature increases in one degree. This value will vary with any modification in the design.

3.1.5.5 Heat exchanger.

This heat generated after the reactions must be removed because otherwise, the stack will increase its temperature, this is done using a heat exchanger. In the following section, there will be more detail about the geometry of the system, but it is a pipe that leaves the housing to be in contact with the water that is inside the AUV. Then the system is an internal flow in a pipe surrounded by water, represented in Figure 3.11.

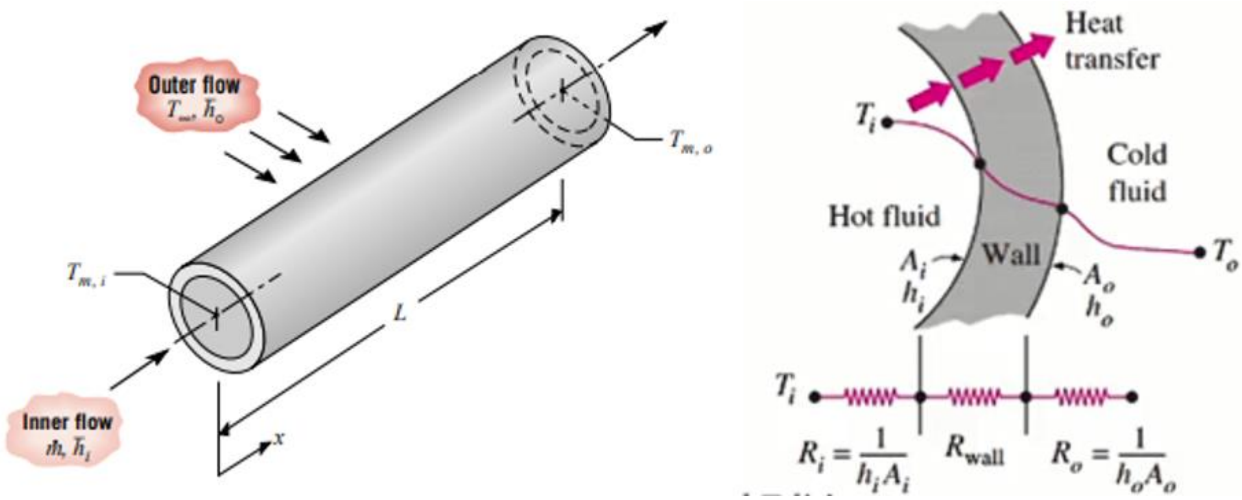

Figure 3.11 - heat transfer in a pipe with internal and external flow. (8), (9)

The heat transfer between the internal and the external fluid is given by the heat transfer equation (*3.17*) which uses a global heat transfer coefficient that accounts for convection (given by the speed of the fluids) and conduction (given by the pipe wall) equation (*3.19*).

$$\varphi = UA_s\Delta T \tag{3.17}$$

$$\frac{1}{UA_i} = \frac{1}{h_iA_i} + \frac{\ln\left(\frac{D_0}{D_i}\right)}{2\pi kl} + \frac{1}{h_eA_e} \tag{3.18}$$

But when the exit and entrance temperatures are known is used the logarithmic mean temperature difference method is, which transforms the equation (*3.17*) into equation (*3.19*). ΔT_i are de differences of temperatures at the ports. (6).

$$\varphi = UA_s\Delta T_{\ LMTF} \tag{3.19}$$

$$where\ \ \Delta T_{\ LMTF} = \frac{\Delta T_1 - \Delta T_2}{ln\left(\frac{\Delta T_1}{\Delta T_2}\right)}$$

The convection coefficients are found with the Nusselt number which depends on the Prandtl and Reynolds number (8). The correlations and equations to find the coefficients are shown in Table

3.8.

Table 3.8 - Correlations used to find the convection coefficient. (8)

Number	Correlation
Reynolds	$R_e = \frac{vD_h\rho}{\mu}$
Prandtl	$P_r = \frac{C_p\mu}{k}$
Nusselt (for convective flows)	$N_u = 0.22{R_e}^{0.8}{P_r}^{0.5}$
Convection coefficient	$h = \frac{N_u k}{l}$

μ : Dynamic viscosity [Pa s]

C_p: Specific heat [J/(kg K)]

C_p: Thermal conductivity [W/(m K)]

v: Fluid's velocity [m/s]

D_h: Hydraulic diameter [m]

Table 3.9 - Convection coefficients

	Internal	External
Nu	46	65
Pr	2,21	2,21
Re	8945	13726
h [W /(m² °C)]	7672	62

After applying the logarithmic mean temperature method and by the definition of the surface areas πDl is found the necessary length of the pipe to obtain a temperature of 60°C.

$$\boldsymbol{length = 804\ mm}$$

3.2 Sealing joints

This is an extremely important part of the design, crucial for the performance of the fuel cell. The ideal case would be that one where the reactions take place in the electrodes and the flows do not leak through the surface contact gaps leaving the stack or mixing with other flows in non-desired places, things that would reduce remarkably the efficiency and even would cause that the fuel cell never works (4). but the reality is that assuring a process without any leak is extremely difficult, but the design can be done such that a near zero-leak state is achieved. The challenging part of designing a sealed joint for this application is the small dimensions and gaps from layer to layer, this section explains the design process of the joint and how it could potentially affect the performance of the fuel cell.

3.2.1 Housing for sealing elements

As has been mentioned before, the membrane electrode assembly is where the chemical reaction takes place, an important piece belonging to this group, that besides keeping the electrodes, membranes, and catalysts together, serves as the housing of the gaskets, is the so-called Housing for Sealing Elements (HSE), this component has an important role when it comes to seal and give stiffness to the assembly of mono-cells (stack). As this part is located between the two bipolar plates (or current collectors depending on the case) it must have some special features and mechanical properties that make the selection of material, not a trivial decision.

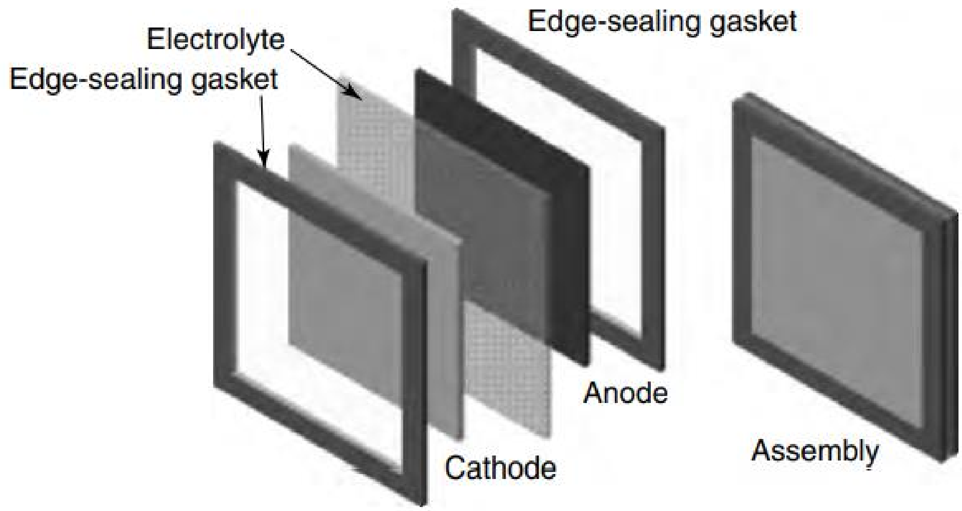

Figure 3.12 - Membrane electrodes assembly. (4)

Below can be found the preliminary properties that this material must have.

- It must be an insulator material: as it will be in full contact with the collector or distribution plate (which is a conductor material), it cannot allow passing the current through itself because it would generate a short-circuit, i.e the generated current would not go through the external circuit, thus the fuel cell would not work.
- It must be an inert material: This component cannot react with the fluids involved in the chemical reaction, i.e it should have chemical compatibility with Hydrogen, Oxygen, Water, and Potassium Hydroxide.
- It must be machineable: the HSE is a part that will have several channels and holes to allocate the gaskets and allow the flow of the fluids, this means that the selected material needs to be able of handling some manufacturing operations and still be a functional and stable part, this is why material functionality must be in line with real production feasibility. Another important aspect is that the functionality must be in line with the manufacturability of the component, thus a properties trade-off is important to create.
- It must be rigid: As fluids will go in the cell at a certain pressure it must withstand a

range of pressure without deflection, because if it deflects it will give space for leakages.

For this component, two materials were analyzed, PTFE (commonly known as Teflon) and PEEK (polyetheretherketone). Some features are listed in Table 3.10.

Table 3.10 – PTFE Vs PEEK (10), (11)

PTFE	**PEEK**
Advantages • High insulation resistance. • High chemical resistance. • Relatively high strength. • Accessible cost. Drawbacks • Very sensible to temperature (Thermal expansion).	Advantages • High-performance polymer. • Its special structure gives a combination of stiffness (by ketone bonds) and flexibility (by ether bonds) creating an excellent balance of mechanical properties. • They are also resistant to chemical attacks and thermal degradation. • It does not absorb moisture. Drawbacks • Extremely high cost.

Even though PEEK would be the perfect material for this application due to its outstanding properties, the selected material is PTFE for several reasons, the first one is the benefit-cost relation, for the development of a prototype this material has an acceptable behavior, another reason is that this material has been used in other projects, then there is a precedent experience working with it. An aspect to be careful about is the thermal expansion of Teflon, it has a considerable change in dimensions as temperature increases (11), the temperature in the process varies between ambient temperature up to 60°C, as geometrical tolerances are small this could affect the performance, anyways this is a point to be tested and verified.

3.2.1.1 Grooves for the gaskets

The preliminary layout for the fuel cell is already known, now is time to define the positions where seals are needed. By definition a sealing element avoids the transition of a fluid from one space to another, this is why that for each type of fluid there is going to be defined a certain number of seals because the selected layout is an internal manifold type, so this increases the complexity of the assembly when it comes to preventing leakages. Thus the sealing elements are defined by each type of fluid as follow:

Electrolyte (KOH)

this fluid enters through the inferior middle port and leaves through the superior middle port, for each MEA the electrolyte must go to the very middle chamber, i.e. between the two anionic exchange membranes, thus it must go through the frontal flange, isolating plate, current collectors and bipolar plates, all this without leakages, then for each hole at the contact surface through which passes the fluid needs a sealing element.

- As it is needed to prevent the mix of the Hydrogen or Oxigen with the KOH outside the electrode, the selected configuration to make this seal is shown in b). c).
- Figure 3.13 a). The seals are going to be compressed against the distribution membrane, in the case of O-rings they are situated face to face. b). c).
- Figure 3.13 a). An aspect to be pointed out here, is that under normal conditions the most suitable way to couple compress an O-ring, is against a wall, in this case, the distribution layer acts as a wall but at the same time it is supported by another O-ring at the other side, this fact could cause problems, thus this is a critical point that needs to be analyzed during testing to know if an acceptable seal is achieved.

- To prevent the KOH from going out of the cell it is needed another set of sealings, this leakage could happen through any of the mating surfaces above the KOH channel, a double-channel in the left and a single channel in the right housing disc is proposed, always pressed against a flat face to ensure the ideal sealing, in this way the three possible scape clearances are covered. Figure 3.13 – Necessary O-rings. b).

- The final component to complete the KOH insulation are the little O-rings situated along the electrolyte feeding channel at the surface of contact between the bipolar plate and HSE. This O-ring prevents the KOH from going to the Hydrogen or Oxygen side chamber, then in this position is needed a groove to allocate the mentioned O-ring. Figure 3.13 – Necessary O-rings. c).

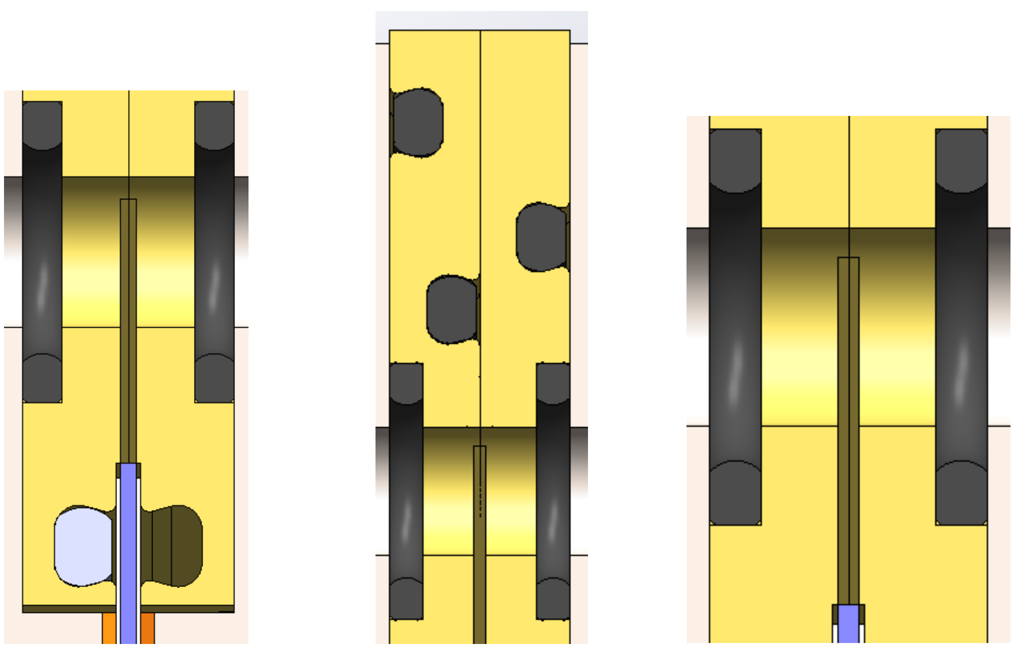

a) *b).* *c).*

Figure 3.13 – Necessary O-rings.

In the frontal view, the entrance of the electrolyte has the geometrical shape shown in Figure 3.14, it has a triangular entrance channel to make easier the entrance of the liquid inside the distribution membrane, thus this is an additional feature that must be machined into this plate.

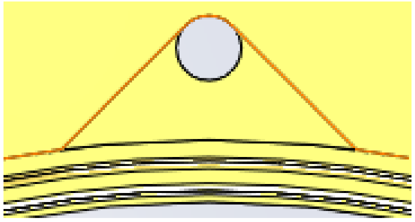

Figure 3.14

<u>*Hydrogen and Oxygen*</u>

The entrance for these fluids has the same configuration, with the only difference that the entrance ports are rotated each other and alternated at the same time, thus the contact surfaces between layers where the fluid does not need to go through, a seal is needed. For this purpose, one groove is needed for each plate of the HSE.

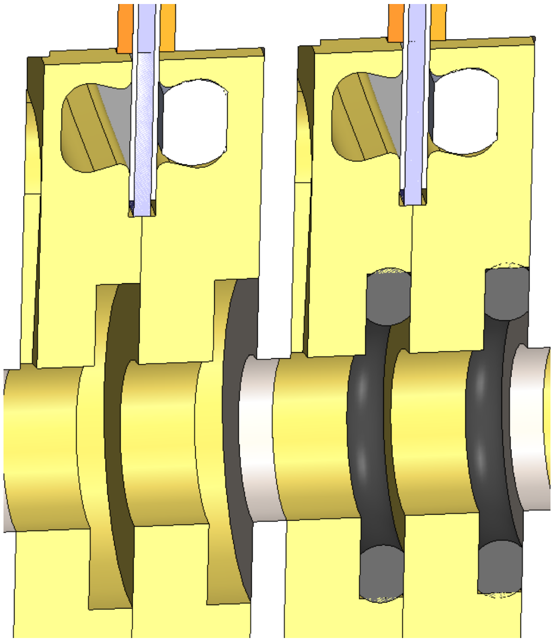

Figure 3.15 – Reactants channels.

The entrance channel in a frontal view is shown in Figure 3.16, this is the selected conduct for the gas entrance, this shape is chosen after analyzing a simulation carried out to understand how would be the entrance gas flow into the chamber.

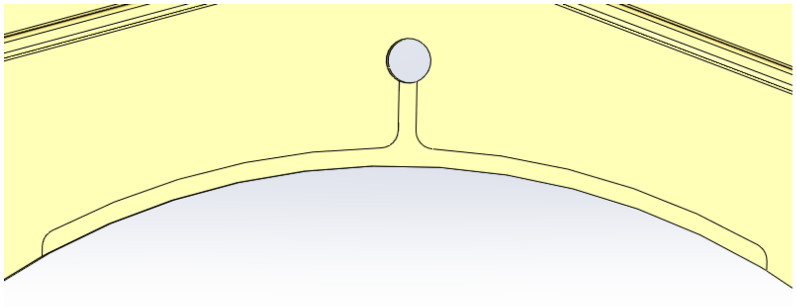

Figure 3.16 – Reactant port in frontal view.

3.2.2 Final part

After the explanation of the grooves for each plate of the HSE, the final part is shown in the Figure 3.17 shows two final models, one for the O-rings and one for the case of plain gaskets.

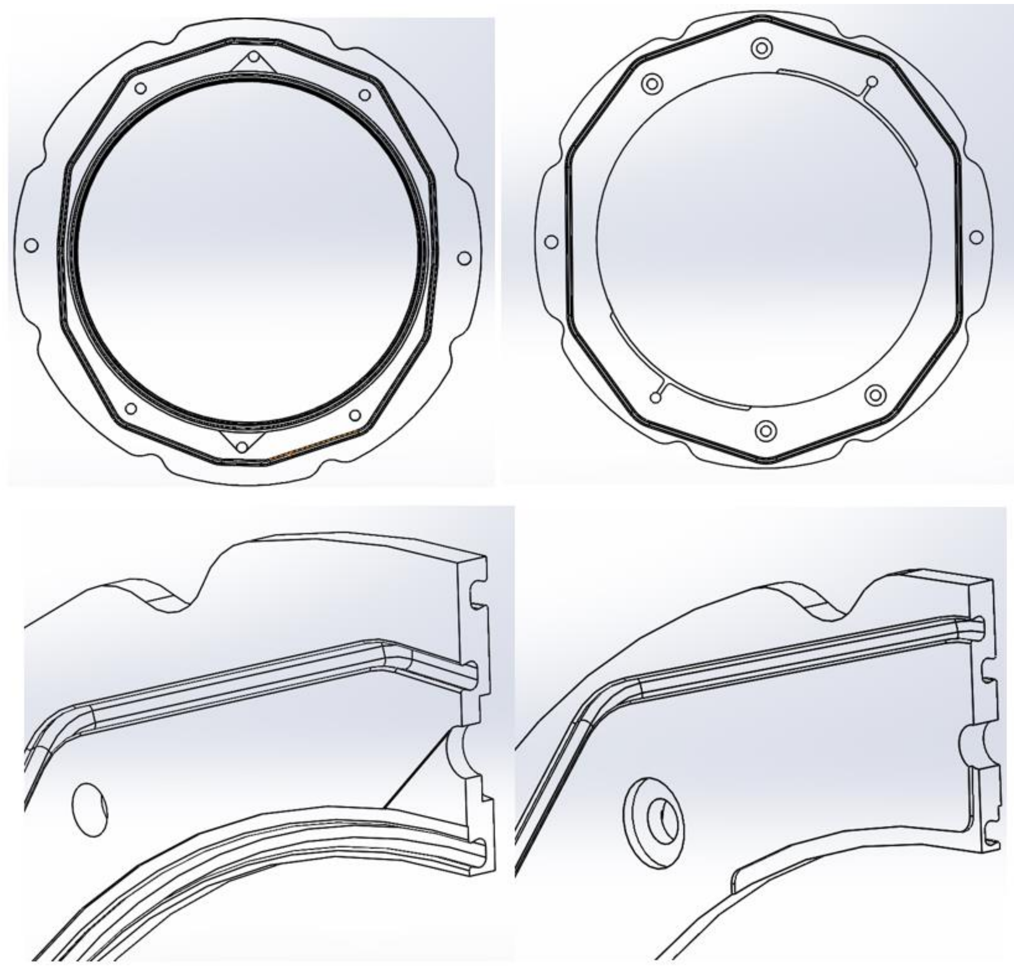

Figure 3.17 – Final HSE.

Comments:

- At the edge, there are small curves to allow the assembly of the bolts.
- The groove for the external sealing has a decagonal shape because there are seals at both sides and if these seals coincide being ain opposite faces this would decrease the thickness of the HSE in the plane between both faces, to less than half of a millimeter, and this is unacceptable for the manufacturing process. Figure 3.18 shows that the grooves do not coincide or cross each other.

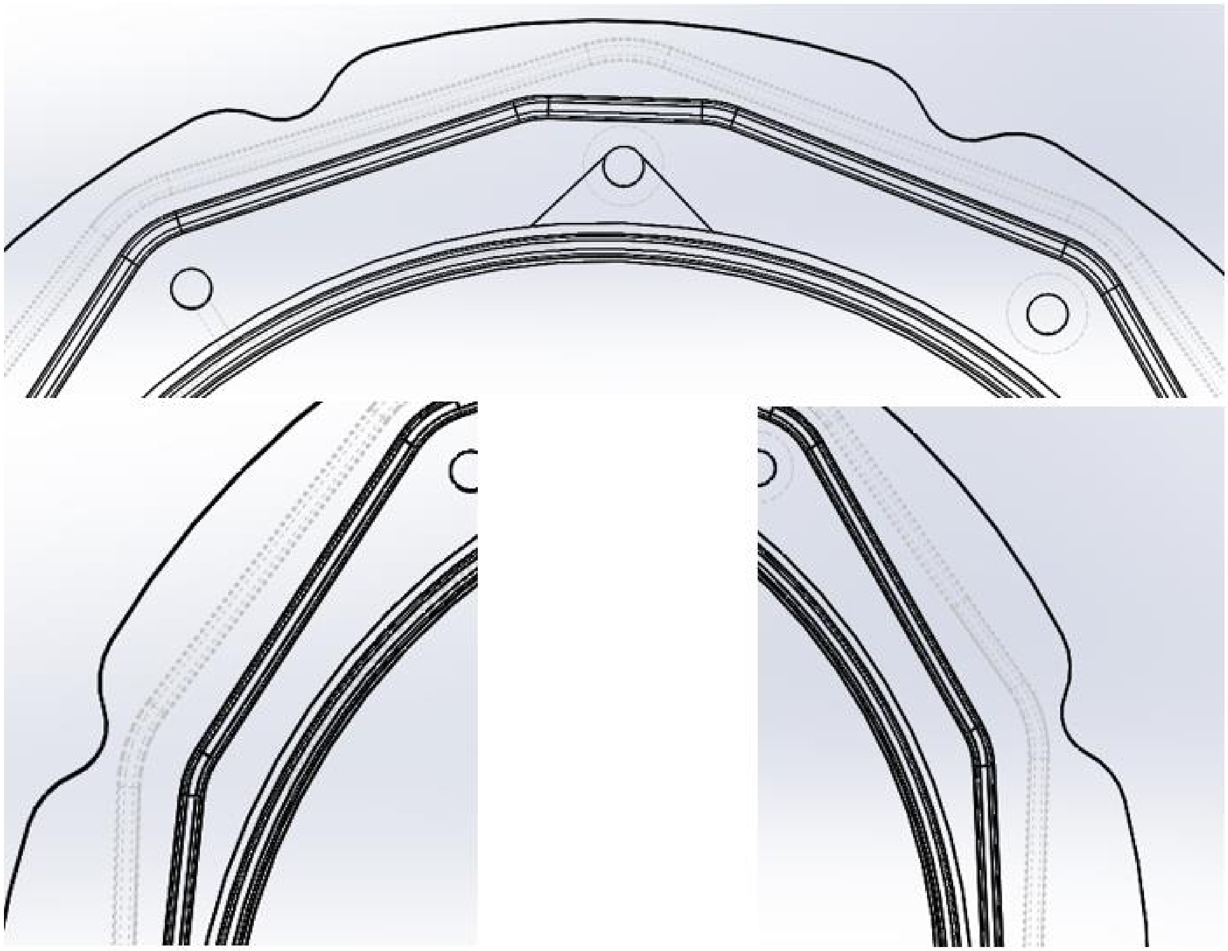

Figure 3.18 – Rotated O-ring grooves and spaces for bolts

- Two extra holes are added because the alignment of these plates is important during the assembly, thus this facilitates this task.
- It is important to notice that the geometry of the HSE plates changes side to side, thus it has a specific order of assembly.

3.2.2.1 Manufacturing method and surface finishing

The entire part is manufactured by cutting and milling, the importance of the manufacturing method goes in the surface finishing that can be achieved with each process, this is a quite important factor for the sealing element selection, if the surface is very rough then a softer material needs to be used. Due to the difficulting of obtaining a predefined roughness, instead of demanding a polished groove, the uncertainty about the roughness of the groove will be taken into account by the time of selecting the O-ring. (11)

Other important aspects in the manufacturing process are the geometrical tolerances and minimum tool sizes available, this creates a new constraint to the design process. In the selection process for the o-ring explained in the next section, is shown that a special groove for the channel has been chosen, thus a special tool is used to create this channel, the constraint generated by this tool is that the smallest tool for the milling process in which the channels are created, creates a channel of 3 mm depth, this means that O-rings with diameters lower than 3 mm do not fit. As the membranes assembled in the HSE are extremely narrow, the machined features in the component are small and difficult to control precision.

3.2.3 Sealing elements: O-ring vs Gaskets

O-rings and gaskets have a similar purpose which is sealing, but they offer different advantages according to the specific application, this section analyzes which one is a better option for this specific fuel cell.

For this application two types of seals can be used, are the O-rings and plain gaskets, an *O-ring* is a ring-shaped mechanical gasket with a and a circular cross-section placed in a groove between two surfaces to avoid the leak of fluid, commonly made of polymers (but there are also metallic), its working principle is the deformation, under certain load they deform and fill out the volume in which they are contained preventing leakages, for this to happen several geometrical characteristics, material properties, and mechanical features must be fulfilled, they will be discussed in the following section. A *Plain Gasket* is a flat piece (metallic or non-metallic) placed between two surfaces, this creates the seal by means of the pressure created by the clamped surfaces, so its working principle is the pressure, the higher the tightening torque supplied to the bolt, the better is going to be the sealing. In Table 3.11 are shown the advantages or drawbacks of each type of sealing element (10), (11).

Table 3.11- Comparisson between O-rings and Gaskets.

	O-rings	**Plain Gaskets**
Advantages	• Even though they need a minimum force deformed to the desired level, it does not work based on the force that is applied. • They can be really small, this is quite beneficial for this application, knowing the limited dimensions. • They seal over a big range of pressures and can resist high operational pressures, as the operating pressure of the cell is small, working with small O-rings dimensions does not cause any problem concerning the pressure. • They have a low weight and the assembly space required is small. • They have a relatively low cost.	• They have a higher area of contact, thus the seal is reached in a higher area. • They come in different shapes. • They are preferred in extreme temperatures applications. • They can be customized almost to any shape, this allows the covering of a wide range of applications.
Drawbacks	• The success of the sealing depends on the roughness of the surface, the better the surface finish, the better is the flow of the element into all the cavities. But in this case, the control of the roughness of the surface is difficult because is a PTFE surface.	• The higher is the clamping force, the better is the seal, but in this case, the force cannot be increased too much because it would cause negative effects on the performance of the fuel cell. • Difficulties in supplying the correct force to each gasket as there are several cells connected in series.

	• Difficult to use in non-circular joints because of its rounded shape.	• Standard gaskets have big dimensions in comparison to this application, thus in case of selection, the gasket must be customized. • In this particular case the space is a limitation.

As a prototype is going to be developed, and now is known the preliminary shape of the stack, as a first option is going to be taken the O-ring's as a sealing element, because of the following reasons:

- The fuel cell has a circular shape
- The minimum forced required for the deformation is not very big.
- They can be standard pieces.
- Low weight combined with a high-pressure resistance.
- Lower cost.

3.2.4 O-ring's selection

3.2.4.1 Operational conditions

To begin is the selection of the O-ring, is important to know the operational conditions and the types of fluids involved in the operation of the fuel cell,

Table 3.12 summarizes the information.

Table 3.12 – Operational conditions.

Fluids	**Gases**	**Liquids**
	Hydrogen, Oxygen	Potassium Hydroxide (KOH), Water (H2O)
Pressure	1-3 bar	
Temperature	50-70°C	

As a first characteristic is known that the operational pressures and temperatures are not that high, this is important because there is a higher degree of freedom to select the O-ring.

3.2.4.2 Materials

The selection of a suitable material is extremely important to obtain a functional sealing, if the material is not chosen properly it may cause different types of failures like swelling or shrinkage due to chemical incompatibility, hardening or softening, due to the wrong temperature conditions, Nibbling, surface cracking, and mechanical failure due to the high stresses and use of a non-resistant material, extrusion due to high pressures and selection of soft material for the application, and defects in the sealing joint for instance leakages thanks to the selection of a hard material placed in a groove with a poor surface finish, further elongation because of a wrong assembly and bad selection of material (11).

The material is selected primarily based on the resistance to the fluid, temperature, and pressure, that is why, before analyzing materials for the O-rings is important to know the effects that cause the main operating conditions of the process. O-rings can be used in applications where the pressure is truly high (even up to 2000 bar) after reaching these values of pressures the seal fails.

As seen before, the operating pressure is low, thus damages like nibbling or extrusion are not likely to happen in this design (10).

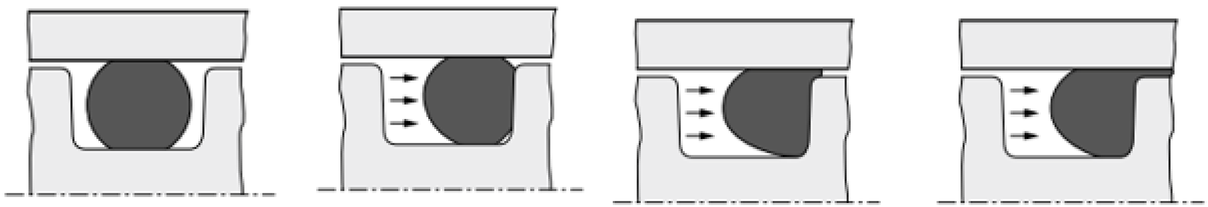

Figure 3.19 – Extrusion failure.

Temperature changes also have a big impact on the performance of the seal, a high operating temperature causes the common know effects on elastomeric materials, for instance, a rise in hardness and a drop in flexibility due to the material's aging, low temperatures causes a low rate of recovery from deformation. Even though the thermal expansion of the elastomers needs to be taken into account in the operating temperature range of the fuel cell, these values of temperatures do not make big changes in the stiffness or hardness of the material (10).

In the case of chemical compatibility, it may vary depending on the material, some are susceptible to inorganic bases, others to acids, some have good resistance to hydrocarbons, oils, and gases, thus this aspect needs to be analyzed material by material, taking into account the fluids involved in the process. As the selection of the material is quite important for the design, some materials are going to be described to analyze which ones could be applicable for the fuel cell. (10)

- *Acrylonitrile butadiene elastomer NBR*: Nitrile Rubber is one of the most used materials to fabricate O-rings thanks to its resistance to oil and greases, they have good wear resistance in comparison with other elastomers. It works perfectly in the range of temperatures present in this fuel cell (temperature resistant up to 100°C with short periods of times above this temperature.) the KOH and oxygen may cause a minor to moderate effect on this material, while they present good chemical compatibility with pure Hydrogen. The main drawback of this material is its limited resistance to weather and ozone conditions. Its hardness is 70 shore A (10).

- *Fluoroelastomer FPM/FKM*: Viton as it is commonly known has excellent resistance to high temperatures (the operating range is up to 200°C), is quite resistant to weathering conditions, in terms of chemical compatibility with the working fluids it has good resistance to the potassium hydroxide and the others fluids, they are not applicable in case of hot water, vapor and low temperatures. The mechanical properties to work as a sealing element are also good, due to its low compression set and excellent aging characteristics. Its hardness is 75 shore A (10).

- *EPDM rubber*: These elastomers work properly under weathering applications are resistant to ozone, hot water, and steam, but are not resistant to oil products like greases, oils, and fuels. In general, they have good mechanical properties (Compression set resistance, heat stability). Its hardness ranges between 70-80 shore A (10).

There are many other elastomeric materials used to manufacture O-rings such as SBR, TPU, FFKM, silicone rubbers (LSR, MQ, VMQ), etc. each of them with specific properties, but the previous three materials are those most suitable for this application.

3.2.4.3 Relation between a proper seal and the surface finish

Is important to make some comments about this aspect before choosing the material, because the roughness of the groove where is held the O-ring, is another parameter that determines what kind of material should be the most suitable for this application. The average surface roughness (Ra) is defined by the mean value between peaks and valleys of a surface, the lower this value, the smoother is the surface. When it comes to sealing, these valleys are like tiny gaps in which the fluid could go through, especially in polymer-based seals (11).

An O-ring material in a groove should fill out as much as possible the surrounding empty spaces to create the perfect seal, based on that, a perfect surface would not have these micro gaps mentioned before and the O-ring would not have problems filling most of the volume (for an intermediate soft material), but this is an ideal case, always there is a level of roughness in any surface, and even more if the groove is used as machined (i.e without any other post-machining process), in this case, the O-ring material must fill the empties even in the valleys to create the seal, difficult task for hard polymer materials (for instance PTFE), due to their inability to flow to all spaces, thus, an important fact to have into account is that the rougher the surface, the softer the material must be to guarantee the maximum flow into the cavities as possible (11).

Special attention must be taken to this, it does not mean that a super soft O-ring material is the best option in case of poor surface finish, it must be also taken into account the pressures involved in the process and the tightening torque exerted in the bolts because super soft materials present the risk of failing by extrusion, thus the idea is to have a balance between hardness and pressure resistance. The ideal surface finish depends on the fluid to be sealed, knowing that a zero-leak joint is impossible to obtain, in Table 3.13 is shown the required surface finish for a certain type of fluid (11).

Table 3.13 – Surface finish for different gases

Application	Surface finish
Helium Gas Hydrogen Gas	0.08 to 0.25 μm

Air Nitrogen Gas Argon Natural Gas Fuel	0.08 to 0.3 µm
Water Hydraulic Oil Crude Oil Sealants	0.08 to 0.4 µm

(12)But one thing that is important to remark is that there is a limitation in the minimum surface finish obtainable according to each type of machining process, in this point, there is uncertainty when it comes to knowing the surface finish of the Teflon which is the material used for the HSE after the machining process because even though there are values of approximate surface finishes for different machining processes, these values are given for metals and not for polymers, thus measuring this roughness in such little grooves is a hard task, therefore will be taken as an assumption a roughness similar to that one obtained with metal under the same machining process and this will be compensated using a soft O-ring material. Table 3.14shows some values for the surface roughness for metals after several machining processes (12).

Table 3.14

Process	Surface roughness (Ra)
Milling	6.3 to 0.8 µm (250-32 µin)
Turning	6.3 to 0.4 µm (250-16 µin)
sawing	25 to 1.6 µm (1000-63 µin)
Drilling	6.3 to 1.6 µm (250-63 µin)

A critical aspect is the presence of a very light gas which is hydrogen, which theoretically for a compliable seal needs a roughness value as much as 0.25 µm in its respective groove, and as the best achievable roughness in the case of the milling process, possibly will be above 0.8 μm, then the idea is to use a material with a hardness non higher than 80 shore A (to ensure an acceptable flow in all the volume) but non lower than 55 shore A (to avoid rapid failure for extrusion).

The selected material for the O-rings is Viton, even though it is not the softest material, it presents a good balance between chemical compatibility, temperature operating range, and pressure resistance, anyways this is under a trial period because it is not the softest available and compatible material to this application, after tests if the leakages are not considerable, this will be the final material.

3.2.4.4 Types of grooves and selection

The shape of the groove depends mostly on the type of O-ring and the manufacturing method, in general, the volume of this channel is 25% higher than the volume occupied by the undeformed O-ring, this is to account for the increase in volume due to thermal expansion and also thinking about the possibility of swallowing (increase in volume due to reaction after the contact with the fluid) (10).

The most used types of grooves are:

- *Rectangular:* The most used grooves, usually with an angle of 5° in its walls for manufacturing reasons. Depending on the side where the pressure is applied, the O-ring is going to be laid, as a general rule it goes laid on the furthest wall opposite to the pressure (internal or external pressure). (10)
- *Dovetail:* These grooves are used in applications where the O-ring must be kept tight to the groove, this type of arrangement exerts slight stress on the sealing elements. (10)
- *Triangular:* Usually used at the corners of an assembly, not suitable for small O-rings (diameters lower than 3 mm), also the O-ring is forced to keep a permanent deformed shape that may shorten its life. (10)

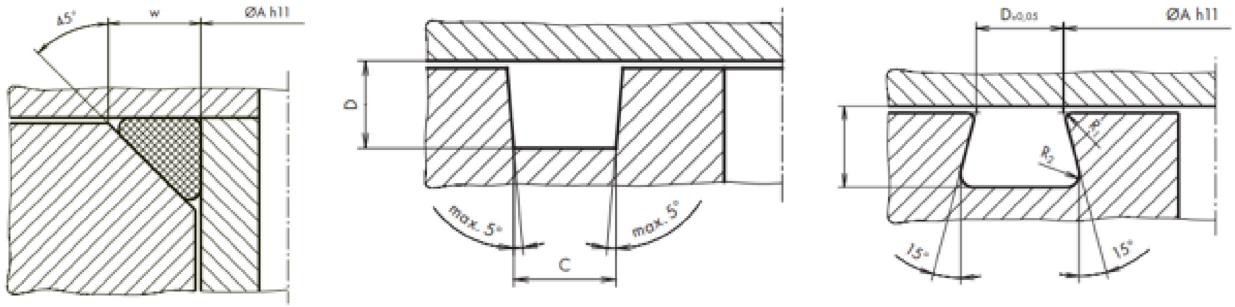

Figure 3.20 - triangular, rectangular and dovetail groove

As is needed to assembly several elements on both sides of the HSE the is needed a groove with the capacity of keeping in their places the O-rings, this is why the dovetail groove is chosen.

3.2.4.5 Assembly parameters

Several physical and geometrical parameters need to be taken into account in the design of the sealing joint, those parameters are defined under certain ranges to guarantee a proper joint. After selecting the dimensions of the O-ring, each one of these parameters is compared with values given by the standards to evaluate the joint. These parameters are defined as follows.

O-ring Stretch/Elongation

Increase of length as a percentage of the initial length equation (3.20), this property gives an estimation about how much deformation is tolerated during the assembly of the o-ring. The smaller the diameter of the O-ring, the more important is the deformation. A notable change in elongation after exposure to fluid is an indication of deterioration of the material. If the reduction is more than 2-3% then this reduction in the cross-section diameter must be compensated by reducing the depth at which it is located to avoid leakages (11).

$$stretch = \frac{ID_{gland} - ID_{ring}}{ID_{ring}} * 100 \tag{3.20}$$

O-ring Gland fil:

How much the O-ring fills the volume after compression, it is expressed as a filling ratio which is usually between 75-90% (11).

$$Gland\ fill = \frac{V_{o-ring}}{V_{gland}} * 100 \tag{3.21}$$

Ring squeeze compression:

This is the amount of deformation that the O-ring undergoes in the percentage of the O-ring diameter, in terms of the gland depth. For flat walls, it is about 25%. (11)

$$Compression = \frac{d_0 - G}{d_0} * 100 \tag{3.22}$$

Compression force:

This is an important parameter, helpful to know what is the force needed to reach the desired deformation and closure of the surfaces, this force is a function of the cross-section diameter, the percentage of compression, and hardness, some manufacturers supply a condensed diagram obtained from the standards where the data exhibited is collected after several tests. Diagram X shows the tables for two different manufacturers (11), (10).

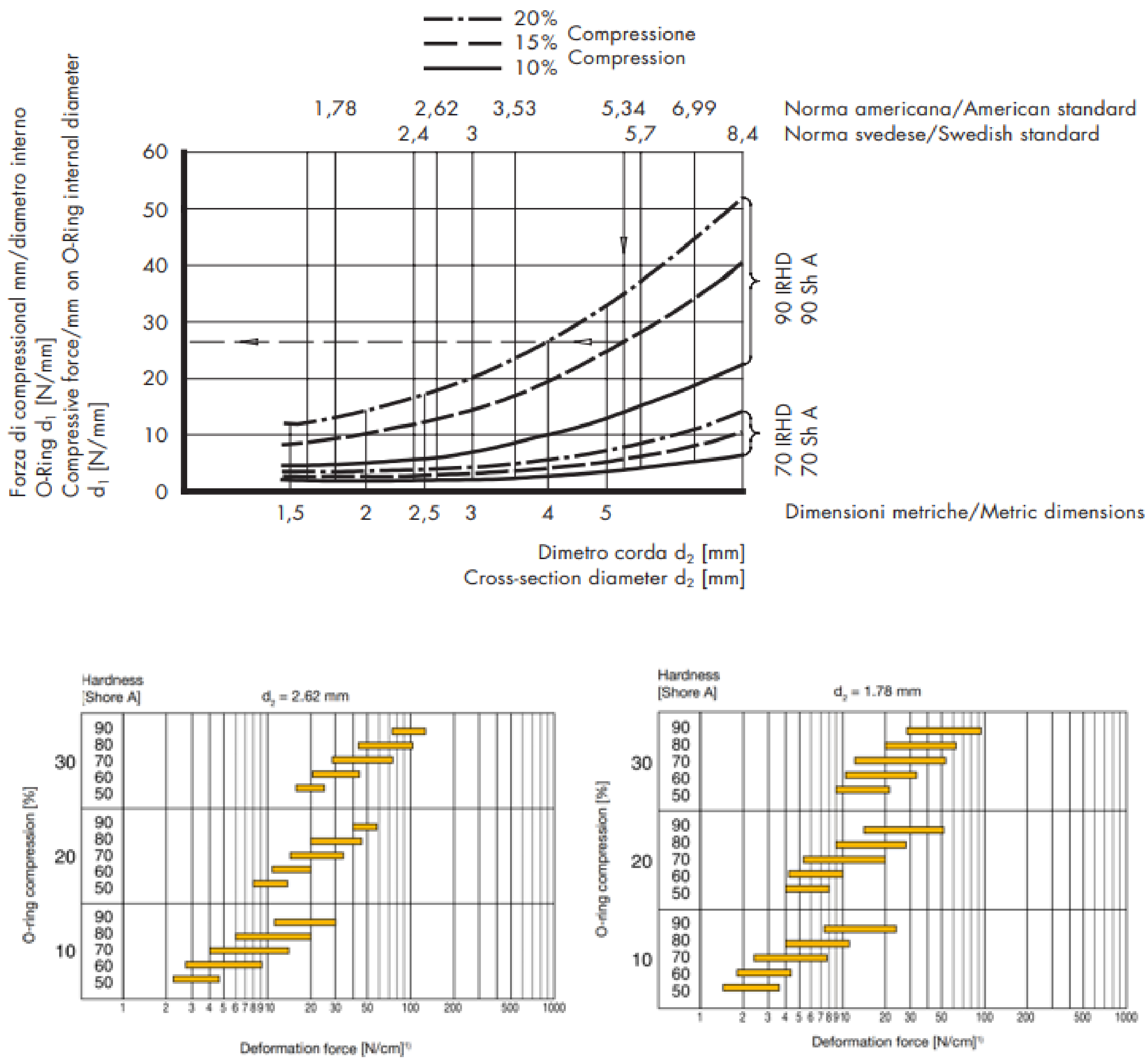

Figure 3.21 – O-ring compression, for a given hardness and diameter. (10), (11)

The process to find the required force is (11):

1. Establish the O-ring cross-sectional diameter.
2. Find material hardness.
3. Establish the internal diameter.
4. Find the design compression of the O-ring.
5. Use the force chart in which is given the force per unit of length for a specific diameter, hardness, and compression.

6. Multiply this force per unit of length by the internal diameter.

Gland clearance gap:

A big clearance can facilitate the failure for extrusion (13).

Gland sharp corners:

If the corners of the groove are not rounded may damage the O-ring during mounting (13).

Gland surface finish:

Important parameter discussed previously to determine the most suitable hardness of the material (13).

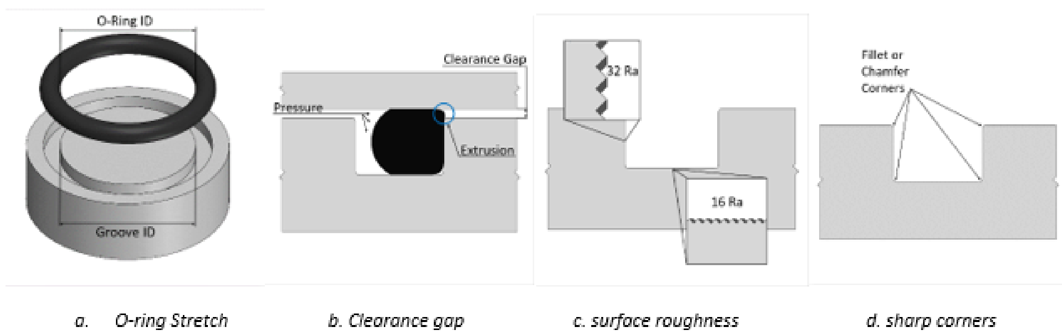

Figure 3.22 – other failure modes (13).

3.2.4.6 Dimensions and results

The final assembly will have four different O-rings, O-ring1, O-ring2, O-ring3, and O-ring4 the assembly parameters, features, and all properties described above, are summarized for each one from Table 3.15 to Table 3.18.

O-ring1:

- This is the O-ring to contains the KOH from going outside the fuel cell.
- In the case of this sealing that has a non-circular shape, is taken an equivalent diameter based on the total length, for both, internal and external diameter.

Table 3.15

O-ring1		
Material	*Viton*	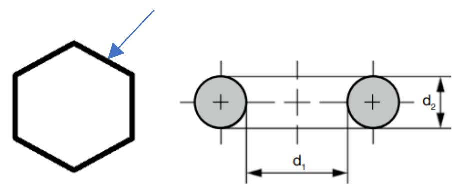
Hardness	*75 shore A*	
Cross-section diameter d_2	*2.62 mm*	
length	*760 mm*	
Eq. Internal diameter d_1	*239.3 mm*	
Eq. External diameter	*244.5 mm*	
Design compression	*20%*	
Deformation force	*2 to 3.5 N/mm*	
Effective force	*432 to 756 N*	
Groove		
Type of groove	*Dovetail*	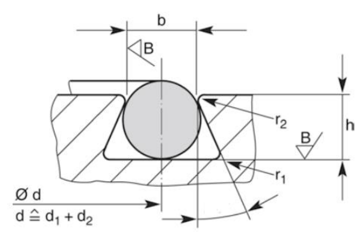
width	*2.3 mm*	
Depth h	*2.05 mm*	
Gland mean diameter d	*246.4 mm*	
r_1	*0.8 mm*	
r_2	*0.3 mm*	
Angle	*15°*	
Stretch	*2%*	

<u>O-ring2</u>

- This is the little O-ring placed at the interfaces of the holes through which all the fluid passes, their function is to avoid the fluid going into the wrong chamber.

- For this O-ring, the groove is not conventional, because it doesn't have two walls as usually, in the internal diameter it is in full contact with the fluid, this sealing joint could be approximated to a triangular joint.

Table 3.16

O-ring2		
Material	*Viton*	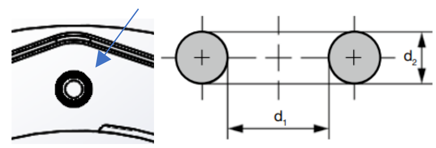
Hardness	*75 shore A*	
Cross-section diameter d_2	*1.78 mm*	
Internal diameter d_1	*6.75 mm*	
External diameter	*10.31 mm*	
Design compression	20%	
Compression force	*0.9 to 2 N/mm*	
Effective force	*6.075 to 13.5 N*	
Groove		
Type of groove	*Rectangular - Triangular*	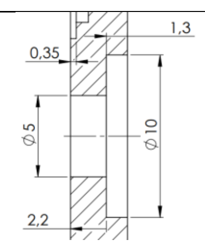
Depth h	*1.3 mm*	
Gland mean diameter d	10 mm	
Stretch	3%	

<u>*O-ring3:*</u>

- This is the O-ring that prevents the mixing of the reactants outside of the electrodes.

Table 3.17

O-ring3		
Material	*Viton*	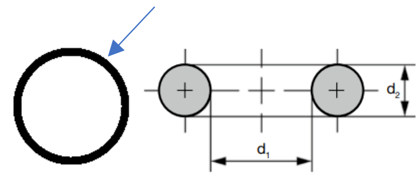
Hardness	*75 shore A*	
Cross-section diameter d_2	*2.62 mm*	
Internal diameter d_1	*164.77 mm*	
External diameter	*170.01 mm*	
Design compression	*20%*	
Compression force	*2 to 3.5 N/mm*	
Effective force	*329.54 to 576.69 N*	
Groove		
Type of groove	*Triangular*	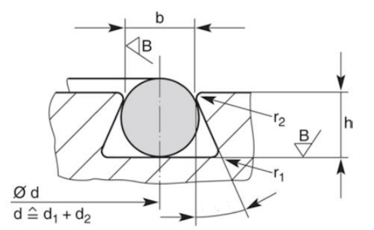
Width b	*2.3 mm*	
Depth h	*2.05 mm*	
Gland mean diameter d	*172 mm*	
r_1	*0.8 mm*	
r_2	*0.3 mm*	
Angle	*15°*	
Stretch	*3%*	

<u>*O-ring4:*</u>

- This is the O-ring at the inlets ports of the flange and of the insulating plates.

Table 3.18

O-ring4		
Material	*Viton*	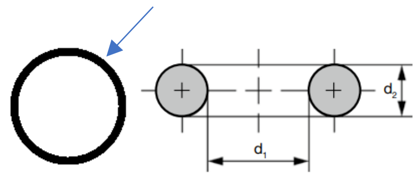
Hardness	*75 shore A*	
Cross-section diameter d_2	*1.78 mm*	
Internal diameter d_1	*20.35 mm*	
External diameter	*23.91 mm*	
Design compression	*20%*	
Compression force	*0.9 to 2 N/mm*	
Effective force	*18.3 to 40.7 N*	
Groove		
Type of groove	*Rectangular - Triangular*	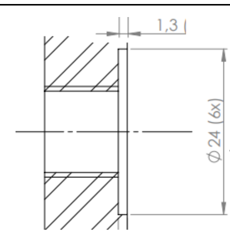
Depth h	*1.3 mm*	
Gland mean diameter d	*24 mm*	
Stretch	*3%*	

3.2.5 Clamping force for the closure of the stack

As there are different materials along the longitudinal direction of the stack, the force distribution may vary from layer to layer, moreover, each O-ring needs its compressive force, thus an important question that comes out is how much clamping force must be supplied to the stack to have a proper closure of the cell without a big impact on the performance? In other words, supplying the required force to press the sealing elements and avoid leakages, reducing the contact resistance between the surfaces of the layers, allowing the mass transport through the membrane electrode assembly (MEA), and finally the capability of the bolt to handle the loads involved. This section describes the design of the joint and the considerations taken to find the optimal clamping force.

3.2.5.1 Required clamping force

As a first step is analyzed the total force needed for the closure of the stack. This is done employing a spring model which represents each one of the sealing elements, where those that are in the same plane are going to be in parallel and the connection between layers will be taken as springs connected in series. As the compression force is already known for each type of O-ring, now the model can be applied. For a layer containing different sealing elements, i.e a parallel arrangement, the total force to compress all the sealing elements is the summation of all the forces needed to compress each one. While for different layers, i.e series arrangement, the load is the same for all the layers, what change is the amount of compression reached in each layer, this is why will be taken the maximum compression force found between all layers. Figure 2.1 depicts the Spring-model.

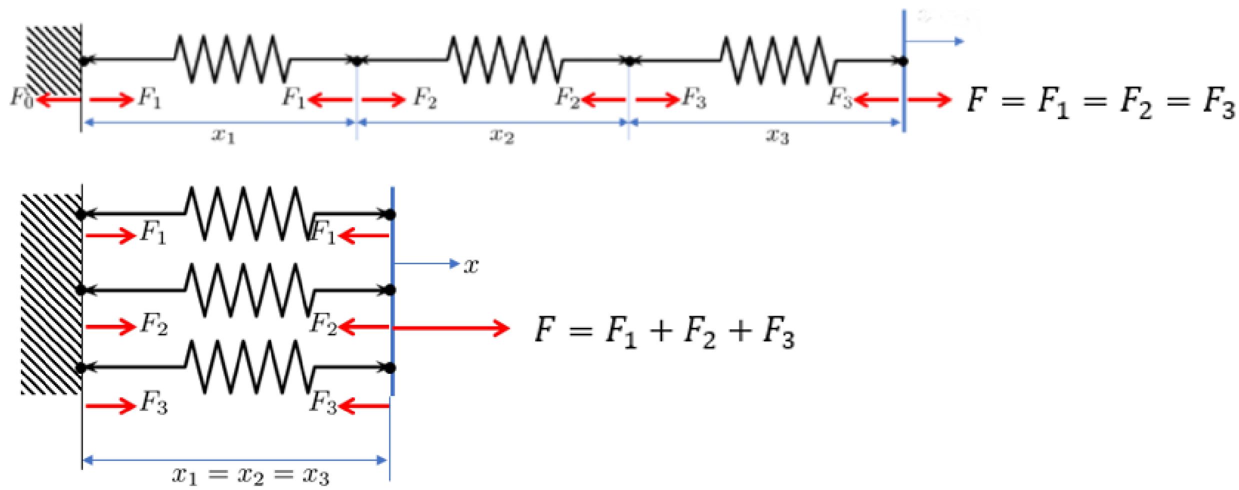

Figure 3.23 – Loads for a set of springs.

To develop the computation of the total load first off is needed the type and amount of sealing elements in each specific layer, taking into account that there are 15 mono-cells in the stack and there are 5 fundamental interfaces with sealings at the boundaries Figure 3.24, the computation can be done by analyzing the forces in each of these boundaries and then can be taken the maximum force value.

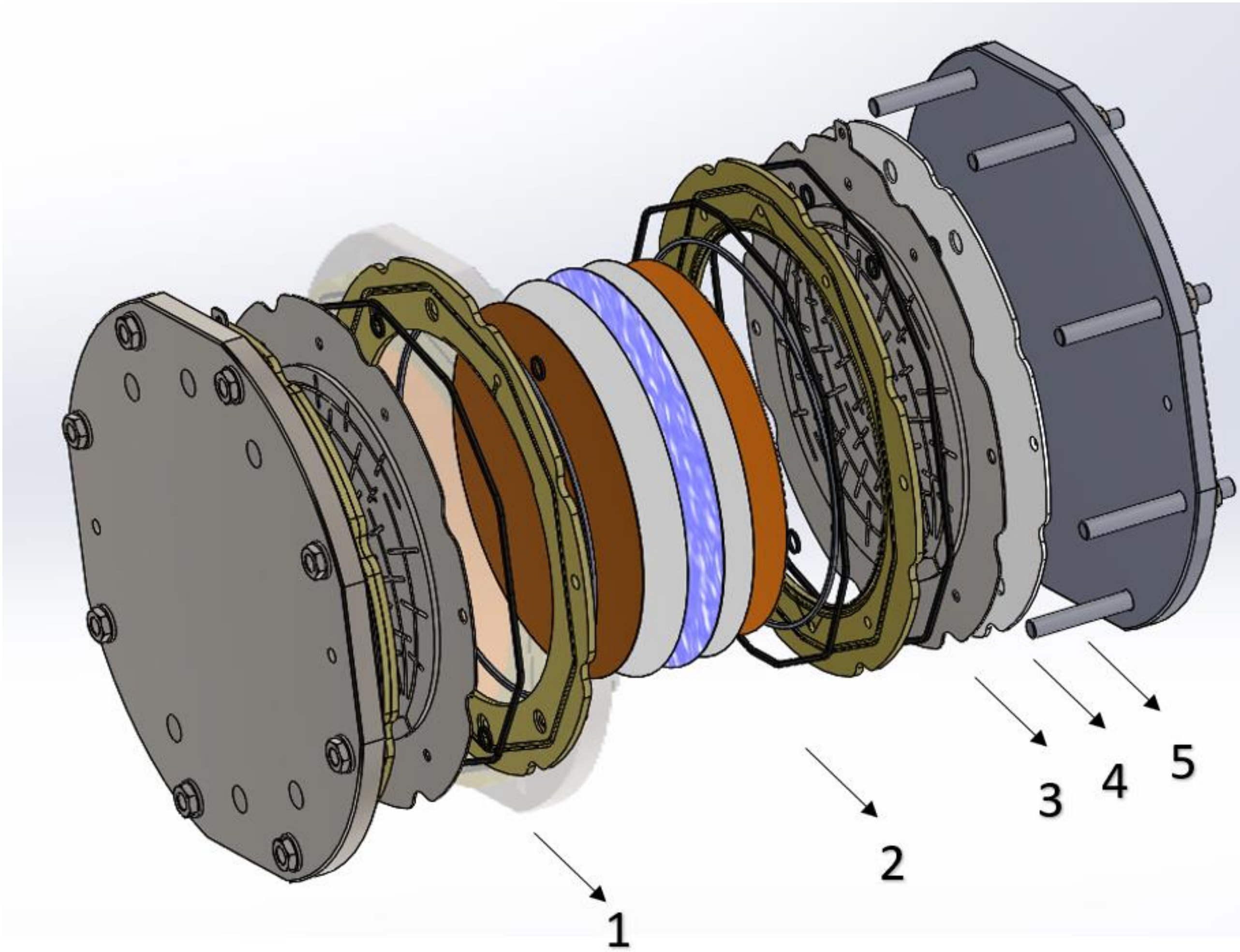

Figure 3.24 – O-rings in each cell.

Table 3.19 - Number of O-rings for each layer.

Layer number	O-ring type and quantity				total force [N]
	O-ring1	O-ring2	O-ring3	O-ring4	
1	1	4	0	0	810
2	1	4	1	0	1386,69
3	1	4	0	0	810
4	0	6	0	0	81
5	0	0	0	6	244.2

Therefore the required force only for the deformation of the O-rings is 1386.7 N. The actual force to create the properly sealed joint is going to be a little bit higher than that one found, because the elasticity of the internal parts is not taken into account, due to this uncertainty will be taken 20%

more of the found force then the force is 1664 N.

3.2.5.2 Maximum force in the bolt

From the company's stock is selected a stainless steel bolt A2-70 which UTS is 700 MPa and the yielding stress is 450 MPa the nominal thread is M8, thus the geometrical features of this bolt are shown in Table 3.20 – Bolt features.

Table 3.20 – Bolt features.

Bolt size	Pitch [mm]	Pitch diameter [mm]	Stress cross section [mm²]	Cross section at minor diameter [mm²]
	P	D_2	A_s	A_{d3}
M8	1.25	7.188	36.6	32.84

For a value of μG= μK = 0.08 for the thread and head friction, the maximum load before yielding that can be exerted on the bolt is **$F_{M,max}$= 13930 N** found with the equation (3.23) that takes into account the axial and torsional effects. For a flange with 8 bolts can be noticed that the force in each bolt due to the compression of the O-rings is **208 N** which is much lower in comparison to the value it can resist.

$$F_{M,max} = \frac{0.9 * R_{p0,2} * A_s}{\sqrt{1+3k^2}} \quad where \quad k = \frac{3}{d_0} * (0.16P + 0.58 d_2 \mu_G) \tag{3.23}$$

The DIN standard proposes a procedure to compute a bolted joint using the joint diagram Figure 3.25 – Tigtheting load and part stiffness according to the DIN standard . where are represented the stiffnesses of the part and bolt to determine when the joint will be overloaded or untightened, the effects of different types of forces on the joint, and the deformation for both, bolt and part? The process establishes an approximated zone that delimits the presence of the stresses and deformation Figure 3.25 this is called the stress or deformation cone. To analyze this diagram the bolt usually is preloaded at a force that makes it very close to its yielding stress, but as the total force needed for the fuel cell is quite lower, is not necessary to carry out this analysis, is more interesting to study what happens to the performance of the fuel cell as the clamping force increases, as there is a wide range of possible compression force (14).

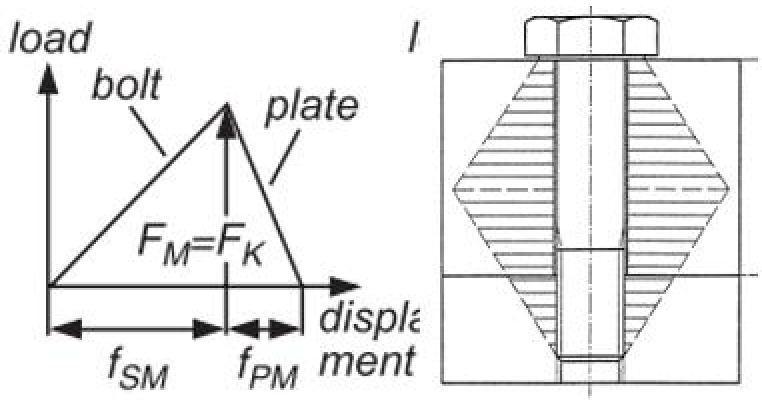

Figure 3.25 – Tigtheting load and part stiffness according to the DIN standard (14).

3.2.5.3 Effects of excess in the clamping force on the performance.

Intuitively could be thought that if the stack is clamped or compressed as much as possible it is beneficial to the performance of the fuel cell, but special attention must be taken in this because it could be useful for some aspects but prejudicial for others. The three parameters most affected by the clamped force are contact resistance, mass transport, and conductivity (7).

The *Contact resistance* is the resistance to the current flow when two surfaces are connected, this is more severe when the two materials connected have very different physical properties, which is the case of the gas diffusion layer and the bipolar plates (a hard material connected with soft and porous material), one way to reduce the contact resistance is increasing the compression force, this would cause an easier flow of current, thus in this case increasing the clamping force would be beneficial to the performance of the fuel cell (15).

The GDL must be porous to allow the triple-phase boundary (the mix of gas, electrolyte, and the electrode), this means that higher clamping force reduces porosity, this reduces the mass transport capability of the system, and as consequence, the three-phase mixture is affected, then the performance of the fuel cell is affected, therefore the excess in clamping force, in this case, is a problem. Then there is an optimal point for the fuel cell, where the clamping force is big enough to reduce contact resistance but not that big to allow mass transport but it is analyzed by tests after construction (15)

Polarization curve

To analyze the effect of tightening torque and all the parameters discussed previously is used the polarization curve Figure 3.26 – Polarization curve., which is a curve that shows the voltage output for a given current density and is widely used to test fuel cells, may work as a troubleshooting tool, to find in what aspects the cell is failing. It has three regions where the voltage drops, which are the open circuit loss due to fuel crossover, the activation losses (also called ohmic polarization, thanks to the electrical resistance of each component), and mass transport losses (can be evidenced by the drop in concentration of the reactants or just by a limited flow of them). Then this test should be carried out after construction to find the correct tightening torque (7).

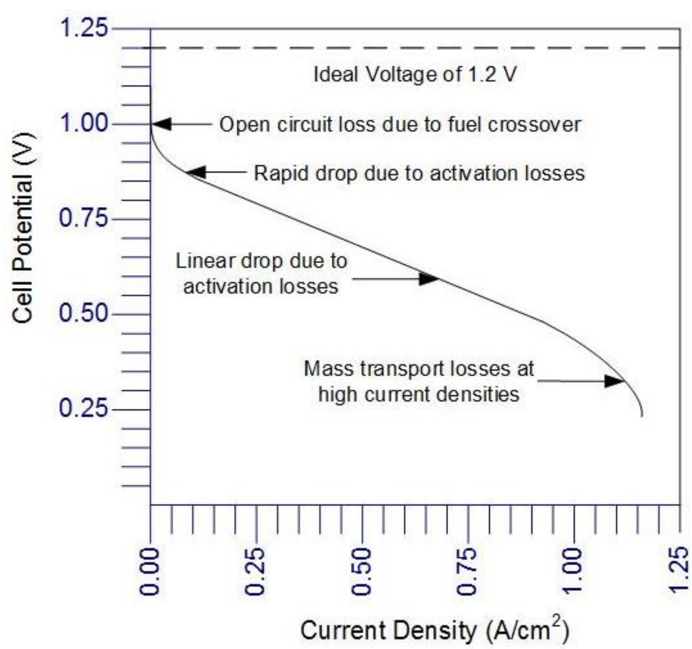

Figure 3.26 – Polarization curve.

3.3 Stack's layout and prototyping

One of the main challenges of this project is to create a functional fuel cell with chamber's thicknesses quite small, thus a proper setup of the different elements inside the stack and very accurate geometrical features are needed to develop the design. Even though there is freedom in the design, there are three initial parameters for the design of the stack:

- The entire system must be contained inside a circular area of diameter 300 mm.
- The maximum thickness for the electrolyte chamber is 0.5 mm
- The required power output is 300W (This is what determinates the number of cells that compound the stack).

This section describes the design procedure for each element of the fuel cell and how the stack is composed.

3.3.1 Main components

As a first step, is important to describe each component necessary for the design of the fuel cell, is known that the bipolar plate that serves as a distributor for the gas, must be in physical contact with the electrode and a catalyzer to increase the speed of the reaction, at the same time the electrode must be in contact with the electrolyte but the reactant gases cannot mix, i.e the must be separated such that the movement of ions is allowed. To reach this, special components are used, such as an Anionic Exchange Membrane that only conducts ions and is impermeable to the reactant gases, a nickel catalyzer that apart from being the electrode also helps to react in less time, and other components that will be described as follows.

3.3.1.1 Membrane Electrode Assembly

This element is the main component of the fuel cell because it is where all the reactions take place. It is composed of two electrode-catalyzer, two Anionic Exchange Membranes, an Electrolyte Distributor placed in the middle, and they are put together by a frame that is going to be called the Housing of Sealing Elements. At the anode is supplied the hydrogen and at the cathode the oxygen, the gas makes contact with the catalyzer, and the electrolyte inside the electrode, creating a three-phase contact, It is called three-phase because it has the contact between the electrolyte (liquid), the reactant either hydrogen or oxygen (gas), and the electrode (solid). Once reached the activation energy, the anionic membrane allows the conduction of the ions and avoids the mixing of the reactants, such that the electrolyte is in all three chambers but the gases always are in their respective space. Thus the MEA is composed by:

- *Nickel catalyzer:* It is placed at the anode, and accelerates the reactions that involve hydrogen

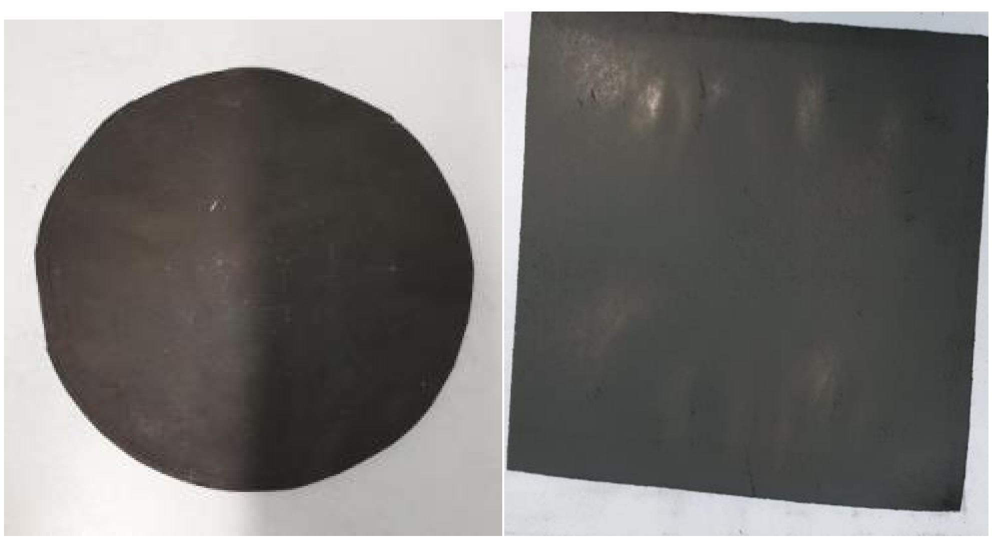

Figure 3.27 – Nickel electrode.

- *Catalyzer for the oxygen:* oxygen-consuming electrode made of siflon (silver) on nickel foam.

Figure 3.28 – Electrode with silver manganese oxide as a catalyst.

- *Electrolyte Distributor:* It is a simple membrane weaved that facilitates the dispersal of the liquid throughout the chamber.
- *Anionic exchange membrane:* It only allows cross-flow of ions.
- *The frame (Housing of sealing elements):* It puts together all the layers to create a unique group, it also allocates the sealings and has the holes for the distribution channels.

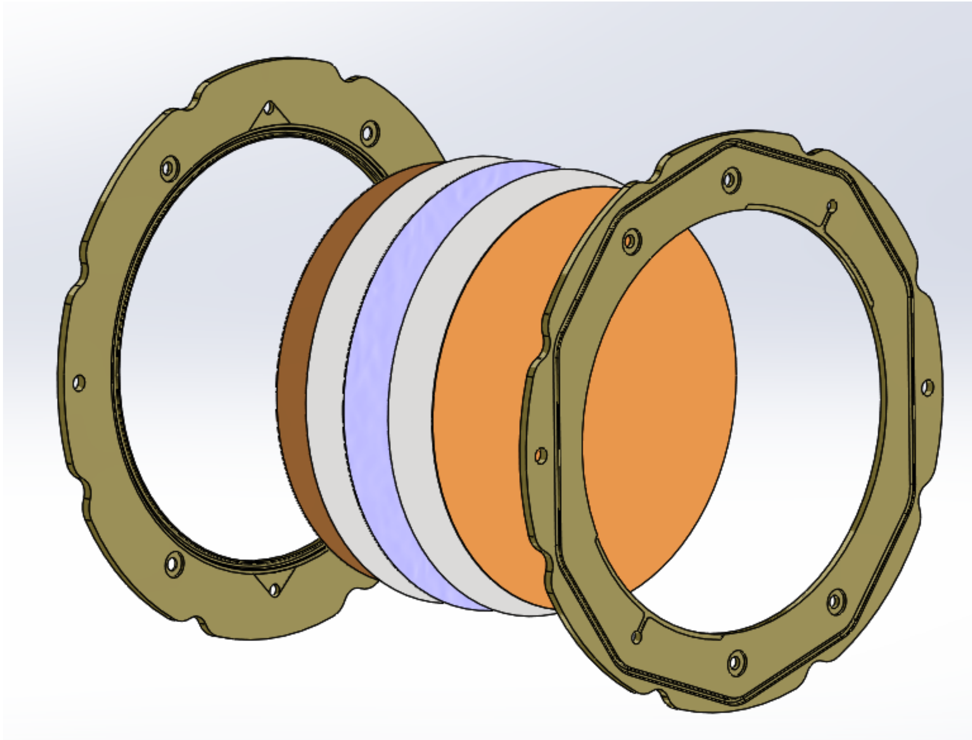

Figure 3.29 - MEA assembly

3.3.1.2 Bipolar plates

A description of the bipolar plates was given in the general overview of the fuel cells, this is a fundamental part to create the stack of fuel cells, because it connects consecutive cells, and also serves as a distributor for the gases. this component has channels machined in its surface to perform this task, as a preliminary step it was done a simulation to understand the distribution of the gas once it enters the chamber, shown In Figure 3.30, this simulation is useful mainly for two things, it gives an idea about how should be manufactured the entrance ports for each MEA group and the geometry of the channels in the bipolar plate can be constructed based on the natural flow.

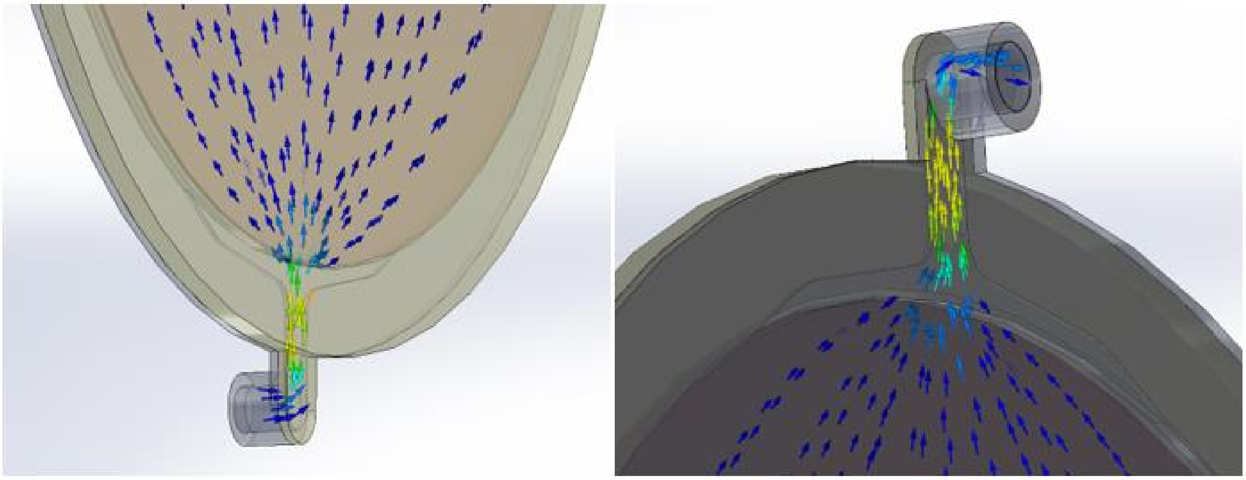

Figure 3.30 - Distribution of gas inside the chamber

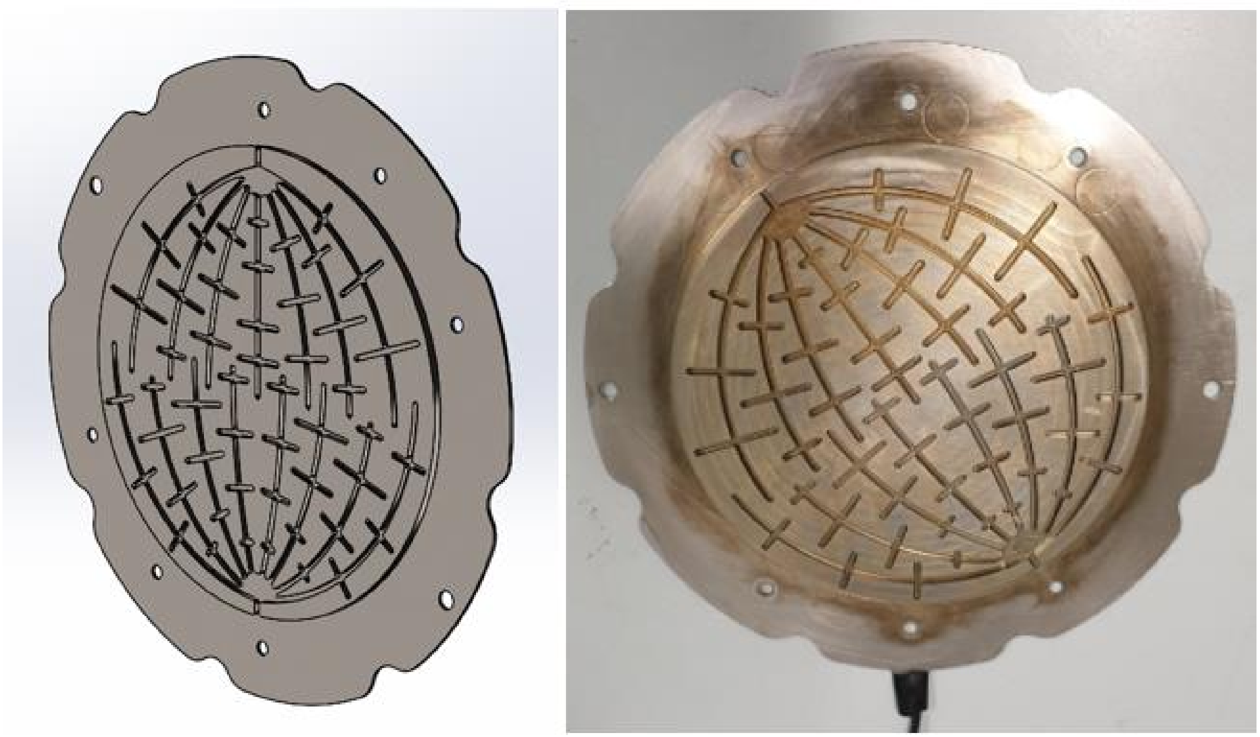

Figure 3.31 – Bipolar plate

3.3.1.3 Current collector

Even though the gas tends to expand inside the volume, channels are created to avoid pressure losses and obtain a better distribution, based on that, has been chosen a random path of channels for the bipolar plate. Figure 3.322 shows the modeled part and the manufactured part. It has been manufactured in stainless steel 316 because it offers good conductivity combined with corrosion resistance.

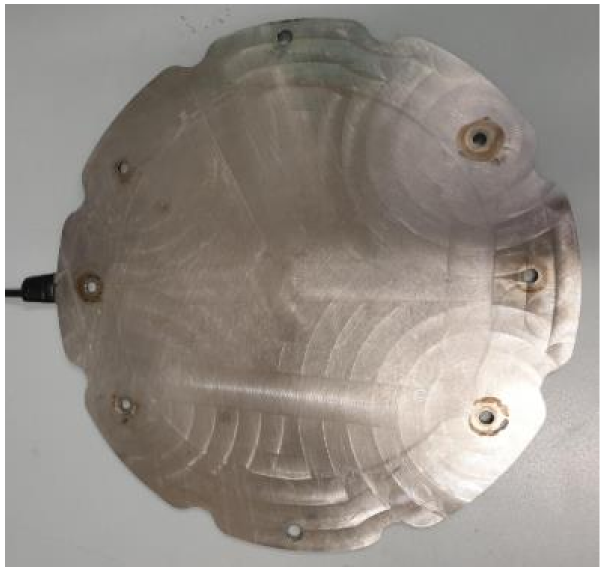

Figure 3.32 – Bipolar plates/Current collector

3.3.1.4 Closure flanges

These are the external caps that hold all the stack together, they must have several mechanical attributes, it must be highly rigid and stiff to do not bend as the pressure inside the chambers increase (this would cause an untightening of the sealing elements, increasing the probability of leakages), also to transmit uniformly the force of the bolts to all the layers without a failing rupture, and they must be corrosion-resistant because it will be in a highly aggressive environment.

To guarantee the compliance of the part, it has been carried out an FEA analysis to the flanges, where its internal face is subjected to a maximum pressure of 3 bar (taking into account that the fuel cells work between 1 to 2 bar) and based on its response, the thickness is chosen for the case in which the maximum displacement under this pressure is not bigger than 0.05 mm in the zone where the sealing elements are located. This is to assure a minimum compression of 20% for the O-rings. Figure 3.33 a). shows the simulation of the flange.

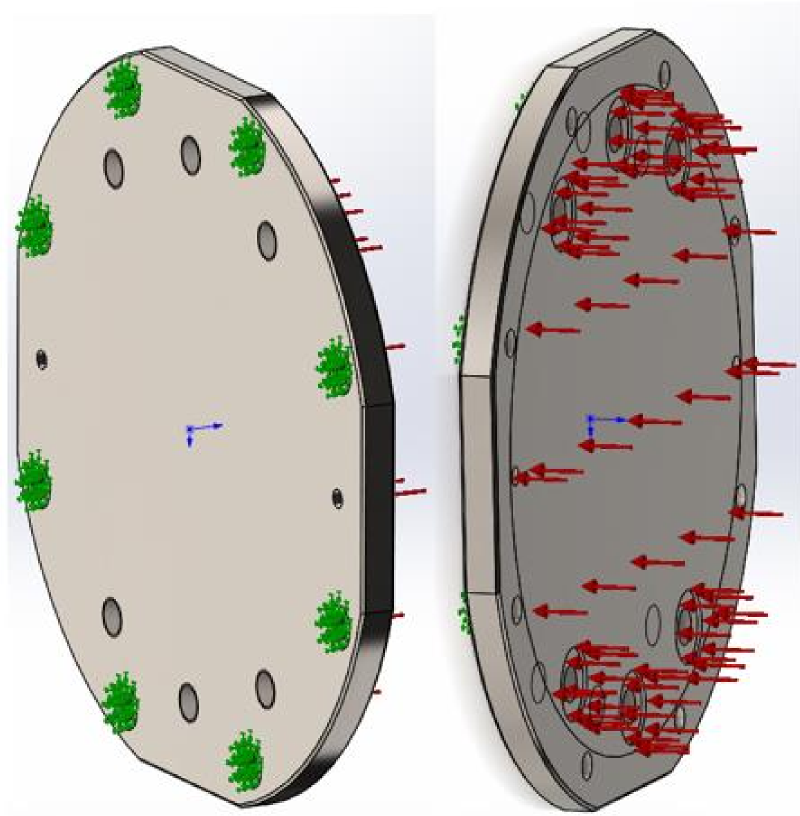

a). Study setup

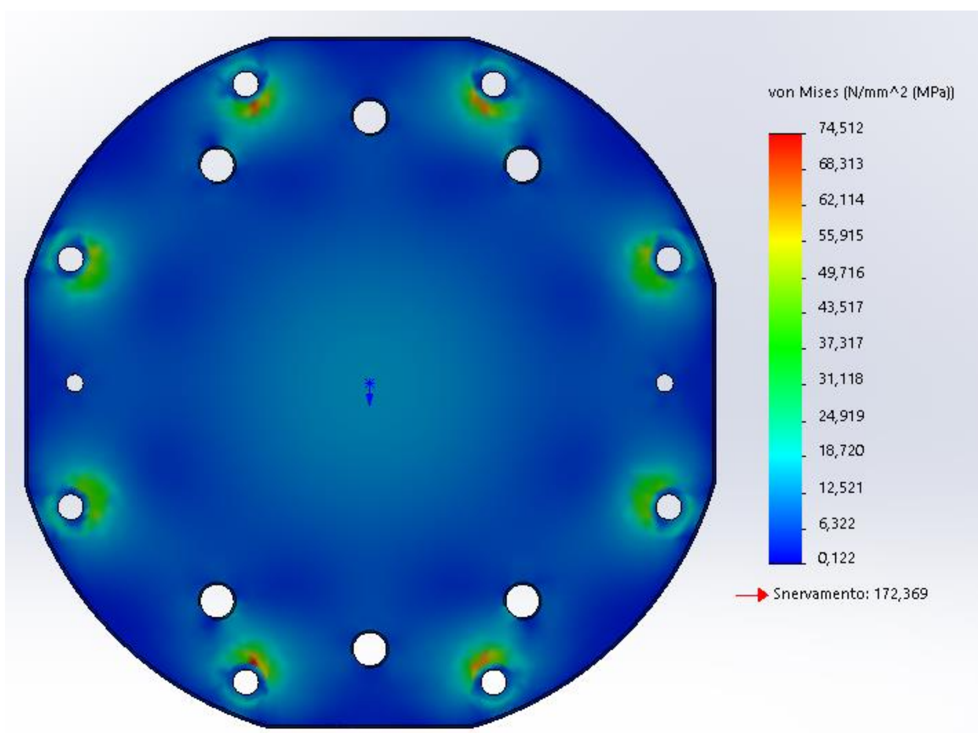

b). Stress results

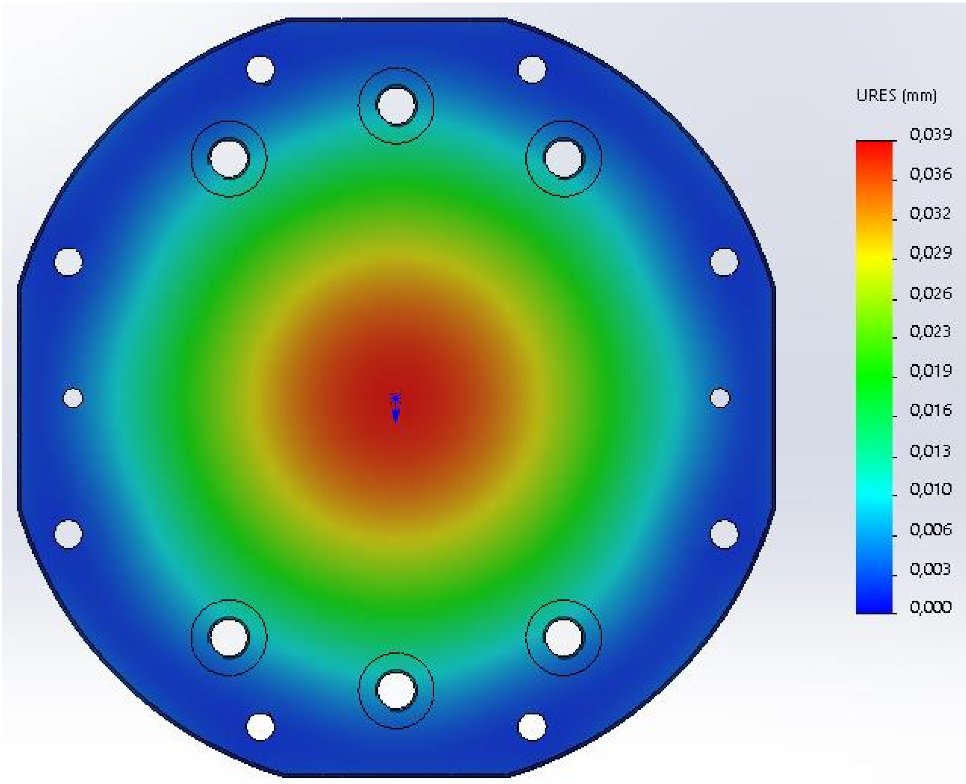

c.) Displacement results.

Figure 3.33 – Closure flange FEA study

As a result, the chosen material of the flange stainless steel 316 With a thickness of 12 mm, image x shows the part modeled and manufactured.

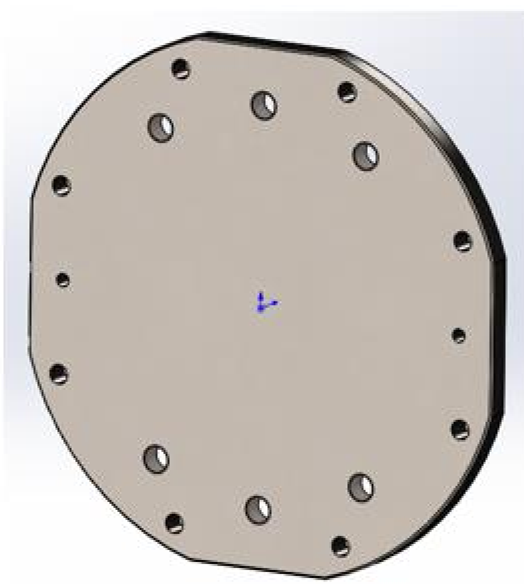

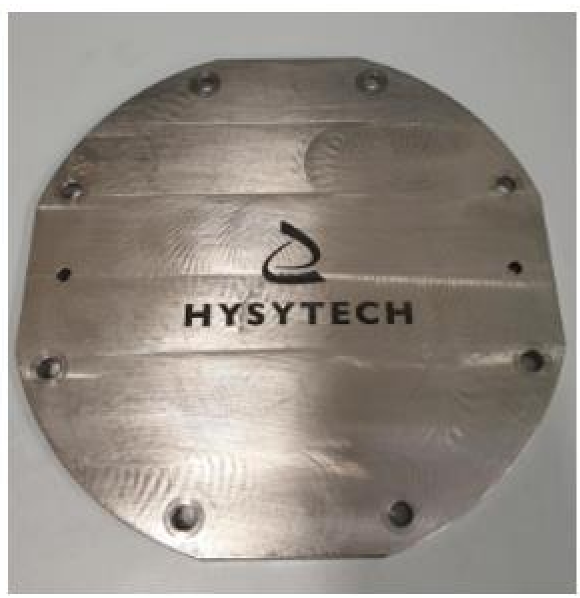

Figure 3.34 - closure flange modeled and manufactured

3.3.1.5 Distribution channels

An internal manifold distribution system is going to be employed for the fuel cell (explained in the "types of gas supply" section), the distribution channels need to have the following features:

- None of the reactant fluids can mix outside the electrode chamber.
- The entrance inside the electrodes for the hydrogen and oxygen sides must be alternated.
- Each fluid has its entrance and exit channel.
- The reactant fluids must expand as much as possible when going inside their respective chambers.

The layout of the channels was determined based on previous projects and after several iterations taking care of all the geometrical constraints and material limitations, Figure 3.35 shows a representation of the working principle of the distribution channel for a stack with three cells, this representation is only to show the paths that the different fluids must take, this is not the final result. It can be noticed that the entrance is at the bottom and the exit in the upper part, for a single cell the electrolyte enters through the middle port and the gasses at the sides, such that the fluid alternates its entrance in the proper chamber. Also is chosen a circular shape to fit in a better way the stack into the housing cylinder, this configuration has as a critical point, the sealing joint for all the holes placed in different layers, a topic that will be discussed in the sealing section.

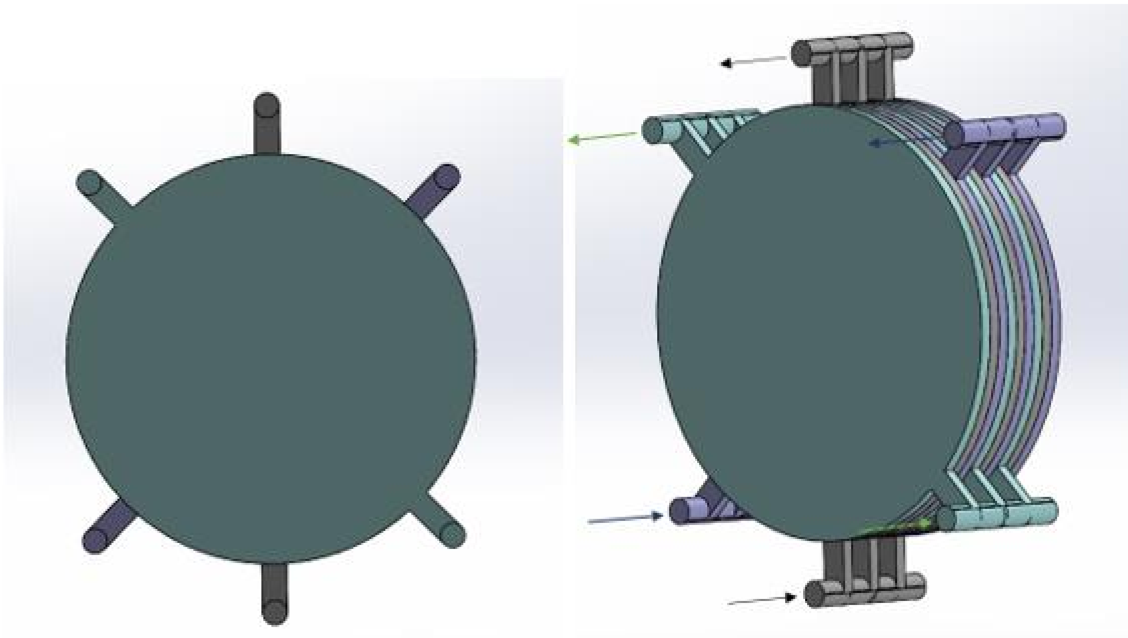

Figure 3.35 - schematic representation for the working principle of the distribution channels

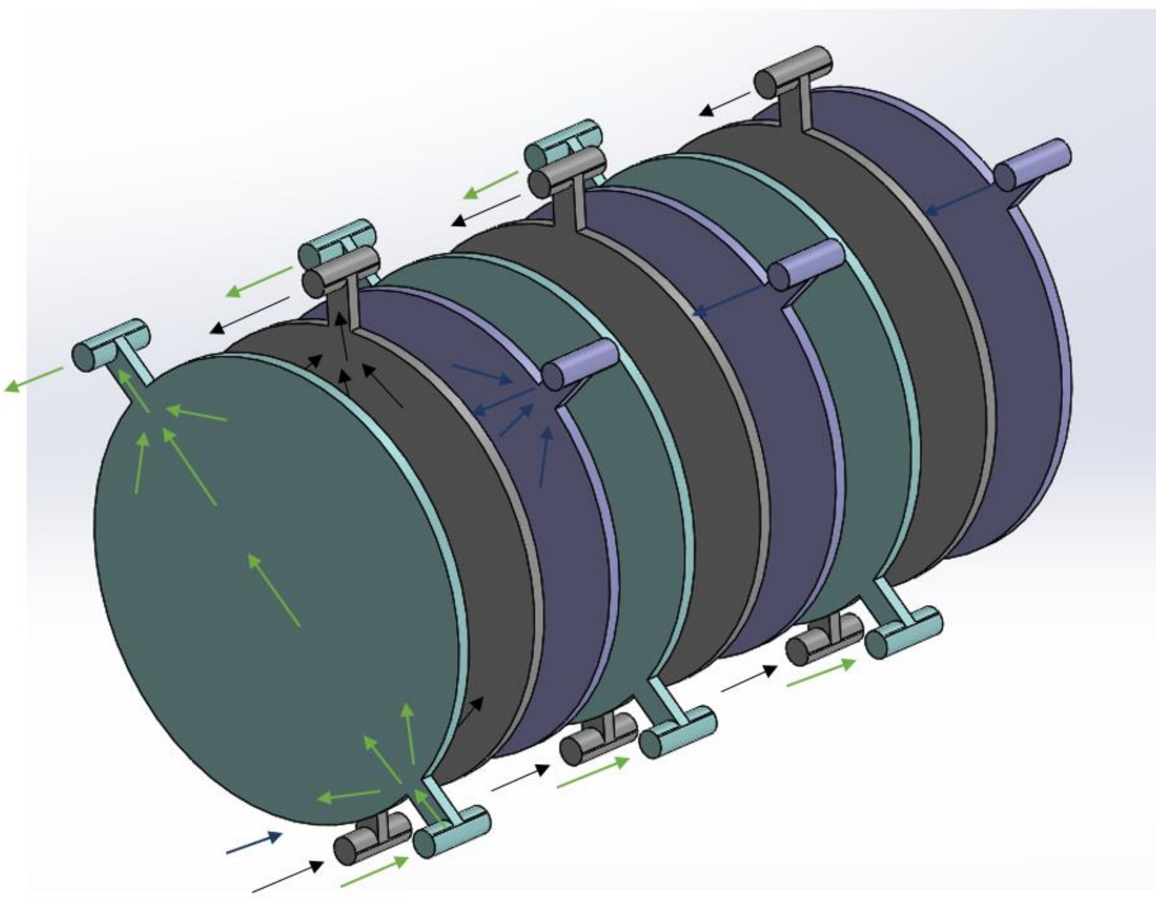

Figure 3.36 – Explousure view for the distribution channels

As is shown in Figure 3.36 the side channels are tilted 30° from the middle port, and the flow is crosswise such that if the fluid enters through the right port it leaves from the left, with this is intended to distribute the fluid as much as possible inside the chamber obtaining a good contact between gases and the electrodes.

These channels are created by making consecutive holes in each layer of the assembly, specifically on the frames that hold together the membrane electrode assembly (MEA), this frame will be defined with more geometrical detail in the section where are analyzed the sealing elements because this element also serves as a house for the O-rings and gaskets.

3.3.2 Final layout

The image x shows the final layout of the stack modeled and after manufacturing, the global parameters of the fuel cell are presented in Table 3.21 – Fuel cell dimensions and characteristics

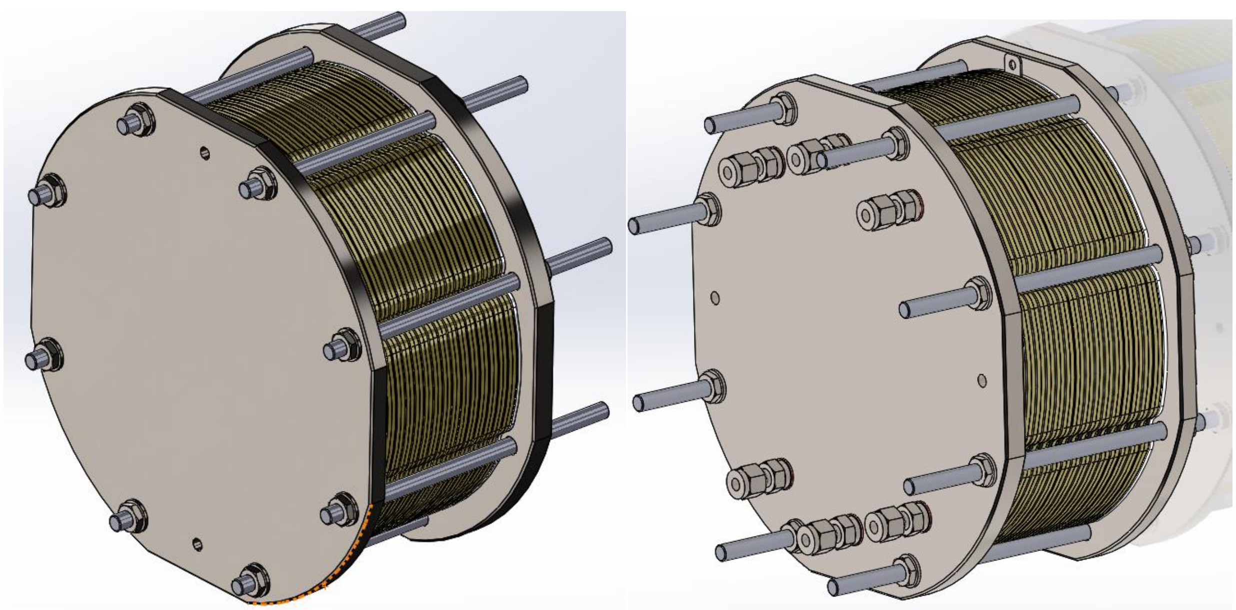

Figure 3.37– modeled stack

Table 3.21 – Fuel cell dimensions and characteristics

Alkaline fuel cell	
Dimensions	114 mm length, 250 mm diameter
Single cell thickness	8 mm
weight	12 kg aprox.
Power output	300W
Number of cells	15
Operation temperature	60-70°C
Operation pressure	1 bar

4. Power bank system

The Fuel cell by itself does not work, it needs additional subsystems to perform, therefore, this section describes the necessary external components to obtain the power bank and also some computations for its design. All this takes as a first reference the constraint in weight and volume given by the neutral buoyancy requirement and the maximum available dimensions to locate the system.

4.1 Neutral buoyancy

Stability and maneuverability are extremely important features for the performance and control of the AUV, to avoid the risks of losing the vehicle during operation. If the internal components do not have neutral buoyancy, either the weight makes it go down or the buoyancy makes it go up.

These facts would make difficult the controllability of the vehicle, that is why is established a special requirement for each subsystem of the vehicle, which is the neutral buoyancy, this means that the weight must be equals to the buoyancy force, equation (4.1).

$$F_{weight} = F_{Buoyancy} \tag{4.1}$$

Equations (4.2) and (4.3) and show the definition of each force (16).

$$F_{weight} = \rho_{system} * V_{ystem} * g \tag{4.2}$$

$$F_{Buoyancy} = \rho_{sea\,water} * V_{submerged} * g \tag{4.3}$$

Then this means that the weight of the displaced volume of water when a component is immersed must be equals to the weight of the component. Thus equation (4.4) shows the relation to obtain the maximum allowed weight (in kgf) (16).

$$M_{max} = \rho_{sea\,water} * V_{component} \tag{4.4}$$

Therefore, defining the initial dimensions for the housing, gives as result the maximum allowed weight to assure neutral buoyancy.

Another important aspect to assure stability is the location of the center of buoyancy, and its relative position with the center of mass. The center of buoyancy is the point at which the buoyancy force is applied, and this point always coincides with the centroid of the displaced volume. Wrong relative positions of these points may cause that the system to never go back to equilibrium after an external force disturbance. Figure 4.1 shows this point.

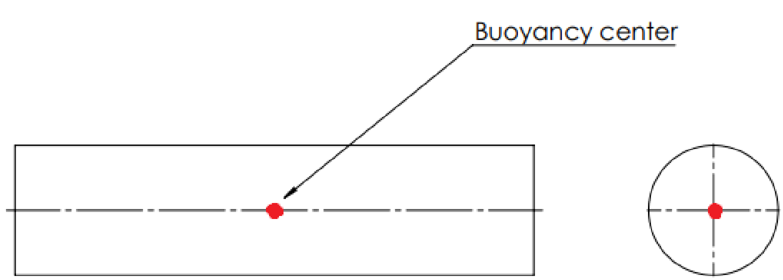

Figure 4.1 - Buoyancy center location

The center of gravity is the point at which the weight load is applied. Thus, when the component is in the water there are two forces applied to two different points, where the relative position between these points may cause instabilities due to the appearance of rotational moments. For instance, Figure 4.2 shows that the buoyancy center and the center of gravity are in different geometrical points, there is created a rotating moment due to the horizontal distance between the forces. The ideal case scenario is to have these two points coinciding in the same geometrical point, in this way there are no resultant rotational moments, and the system is stable.

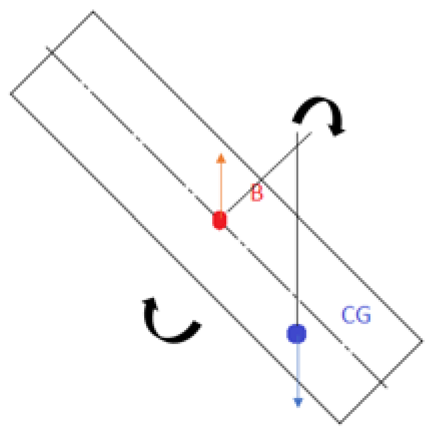

Figure 4.2- Different positions for the buoyancy center and center of gravity

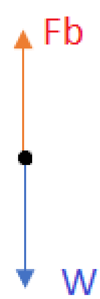

Figure 4.3- Buoyancy and weight in the same point

When is not possible to have both points coinciding, then the ideal case is to have the center of gravity in a lower position from the buoyancy center. Figure 4.2 shows the CG in a higher position than B, if an external moment is applied in the correct direction the system will begin to rotate because their relative position causes instability, while in Figure 4.3 when there is an external disturbance to the system appears a restoring moment because CG is in a lower position, and tends to stabilize the system.

a). CG above B, unstable system *b). CG below B, stable system*

Figure 4.4 - Relative positions of the center of gravity and buoyancy center.

From now are established two conditions for the layout of the system, the first one is that once the dimensions are chosen, the maximum allowed mass is fixed, and the second condition is that the layout of the power bank must be created such that the center of gravity is in the centroid of the housing (or at least very closely) or below to avoid instabilities. Then after several iterations, the selected geometry is shown in Figure 4.5. For these dimensions, the total volume is $0.084\ m^3$ therefore the maximum allowed weight found with equation (4) is 86.7 kgf

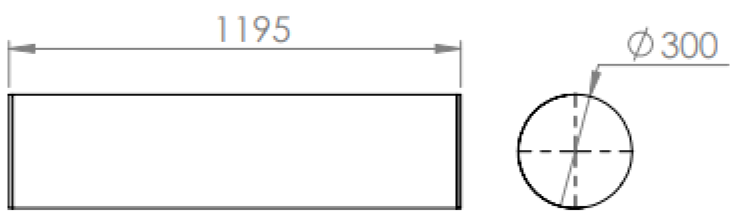

Figure 4.5

4.2 Piping and instrumentation diagram

The P&ID shows the piping, equipment, instrumentation, and control devices needed for the chemical process, for the consequent layout design of the system. With this diagram are defined the components that must be designed (modeled and simulated), to create the assembly. The total diagram will be explained by parts and consequently, the different components will be defined.

4.2.1 Reactant's entrance

Figure 4.6– P&ID reactants entranceshows all the involved components before entering the stack. Outside the system, are located the tanks that have pressurized hydrogen and oxygen connected with a valve that reduces the pressure to enter the system, the dotted line delimits the power bank, therefore these tanks are outside the system.

The first component located Inside is the reservoir for the electrolyte, which sends the KOH inside the stack employing a pump located between two valves to control the flow. The tank receives the recirculation of the non-used electrolyte and the product water and also has an outlet port to extract the merged gas in the recirculated stream.

At the sides are situated the entrance pipes for the reactant gases. The first flow control found is an electrical plunger valve that closes the entrance in case of emergency, then are placed ball valves before a recirculating line. Before entering the stack, the flow must pass for a digital flowmeter that exerts control on the mass flow. Table 4.1 shows the initial parameters for the components and the final component modeled.

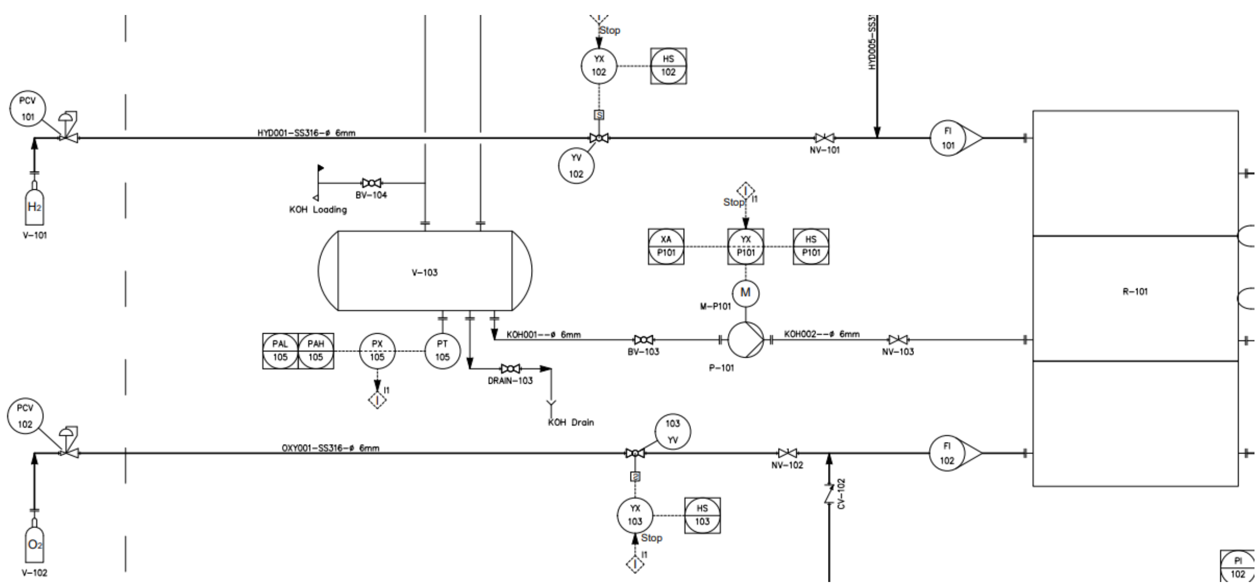

Figure 4.6– P&ID reactants entrance

Table 4.1 - Main components for the reactants entrance

Component	**Features and parameters**	**Modeled part.**
KOH Tank	• Volume=11L • Non-increasing pressure. • Chemical material compatibility with KOH. • Five ports.	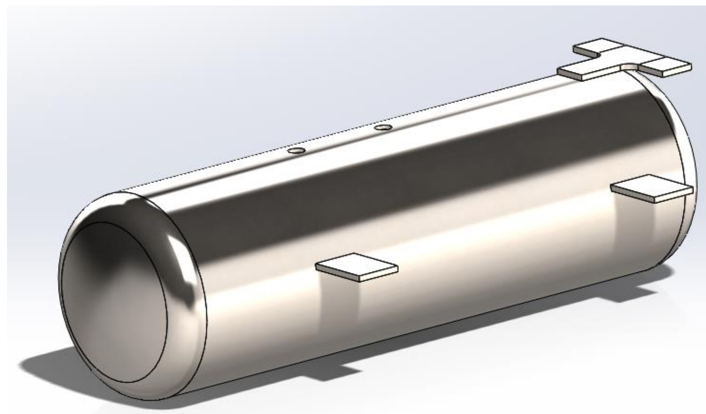
Needle valve	• Commercial valve for a 6 mm pipe	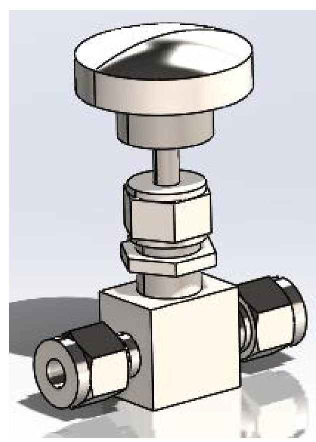

Plunge valve	• Commercial valve for a 6 mm pipe	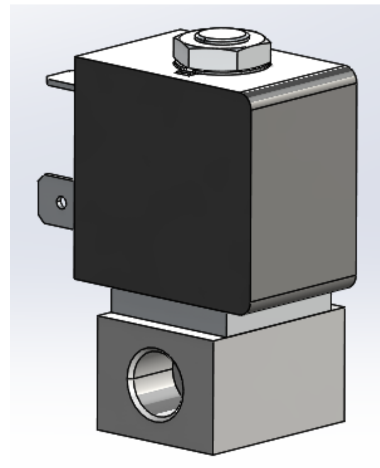
KOH pump	• Commercial pump • Needed flow rate= 0,0047 g/s • Chemical compatibility with KOH. • 12 V / 33 W / DC	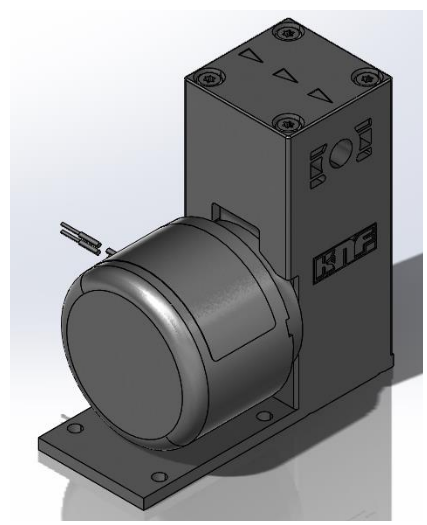

4.2.2 Outlet ports

The gasses leaving the stack go to a separation tank where is condensed the water present in the flow (gas-vapor) and then the separated gas goes to a reactor to eliminate the present particles of the other reactant, i.e. the reactor in the hydrogen side eliminates the small portion of oxygen present, and in the oxygen side happens the opposite.

In the diagram also appear two electrical resistance connected to the closure flanges to warm up the stack and obtain the required operational temperature. In the stream of the electrolyte leaving the stack is measured the pressure and temperature, being the last quite important for the process, since the fluid is constantly increasing its temperature thanks to the exothermic reaction. Table 4.2 shows each modeled part and its characteristics.

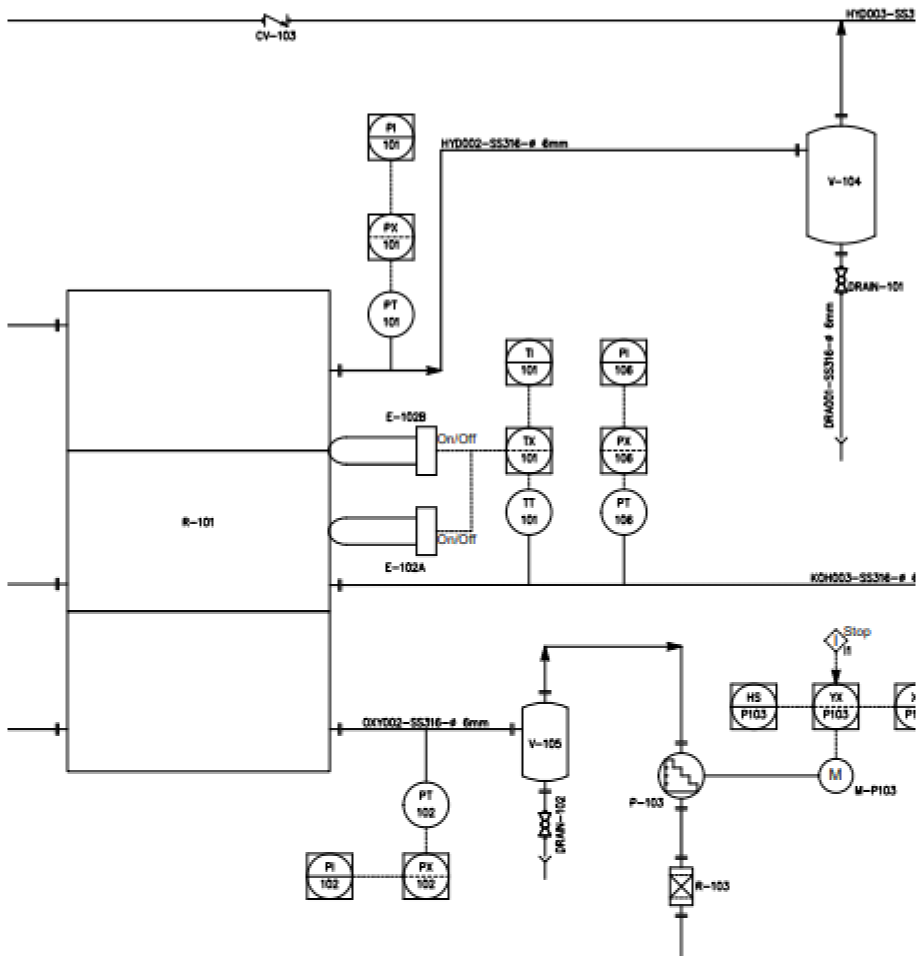

Figure 4.7 - P&ID Stack's outlet

Table 4.2 - Main components at the outlet

Component	Features and parameters	Modeled part.

Separator **Tank**	• Volume=0.5 L • Non-increasing pressure. • Chemical material compatibility with KOH. • Three ports.	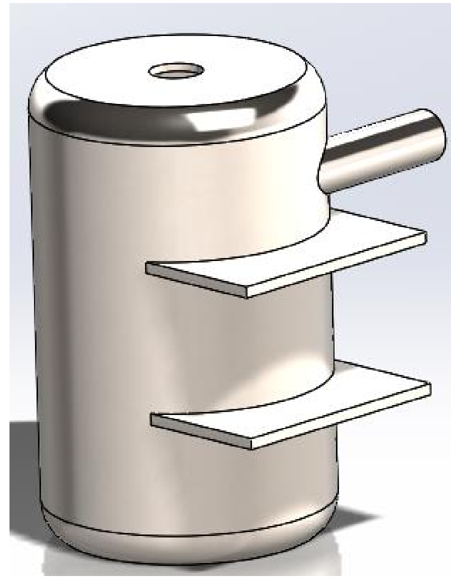
Reactors	• Container for Palladium on alumina spheres. • Spheres 2-4 mm diameter. • Bulk density 750kg/m^3. • 0.15 g of spheres needed • Tank volume=0.0002 m^3 • Tank diameter 2”	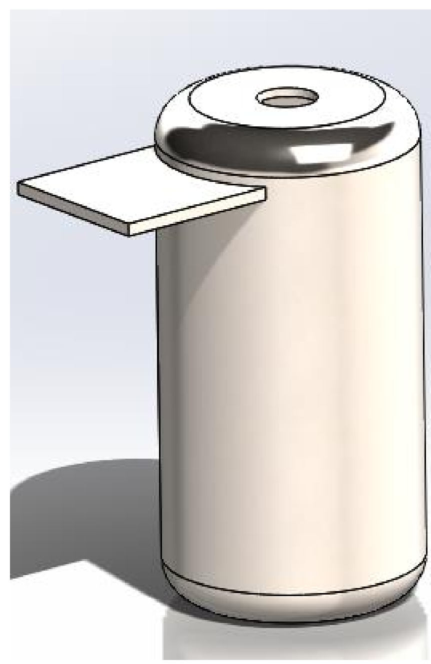

Electric heater	• Commercial component • Desired temperature = 60 °C • Small dimensions	
Gas pumps	• Commercial pump • The lowest needed flow rate= 0,0338 g/s. • Special pump for gases. • Suitable to work with hydrogen and oxygen. • 12 V/ Imax= 0.85 A (10.2W) / DC	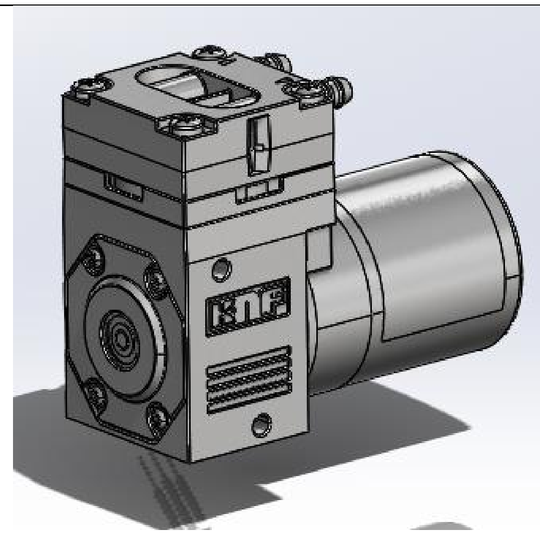
Thermocouple	• Commercial	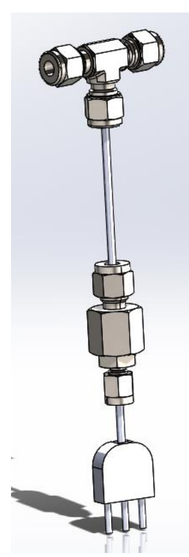

Pressure transmitter	• Commercial pressure measurer. • Small dimensions. • Digital signal.	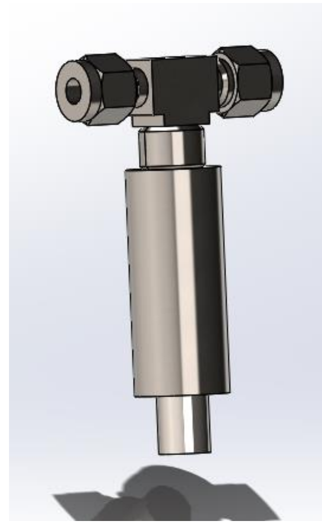

4.2.3 Recirculating system

The non-used gas is injected back into the circuit after leaving the reactors, this happens on both sides, the hydrogen and oxygen side, the circuit is simple, it only uses a check valve to avoid the backward flow of the separated gas. There is a special feature in the recirculated circuit at the hydrogen side, some gas that reached to go inside the electrolyte tank is injected into the stream before reaching the reactor, where again the presence of oxygen is burnt.

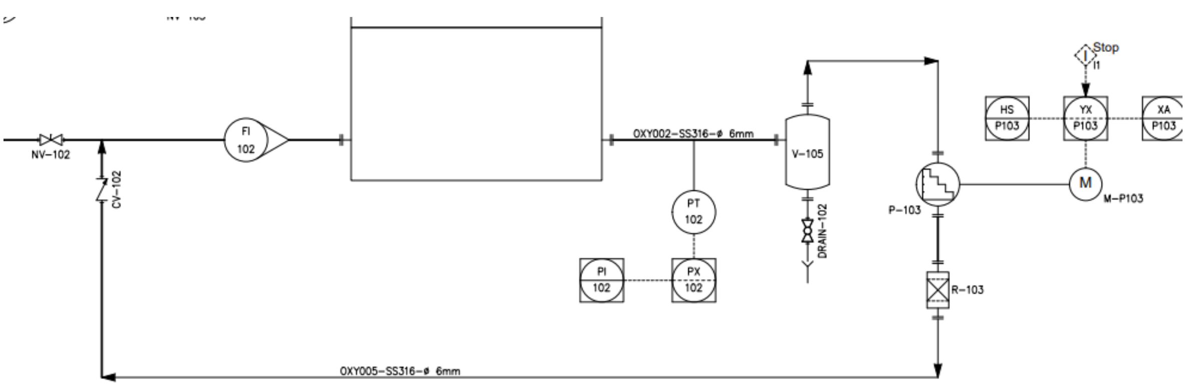

Figure 4.8 - P&ID Recirculating system.

4.2.4 Heat exchanger

The heat produced inside the electrolyte is taken with the mixed solution of water-electrolyte, i.e this fluid besides enabling the chemical reaction it also works as a cooling fluid, but before reentering the recirculating circuit it must be cooled down again employing a heat exchanger. This heat exchanger is just a pipe that leaves the housing and cools down the electrolyte using the water present in the chamber of the AUV. The cooled water-KOH is sent to the tank, as the process goes on the concentration of the electrolyte decreases since more water is going inside. Table X shows the modeled component.

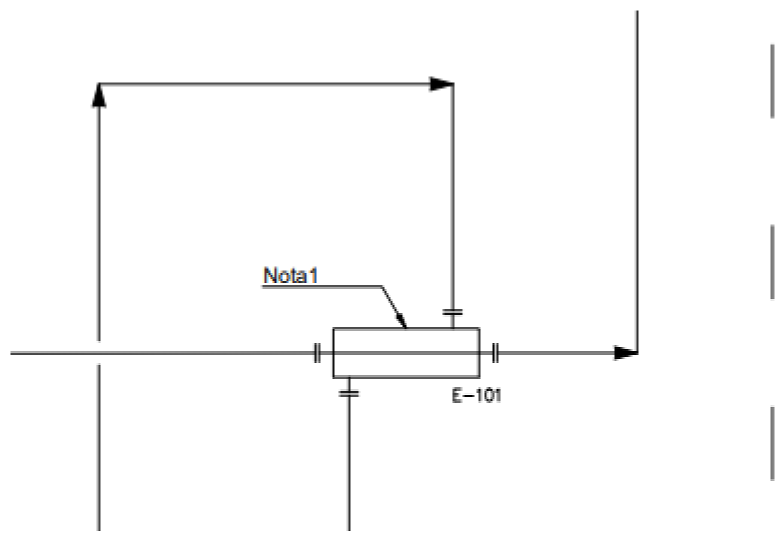

Figure 4.9 - P&ID Heat exchanger.

Table 4.3 - Heat exchanger characteristics.

Component	Features and parameters	Modeled part.
Heat exchanger	• Entrance temperature of the KOH=76°C • The temperature of KOH at the outlet= 60 °C	

		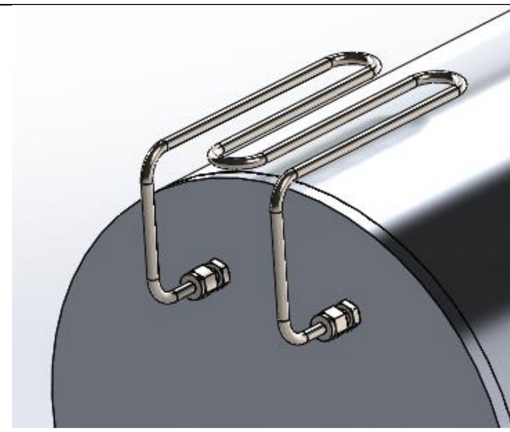

4.3 Layout construction process

The first challenge during the assembly process was the accommodation of the components in a constraint space, the effective dimensions available were: 277.4 mm of diameter and 1135 mm of length, considering that inside this volume also must be the frame. An iterative procedure was carried out measuring the center of mass each time after locating a new component.

The most massive components of the entire system are the electrolyte tank and the stack, therefore these two were the first components to be placed inside the available volume. As the setup must be such that the center of gravity is below or coincident with the center of buoyancy, these components are accommodated on opposite sides.

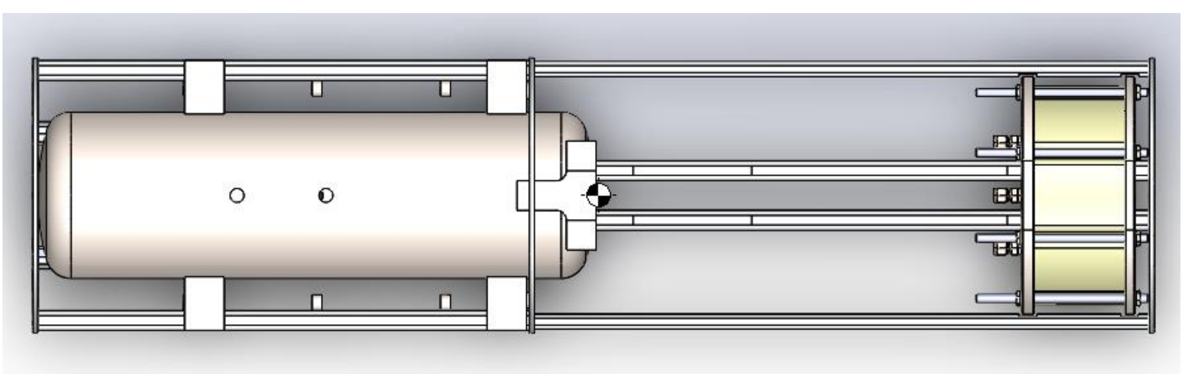

Figure 4.10

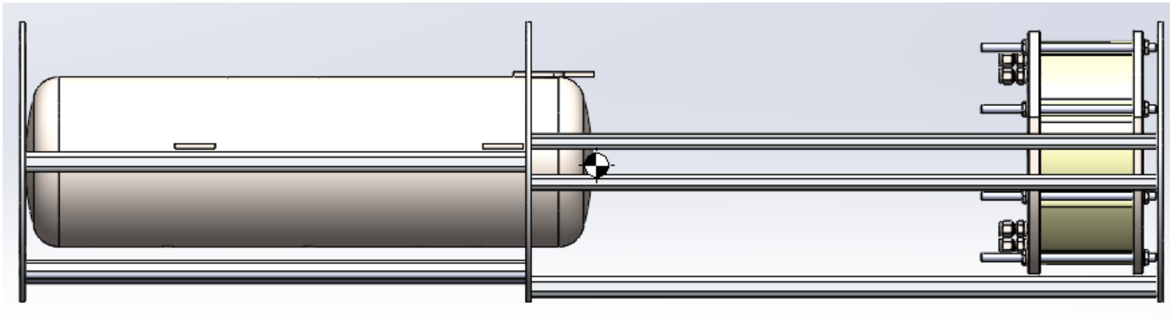

Figure 4.11

Then the other of the assembly was to accommodate each part from the bulkiest to the smallest, thus the consequent step was the assembly of the reactors and separation tanks, which were attached to the KOH tank to balance the weight out.

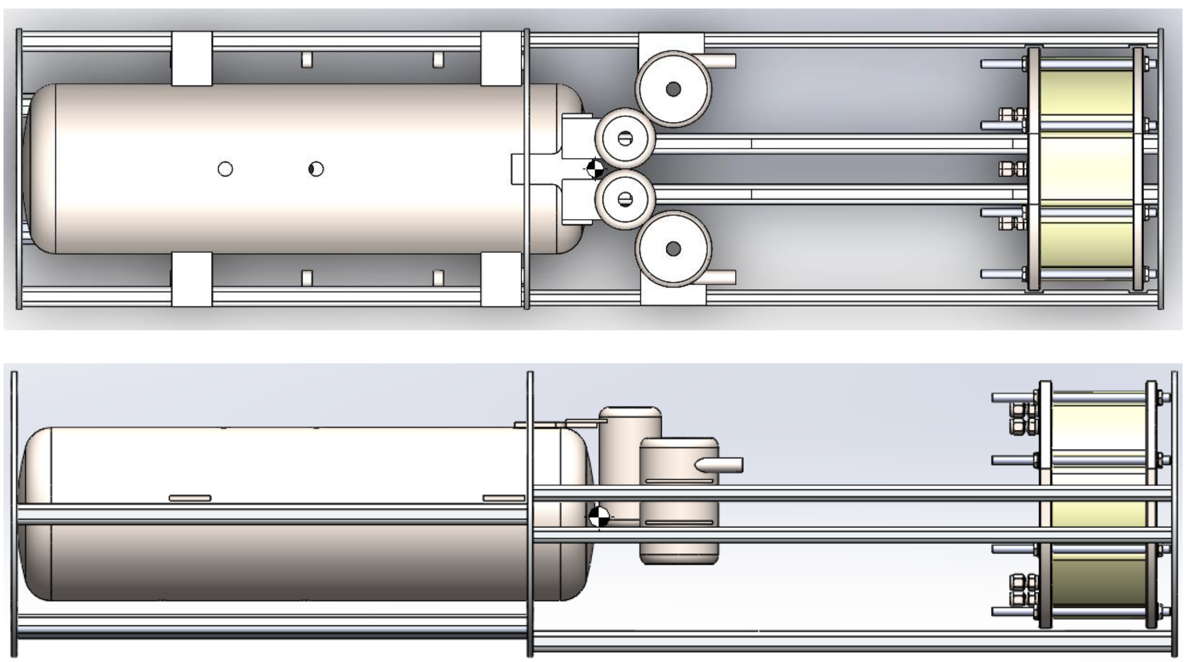

Figure 4.12

Then the KOH pump was placed after several iterations to avoid interference with the flowmeters and the pressure transmitters.

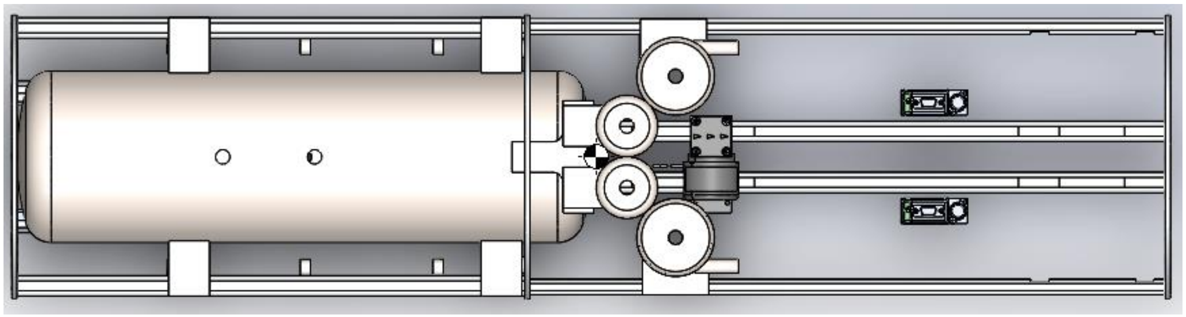

Figure 4.13

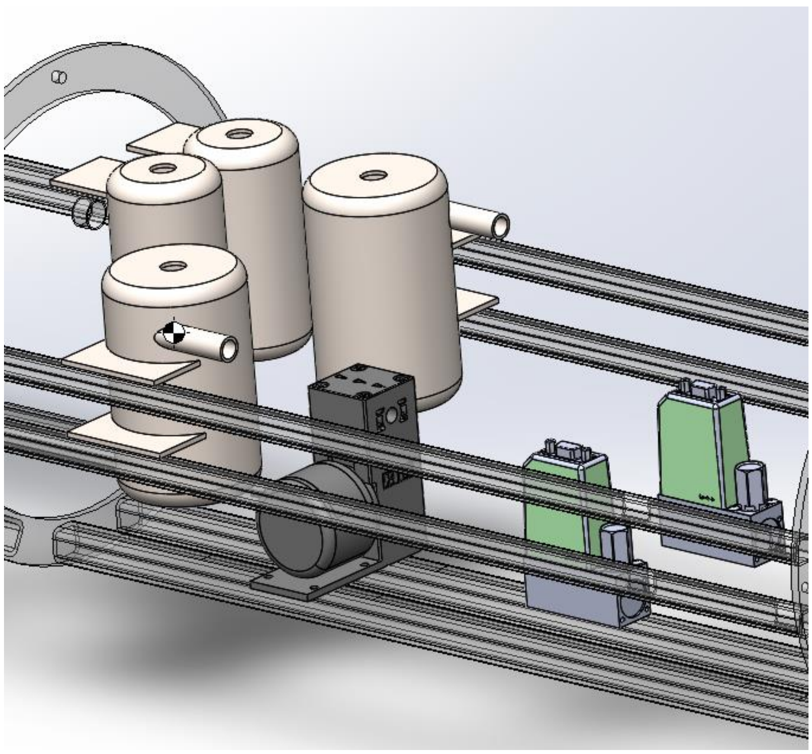

Figure 4.14

Also were defined the entrance channels to locate the plunger valves, and the tube fittings needed for each connection or port, special attention was taken to locate each port in the proper direction to avoid piping interference.

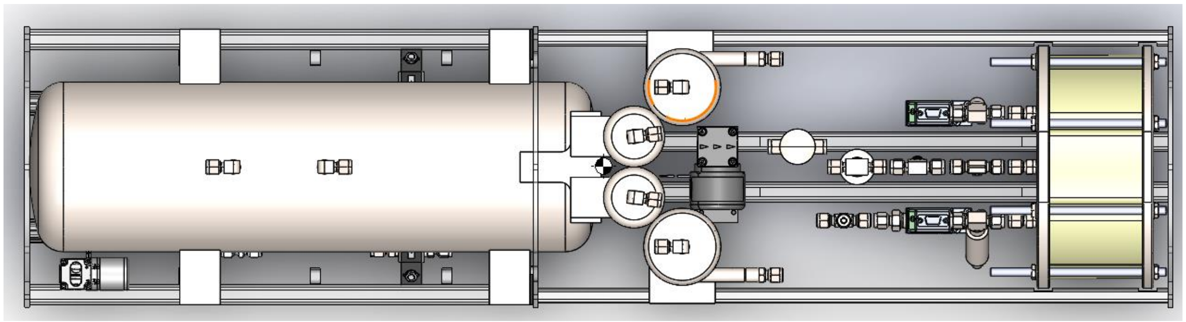

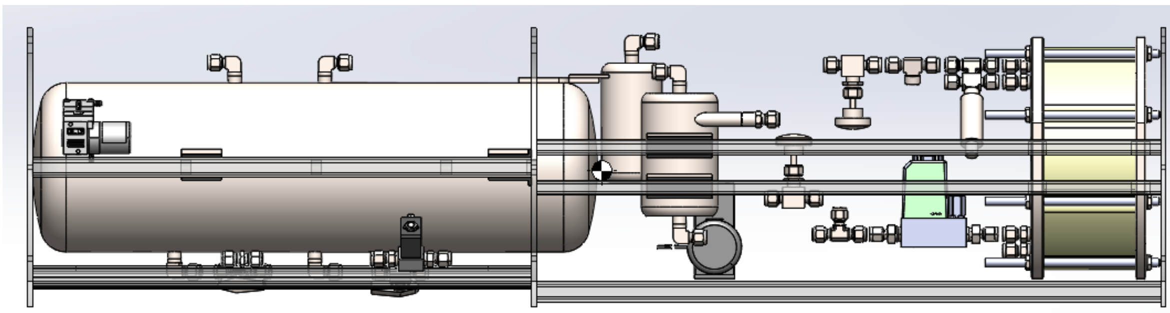

Figure 4.15

Finally, the piping process, the pipes are a combination of stainless steel and Teflon pipes, the pipes connected to the interface at the entrance cap, were made flexible to avoid the assembly and disassembly of the cap and at the stack level to ease the connection as the entrance and outlet ports for the gasses are crossed. The rest of the piping connections were rigid metallic pipes, the most important thing to consider during the assembly of these pipes is that the minimum bending radius is three times the pipe diameter.

5. Structural and buoyancy Analysis

This section studies the capability of each structural component that belongs to the global system to undergo the loading conditions during operation, the main structural components are the external housing, which undergoes the external pressure caused by the column of water above the vehicle, the internal frame where are placed all the internal components, and different connectors that hold tanks in their positions. This was assessed employing analytical formulas and simulations.

5.1 Housing design

The housing is the most important structural element because it creates a sealed environment to avoid the entrance of water, and also it protects the components of the system from the ocean pressure at the operational depths. The goal is to design the pressure housing for a maximum ocean depth of 1000 m. The most used materials in these types of applications will be assessed for both, the cylinder part and the end caps, and also will be analyzed the different configurations for the bolted joint.

5.1.1 Parameters

5.1.1.1 Load conditions:

The maximum pressure reached is approximately 100 bar which takes place at the maximum depth of 1000 m. But the study will be aimed to resist a pressure of 150 bar, taking a safety factor of 1.5.

5.1.1.2 Geometry:

The base dimensions to begin the analysis are shown in Figure 5.1Table 5.1 And the initial design is in Figure 5.1Table 5.1

Cylinder		**End Caps**	
Length	750 mm	Thickness	10 mm
Outer diameter	300 mm	Outer diameter	300 mm

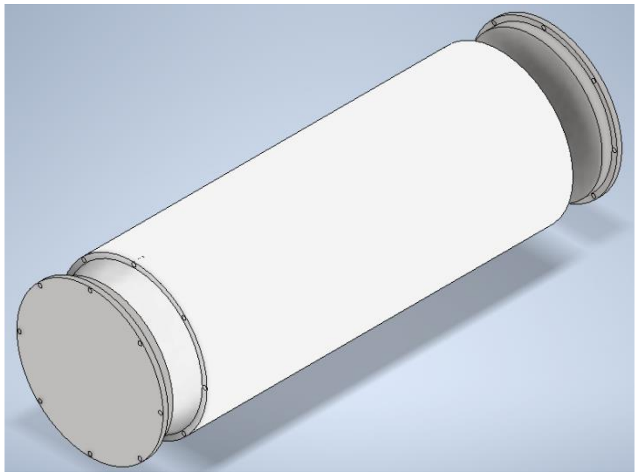

Figure 5.1

5.1.2 Materials

The most used materials are the aluminum alloys 7075 and 6061 T6, the titanium grade 5 (Ti 6Al4V), and the stainless-steel alloy 316L (This information is taken after researching similar devices in the market). Their mechanical properties are shown in Table 3.1 – AFC and PEM features

Table 5.2

	Al 7075	**Al 6061 T6**	**Ti 6Al-4V**	**316 L**
Modulus of Elasticity [GPa]	71.7	70	113	193
Tensile Yield Strength [MPa]	503	276	830	205
Tensile Ultimate Strength [MPa]	572	310	900	515
Poisson 's ratio	0.33	0.33	0.35	0.25
Density [g/cc]	2.81	2.7	4.4	8

5.1.3 Possible configuration of bolted joints

The three most common configurations for the bolted joints are shown in Figure 5.2 where each one has its pros and cons, the radial configuration may present problems insulating the internal part of the housing, while the axial configuration may present problems at the time of designing the joint for not having enough thickness (this will be analyzed later), the axial configuration with flange solves the two previous problems but the flange would make difficult mounting the external pressure cylinders for hydrogen and oxygen storage, besides the additional manufacturing process that it would need.

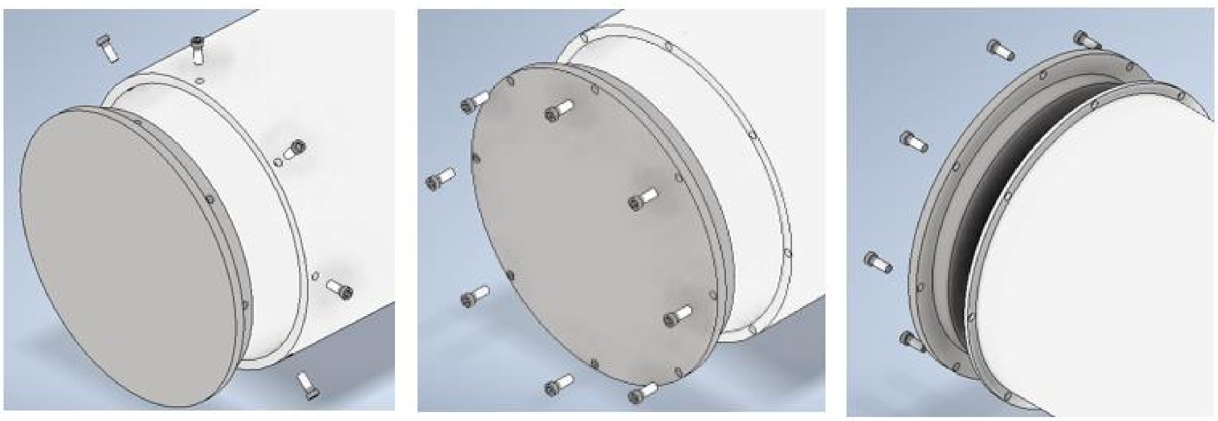

a). Radial *b). Axial* *c). Axial with flange*

Figure 5.2 - Configurations for the bolted joint

Note: Figures are just descriptive, many other elements and features are lacking in the joint.

5.1.4 Analysis type

The structural calculations were carried out in two ways: analytically and Finite Elements Analysis (FEA). Initially, the geometry of the different elements is taken without holes and other features to simplify the analysis, thus after designing the bolted joints, adding the channels for the sealing rings, and adding the holes for the different pipes, the analysis will be carried out again to verify that they do not fail. Also is important to mention that the housing is assessed separately (Cylinder and Endcaps).

5.1.5 Analytical calculation

The structural calculation is divided into two parts, analysis against static failure and analysis against linear buckling.

- For static failure were used the equations for thin-walled cylinders (17) (a thin cylinder is considered when the value of ten times the thickness is lower than the average radius, equation (5.1)), thus by the static analysis was found the circumferential stress (hoop) and the axial stress equation (5.2). The radial stress in thin-walled cylinders is approximately zero.

$$if\ \ 10t < r_{av} \rightarrow thin - wall \tag{5.1}$$

$$\sigma_t = \frac{P_r}{t} \rightarrow Hoop\ Stress \qquad \sigma_a = \frac{P_r}{2t} \rightarrow Axial\ Stress \tag{5.2}$$

- In the case of buckling analysis, Roark's equations (17) were used for thin-wall cylinders and external pressure. Were computed the pressures needed to deform the cylinder if it has a thickness t in two cases, thin tube with closed ends: if the expression (5.3) is fulfilled then the pressure can be approximated to that one in the equation (5.4) and thin tube with open ends equation (5.5).

$$if\, 60 < (\frac{l}{r})^2 * \frac{l}{r} < 2.5(\frac{r}{t})^2 \tag{5.3}$$

$$P = \frac{0.92E}{\frac{l}{r} * (\frac{r}{t})^2} \tag{5.4}$$

$$P = 0.807 \frac{Et^2}{lr} \sqrt[4]{\left(\frac{1}{1-v}^3\right) * \left(\frac{t}{r}\right)^2} \tag{5.5}$$

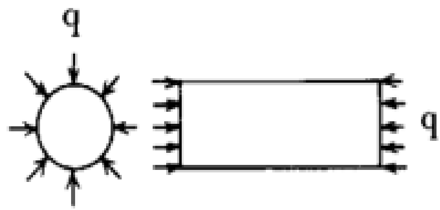

Figure 5.3

This calculation will be carried out in more detail after having the components assembled, once it is known the final weight of the complete system to calculate the forces that will act in each screw. But as a preliminary step and to be sure that the dimensions of the screws will not change dramatically the geometry of the components, a simple calculation of the needed area for the screws is carried out for each material assuming that the final weight is 800 kg, in Table 5.3 are presented the approximation of the ranges in which the diameter of the screw could be. It is noticed that the possible sizes are around low values that could adjust perfectly with the design.

Table 5.3

screws	min. Area [mm^2]	min. Diam [mm]
Aluminum	28.4 – 14.2	6.0 – 4.3
S.S 316L	8.9 – 4.4	3.4 – 2.4

The critical type of failure in the cylinder is due to buckling, this can be seen in Table 5.4 where it is compared the pressure needed to cause a buckling and a yielding failure, this can be noticed from the analytical calculations. therefore the FEA only will be done for linear buckling analysis. In the case of the Endcaps, the analysis will be static.

Table 5.4 - Example of failure for 7075 T6.

Yield failure occurs at a pressure quite bigger than the buckling failure.

Type of failure	Failure pressure [bar]
Buckling	144.8
Yielding	335.33

5.1.5.1 Cylinder

The assessment is carried out by analyzing the mode shapes, which are the shapes of deformation that the cylinder will undergo as the pressure increases, in this study the failure pressure is going to be the one that causes the first shape mode. The pressure of failure is going to be assessed for several thicknesses and the materials shown before, choosing the thickness that presents a failure pressure of 150 bar (1500 m depth) for the design.

Mesh convergence

An iterative process is followed to choose the most appropriate mesh size, the main purpose is to have a good balance between a good approximation in the results and not too long simulation time. The mesh size selected is 10 mm and the study is shown in Graph 5.1.

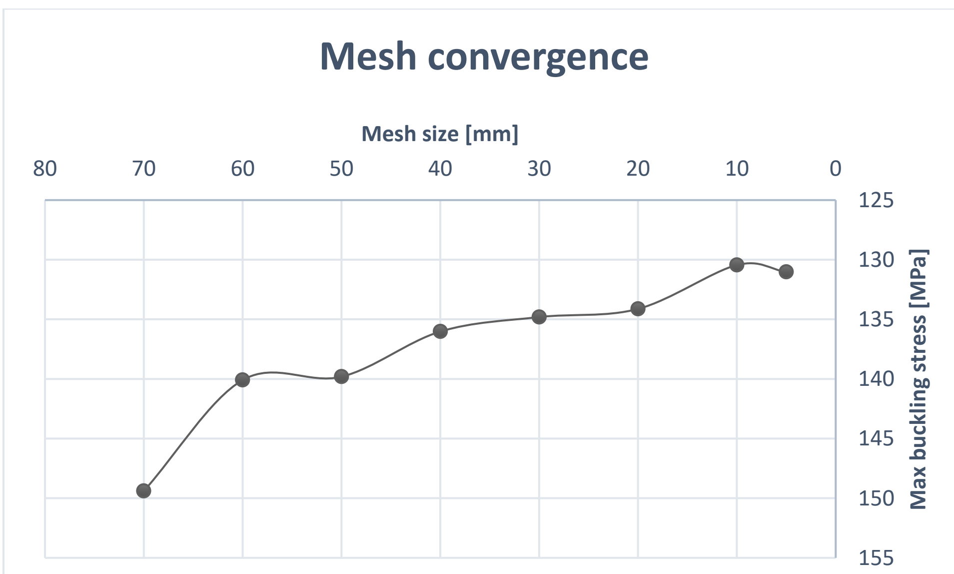

Graph 5.1

Boundary and loading conditions

The cylinder surface is loaded with hydrostatic pressure. In one of its ends, the pressure is distributed along the edge where the cylinder makes contact with the Endcap; in this edge the nodes were constrained in all directions except the axial direction, letting it free to move in this direction. The constraints at the other end were fully fixed in all directions, in Figure 5.4 It is shown the loading condition.

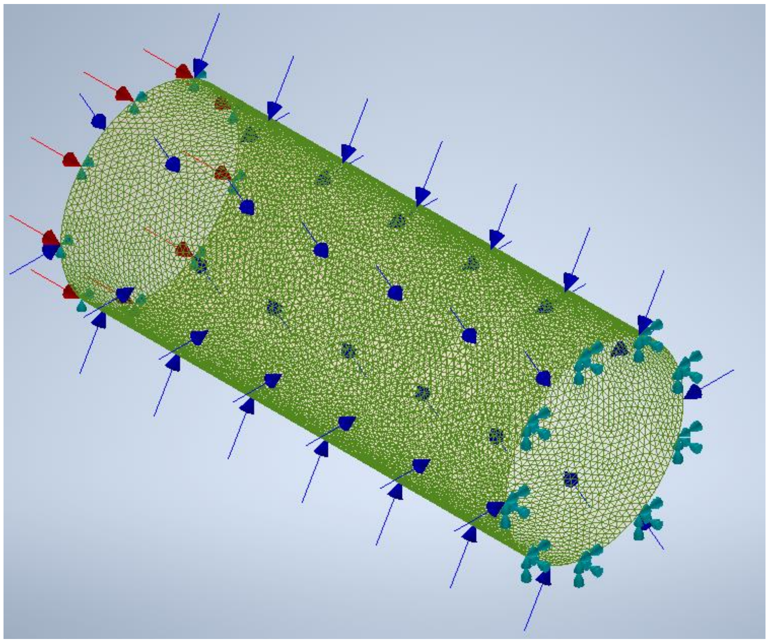

Figure 5.4

5.1.5.2 Endcap

A linear static analysis is done for the Endcaps, analyzing what is the ideal thickness of the flange that goes inside the cylinder, and verifying that the maximum stresses are below the yielding stress. Thus the simulation is carried out for several thicknesses.

Convergence mesh

In this case, the method is a little different because it is a process that the software does automatically. Mesh size is set and then a convergence analysis is done Graph 5.2, if it converges it means that the mesh size selected is appropriate.

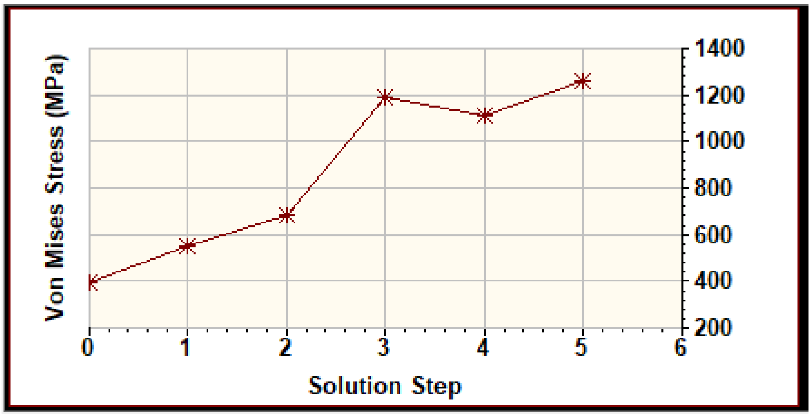

Graph 5.2

<u>*Boundary and loading conditions*</u>

The contact face is constrained by the cylinder's face, then these nodes are fixed. Uniform pressure is located in the external face of the cap.

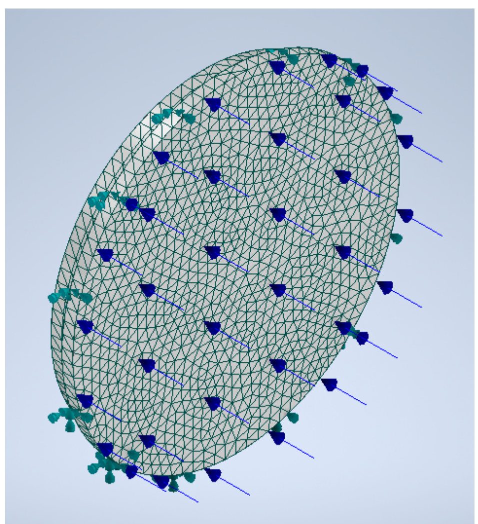

Figure 5.5

5.1.6 Results

5.1.6.1 Cylinder

Graph 5.3. shows the variation of the thicknesses with the pressure, the theoretical and simulated curves are plotted to obtain the optimum thickness at 150 bar, the ideal thickness is the intersection between the reference and the theoretical or simulated curve.

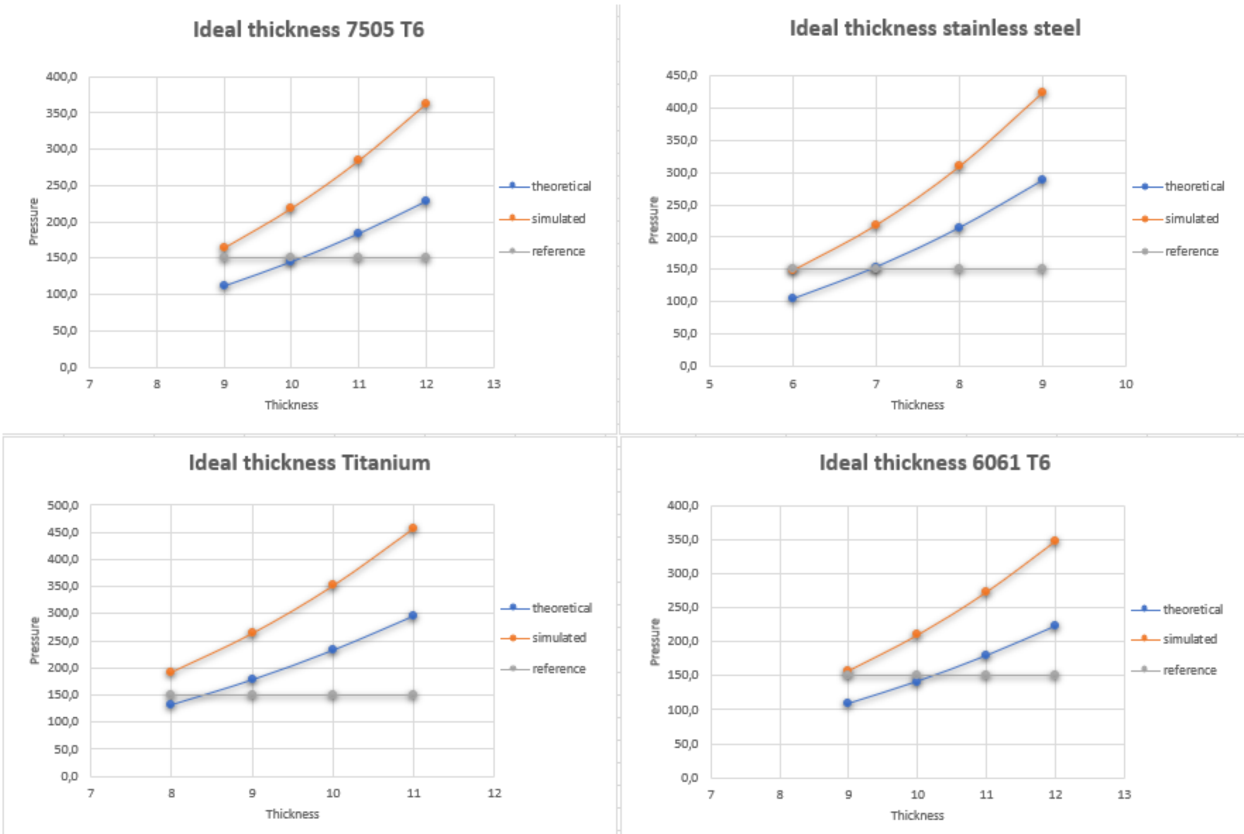

Graph 5.3 - Ideal thickness for each material for 1500 m depth.

During the simulations were used five modes to see how the housing will deform as the pressure increases Graph 5.4 The pressure limit is taken from the first mode which is the beginning of the deformation.

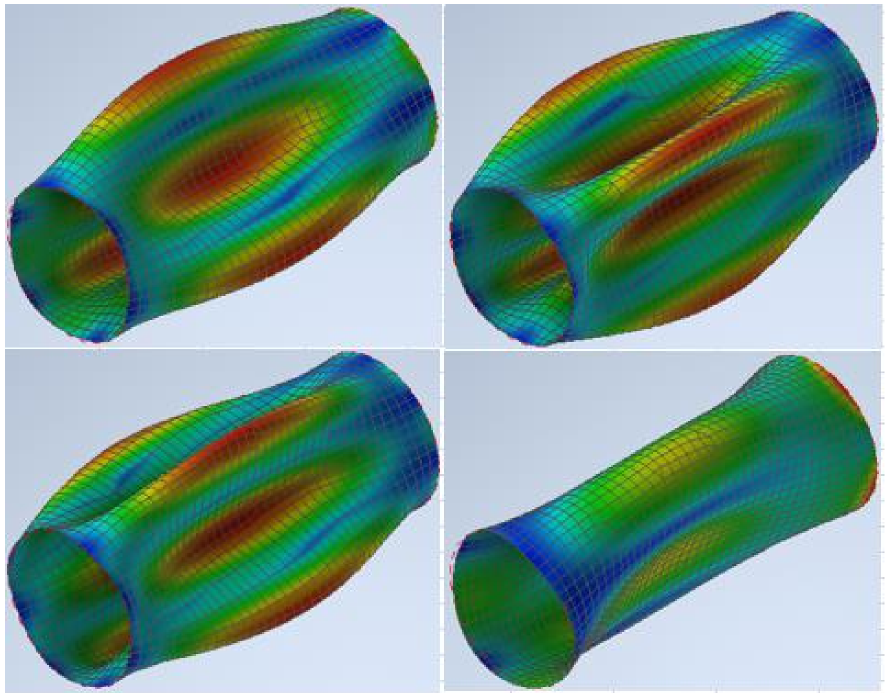

Graph 5.4

5.1.6.2 Material selection and dimensions

Graph 5.5 shows the material's weights and the prices of a standard tube adjusted to the dimensions and weights of the cylinder (these prices are just to make a comparison because it was taken a price of a standard tube then adjusted to the magnitudes for each material) . (18)

The material selected is Aluminum 7075T6 Because it is lighter, and the price is not so high compared with the other materials. A good option also could be 6061 T6. Titanium is too much expensive and stainless steel is too heavy and its price is higher than aluminum.

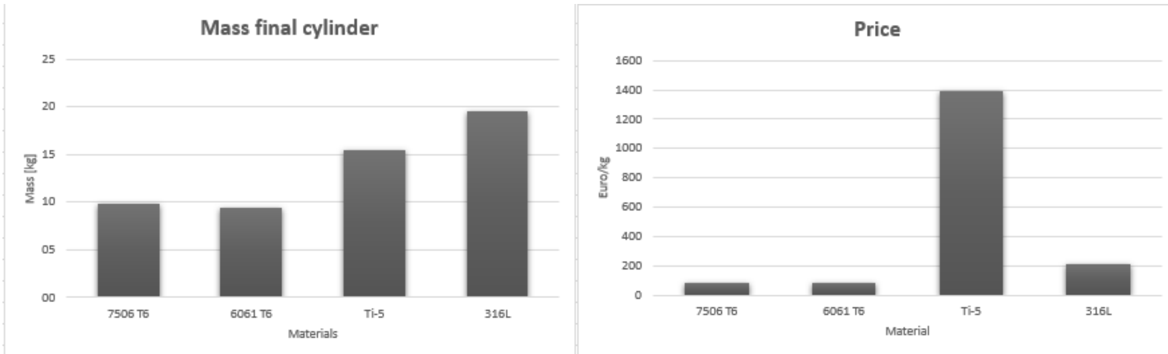

Graph 5.5

The maximum theoretical and simulated stresses for the selected material are shown in Table 5.5. In the case of buckling analysis, the maximum stress was found in mode number four, it must be verified that this stress does not cause yield. If a structural safety factor of 1.5 is taken, can be noticed that all stresses are lower than the admissible stress.

Table 5.5

<table>
<tr><th>Buckling - FEA</th><th colspan="4">Static analysis</th></tr>
<tr><td rowspan="3">238.6 MPa</td><td colspan="2">Analytical stresses</td><td>Admissible stress</td><td>Yield stress</td></tr>
<tr><td>Hoop</td><td>Axial</td><td rowspan="2">335.3 MPa</td><td rowspan="2">503 MPa</td></tr>
<tr><td>225 MPa</td><td>112.5 MPa</td></tr>
</table>

An additional graph is added for the selected material to observe how the depth endurance decreases as the thickness decreases. Noticing that at big depths decreasing one millimeter of thickness would drop the endurance in a higher magnitude than in low depths. To optimize the design the idea is that the reduction in thickness affects as lower as possible the endurance.

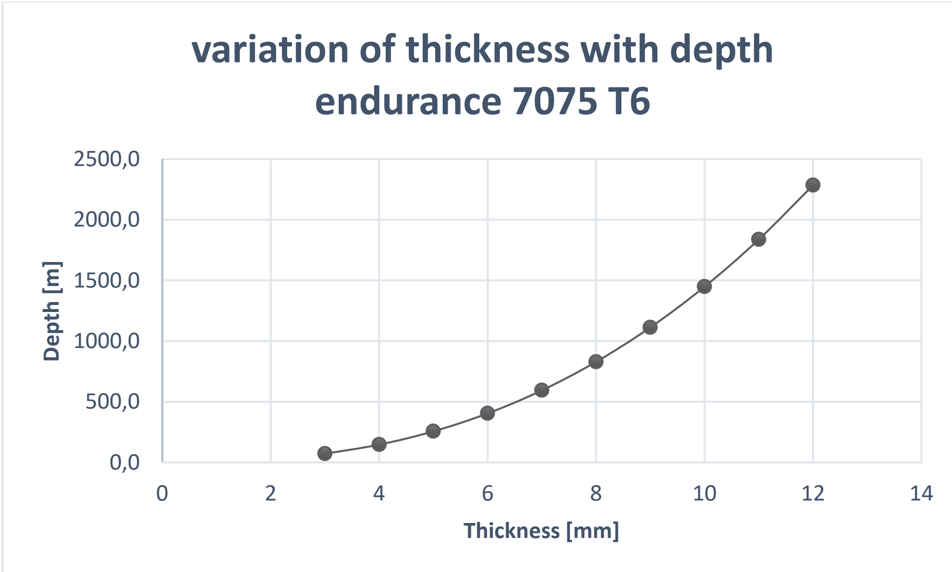

Graph 5.6

5.1.6.3 End caps

Figure 6 shows the FEA maximum Von Misses stress and the maximum displacement of the cap. In the contact edges are located the maximum stresses (Figure 7) but those stresses are quite big due to the stress concentration for the change in cross-section, the location of the nodes right in the edge, and the constraining boundary conditions. That is why the maximum stress is taken at the point where the maximum displacement is located. In Table 5.6 are presented the results of the same test for different thicknesses, where the caps with a flange length between 15 mm and 20 mm satisfy the structural conditions (The maximum stresses found are lower than the yielding stress, 503 MPa). It is proposed to use the cap with a flange length of 20 mm because it guarantees a structural safety factor of 1.5, (on the base of 1500 m), this overcalculation could help to account for all the features that were not considered in the geometry and the cap does not suffer much deformation during operation, but it is worth mentioning that 15 mm also could work.

Table 5.6

flange length	max stress	structural safety factor
10	600	Fails
15	460	1,1
20	344	1,5

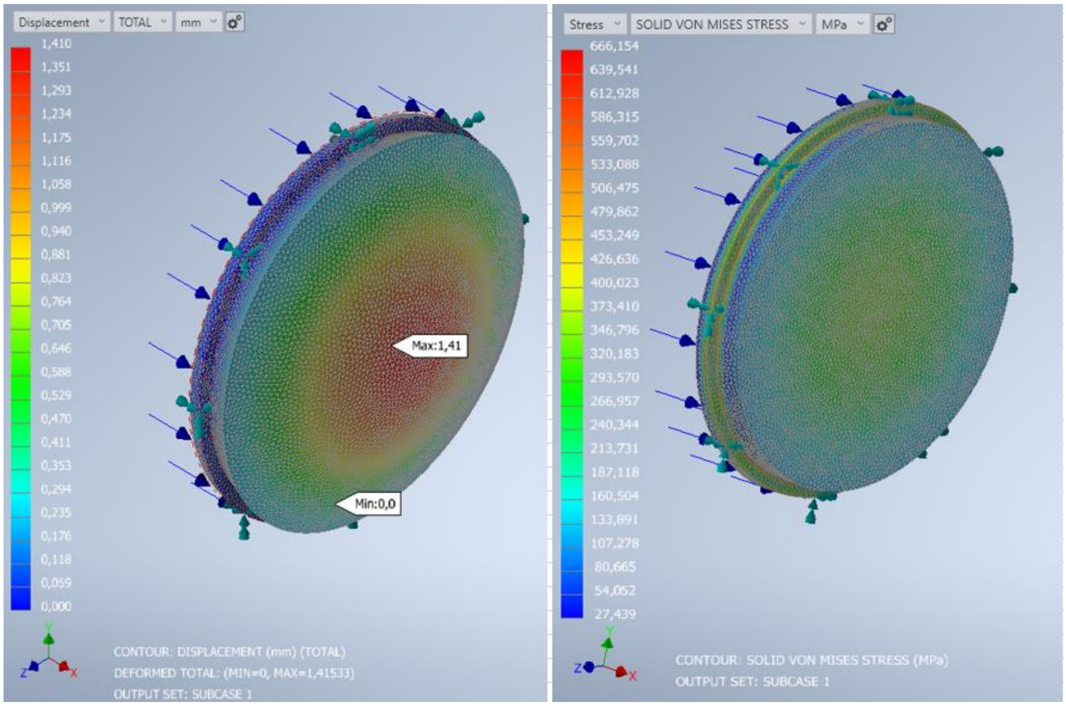

Figure 5.6 - Results for a flange thickness of 20 mm.

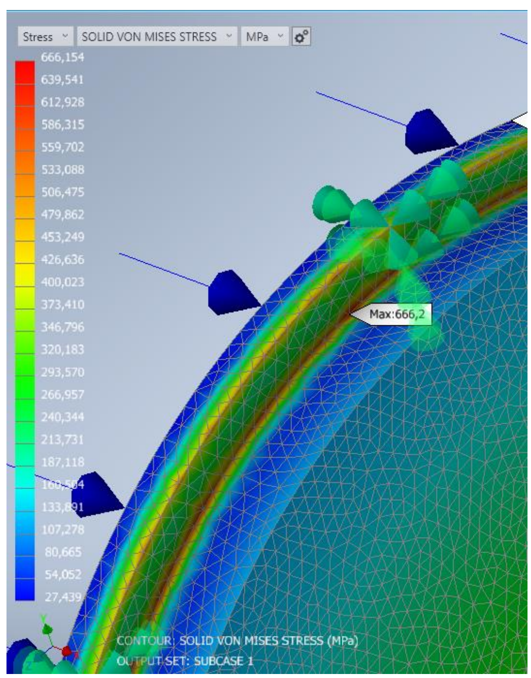

Figure 5.7 - Stress concentration at the edge.

In the first analysis, the housing was assessed to endure 1000 m with a safety factor of 1.5, it was verified that the main components do not reach failure under operation, but there were several modifications in the project in which the available space for the housing was increased to a diameter of 550mm and a length of 1285mm, also the maximum operation depth was decreased to 800m, to increase the maximum allowed weight of the system to guaranty neutral buoyancy, thus under the same analysis presented before, the housing elements were recalculated. Table 5.7 shows the initial parameters and the results obtained after the modifications. The obtained results are summarized below.

Table 5.7 - changes in the parameters for the housing

	Length	thickness [mm]	volume [m3]	maximum total weight [kg]	Housing weight with caps [kg]	Pressure [bar]
initial	750	9,43	0,053	54,39	27,1	1,5
modificated	1195	11,36	0,084	86,66	43,4	1,3

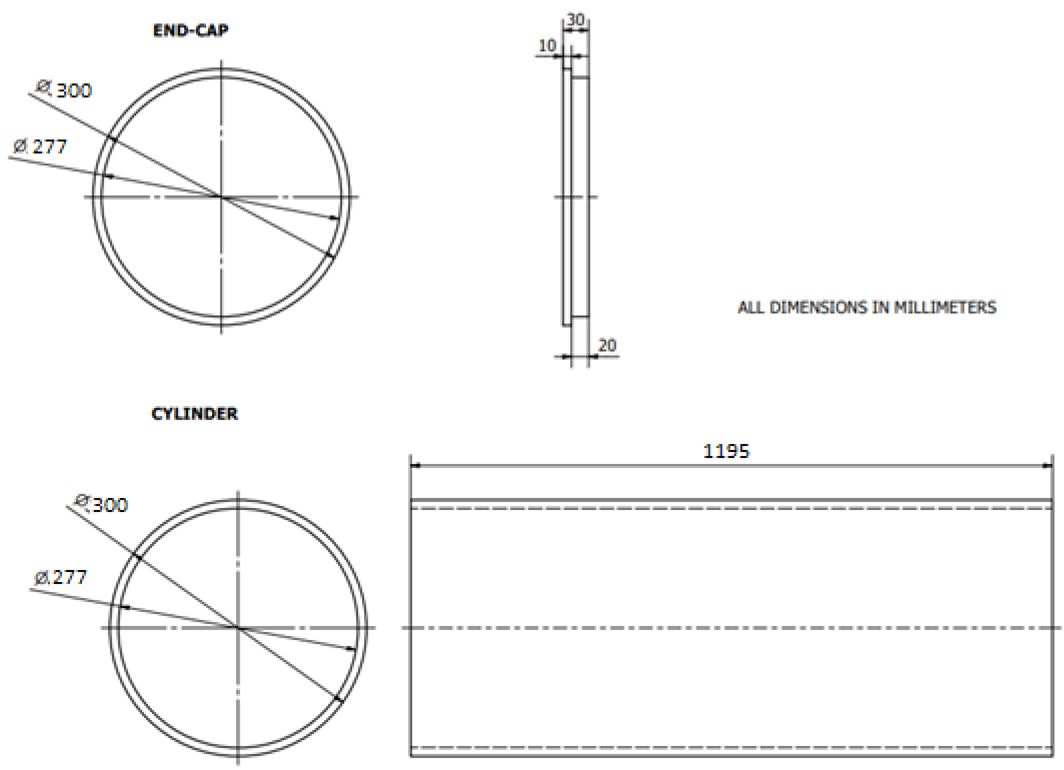

Figure 5.8 - Initial dimensions

- Materials: Aluminum 7075 T6. For both parts (The idea is to have the same material in all components, even the screws to avoid galvanic corrosion).

- Outer dimensions: ⌀300 mm x 1215mm.
- Inner dimensions: ⌀280 mm x 1155 mm.

5.2 Structural elements

5.2.1 Inner structure

The internal frame was designed based on the desired positions of the internal components, the geometrical constraints are given by the housing, and the simplicity of manufacture, always aiming for the minimum weight. It is composed of square aluminum tubes and three sheet rings that hold the tubes. The material was chosen from the beginning to have the same material as the housing and also to obtain a light structure the weight.

The layout process of the structure was iteratively carried out after having the final positions of the elements and the final weight, the first estimation of the beam profile was done with the bending stress formula, where was taken available commercial tubes and based on its dimensions and material, the resulting stress under the total load was compared with its yielding stress, varying the tube dimensions up to obtaining a safety factor of 1.5.

$$\sigma = \frac{My}{I} \ \textit{Stress due to bending} \tag{5.6}$$

The total weight of the internal elements is 87 kg exerted in the center of gravity and held in several points. As for the initial estimation, the weight used to compute the stress is the total weight and is already known that the weight is going to be distributed along all the square tubes, a simulation is carried out to optimize the final size of the bars, Figure 5.9, shows the location of the center of gravity, the points where the load is supported and the selected layout, one aspect to remark is that the layout was selected trying to keep the center of gravity of the structure in the geometrical middle point.

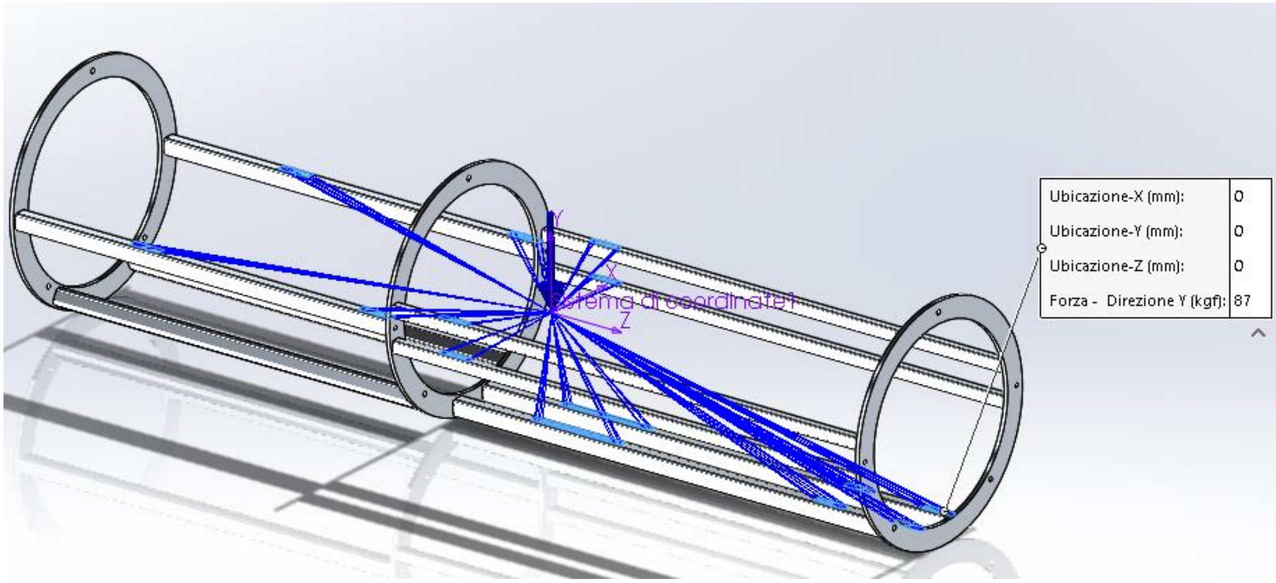

Figure 5.9

The selected material is aluminum 7075 T6 where its yield stress is 503 MPa. Several scenarios were analyzed to study the compliance of the structure:

- <u>The system held from the outer rings</u>

The first case is in which the system is grabbed from the two outer rings, obtaining the results shown in the Figure 5.10, where the maximum stress is 90.4 MPa and the maximum displacement is 3 mm approximately. Is important to notice that, the displacement is not that important as long as it does not cause the failure of the structure.

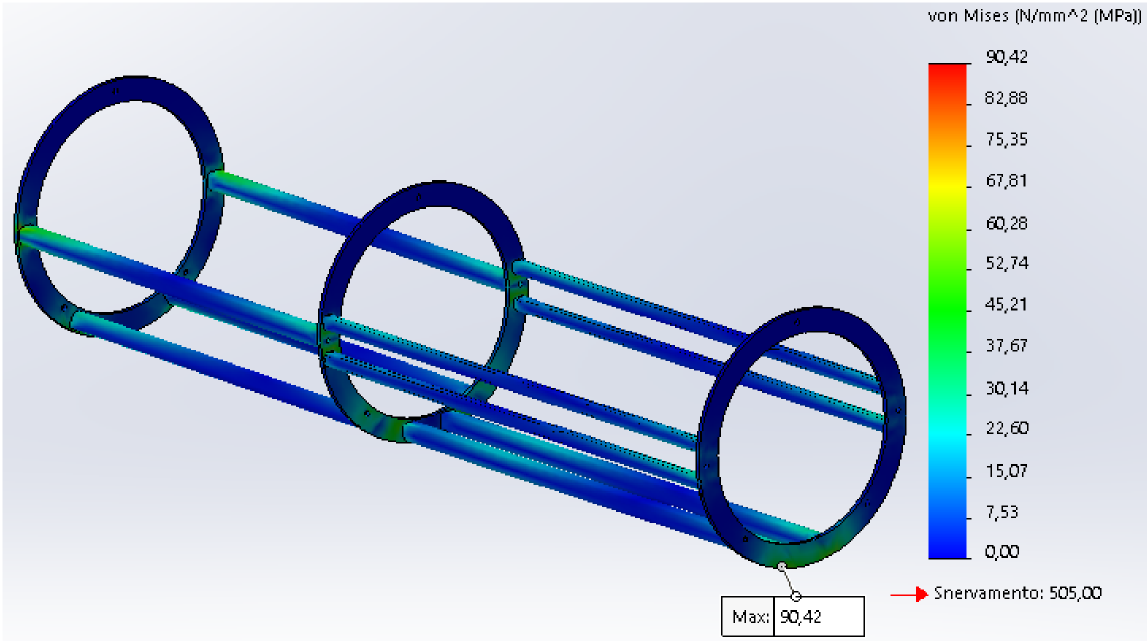

Figure 5.10 - Simulations of the structure, cantilevered case. Stress analysis.

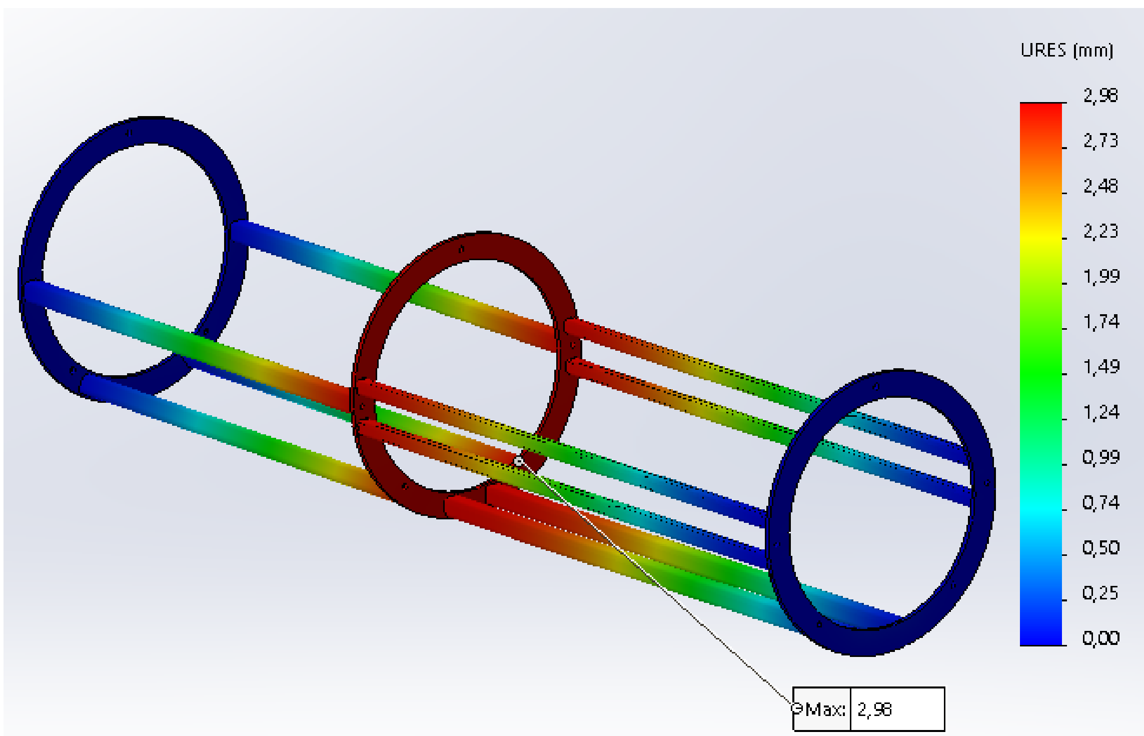

Figure 5.11 - Simulations of the structure, cantilevered case. Displacements analysis.

After iterations in the simulations varying the size of the commercial tubes, the selected components are shown in Table 5.8.

Table 5.8

Component	**Dimensions**	**Material**	**Quantity**
Square tube	15x15 mm		4
Square tube	20x20 mm	Al 7075 T6	6
Rings	⌀ x5mm thickness		3

5.2.2 Brackets and supports

This analysis was carried out to assess the capability of the structural elements that support the tanks to undergo the present loads. This study was carried out employing an FEA analysis in the software Solidworks, there are three studies:

- <u>Electrolyte tank brackets</u>

  This analysis takes into account the electrolyte and tank's weight when it is at full capacity. Is important to remark that the material of these tanks is 316 stainless steel, which has a yielding stress value of 515 MPa, and the maximum present von misses stress is 0.88 MPa, therefore the capability of the brackets is verified. Image x shows the setup and study results.

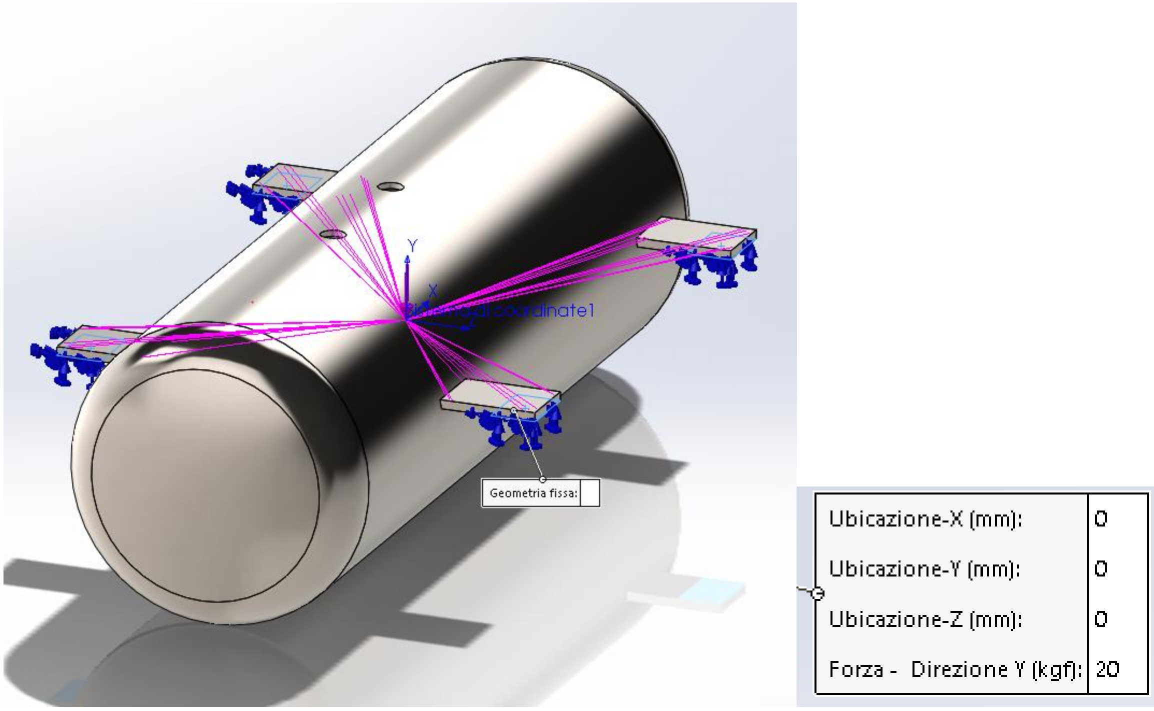

a). Study's setup.

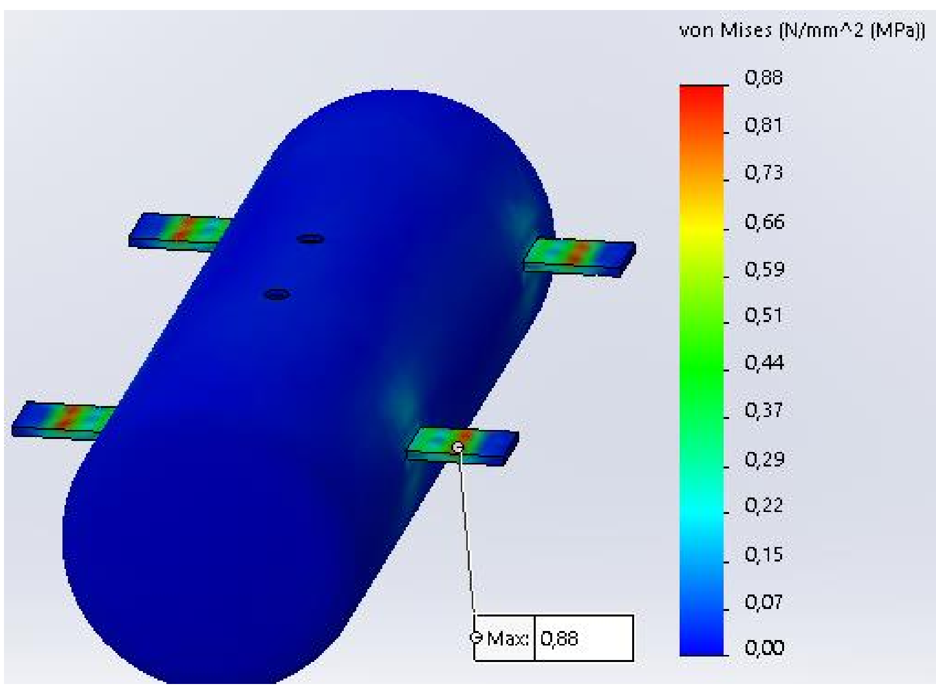

b). Stress results.

Figure 5.12– Simulations of the brackets for the electrolyte tank.

- <u>Brackets for the reactors and the separation tanks</u>

  For these simulations, the taken weights were 0.5 kg for each reactor and 0.7 kg for each separation tank, obtaining the results shown in the Table 5.8, verifying the structural resistance of these brackets.

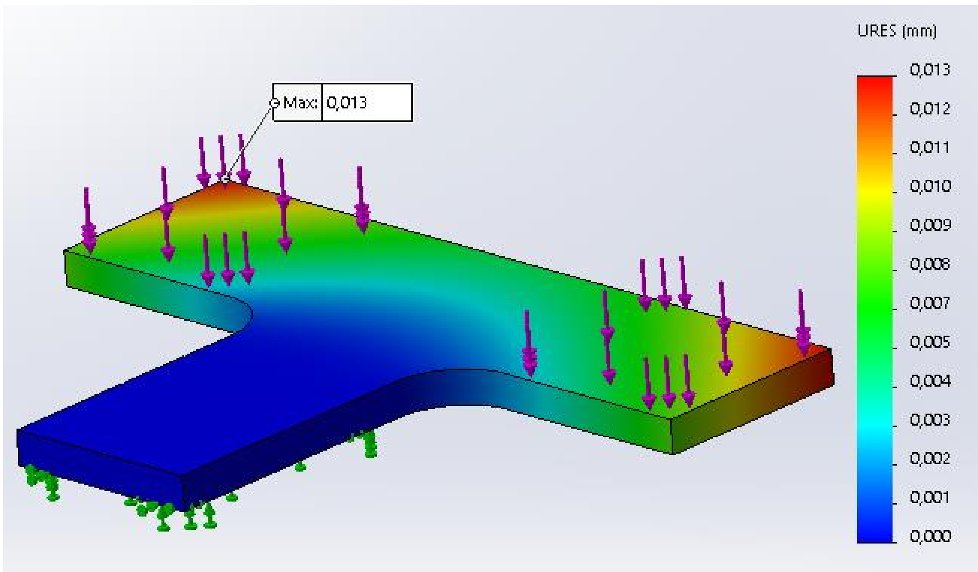

a). Displacement reactors bracket.

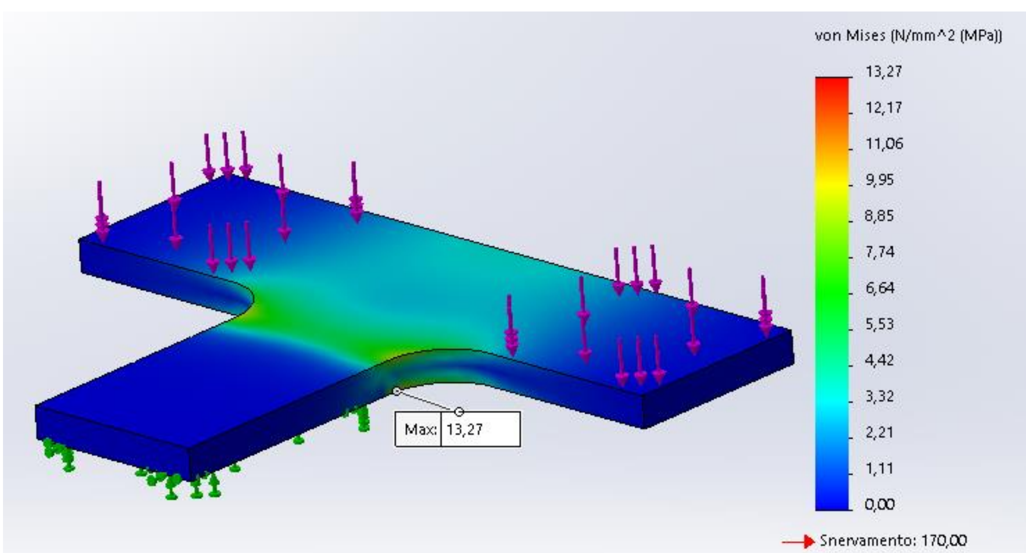

b). Maximum stress reactors bracket.

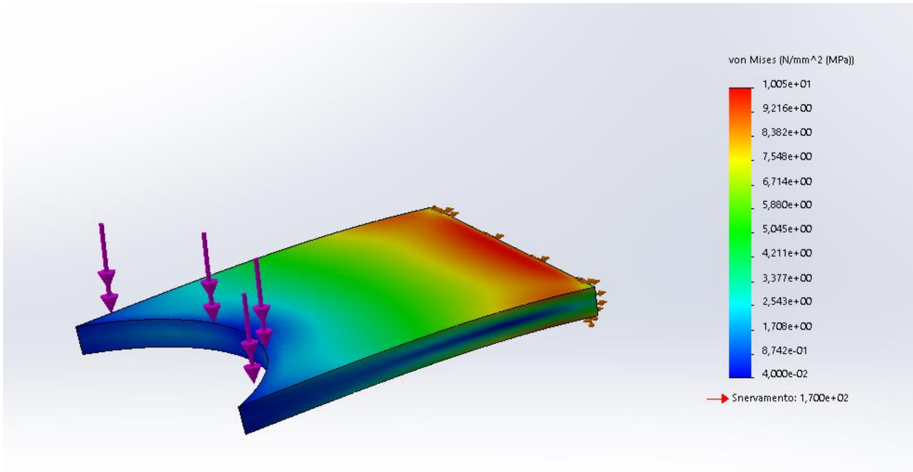

c). Maximum tress reactors bracket.

Figure 5.13– Simulations of the brackets for reactor and separating tanks.

5.3 Neutral buoyancy verification

After having all the components assembled is time to verify the requirement of neutral buoyancy. As it was shown in the computations section, the maximum allowed weight to have neutral buoyancy is 86.7 kg. Table 5.9 shows the weight of each component in the system.

Table 5.9– the weight of the present components

Part	Weight [g]	Part	Weight [g]
KOH tank	9087	PT's	600
Reactor1	454	Flowmeters	560
Reactor2	454	Isolants	128
Separator1	678	KOH Pump	500
Separator2	678	Gas pumps	340
Stack	12000	Plunge valves	200
Structure	2816,38	Support sheets	148
End cap1	5287,3	Tube fittings	1674,97
End cap2	5397,5	Tubing	510
Housing cylinder	32974,98	Termocouple	158
Flexible tubing	194,25	Tube fittings	416,36
check valves	95,52	Bolts and screws	300

The entire system without being loaded with the initial quantities of fluid weights 84 kg, at the beginning and the end of the mission the liquid in the tanks (KOH and water) weights 8.6 kg and 13.86 kg respectively, obtaining a maximum weight of 89.8 kg for the entire system. Then can be concluded that neutral buoyancy was achieved, the total weight is around the required value.

Table 5.10– Comparison between obtained and allowed weights

Total weight	84.54 kg
Allowed weight	86.7 kg

5.4 Barycenter displacement

Another important analysis is the location and displacement of the barycenter. The study is important in this specific application because of the stability and maneuverability of the AUV since it uses an intelligent system of controlled flood to take the vehicle upwards or downwards and with help of sensors, the control system dictates the direction of movement. If the power bank's barycenter moves relative to the center of mass of the vehicle in a wide region and at a high speed, this may cause a loss in the stability of the vehicle and even a malfunction of the control system.

As a first step Figure 5.14– location of the center of mass of the power bank system. shows the location of the center of mass of the power bank system, relative to the reference frame situated in the geometrical center of the system, where all the components were placed strategically to obtain a center of mass as closest as possible to this reference frame.

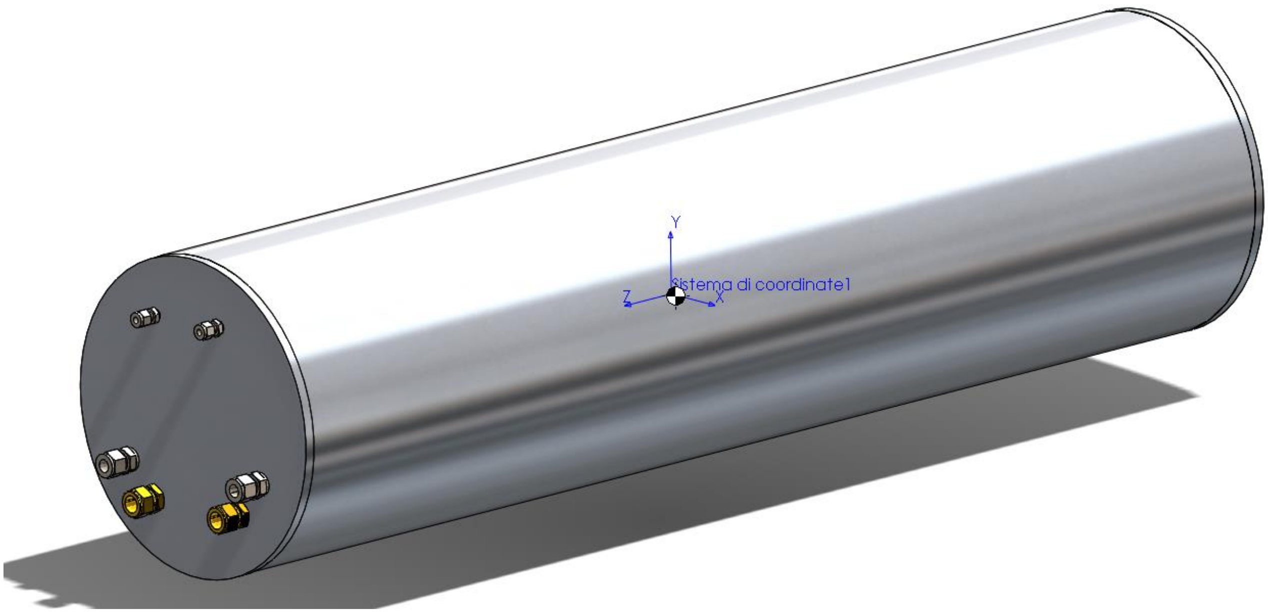

Figure 5.14– location of the center of mass of the power bank system.

The following analysis is to find the location of the center of mass simulating several scenarios that may occur during operation due to the movement of the liquids, which are: the system in a horizontal position at initial, medium, and full capacity, and the tilted scenarios where the center of mass may undergo a bigger displacement, which is the case of initial capacity because the fluid has a higher space to move.

To understand the analysis must be taken into account that at the beginning the electrolyte tank has an initial amount of liquid of 4 L with a concentration of 15 M, (15 moles of KOH/ liter of water). As the process goes on, the electrolyte tank begins to fill up, up to 11 L where the electrolyte concentration drops up to 7 M thanks to the water produced during the reactions, thus the weight contained in the electrolyte tank must be found according to the molar concentration in each case. Below is shown each case with a table summarizing the weights and the location of the center of mass for the power system taking as a reference the already defined reference frame.

- *Horizontal position: Initial capacity.*

  The starting point, with 4L of liquid and a molar concentration of 15M.

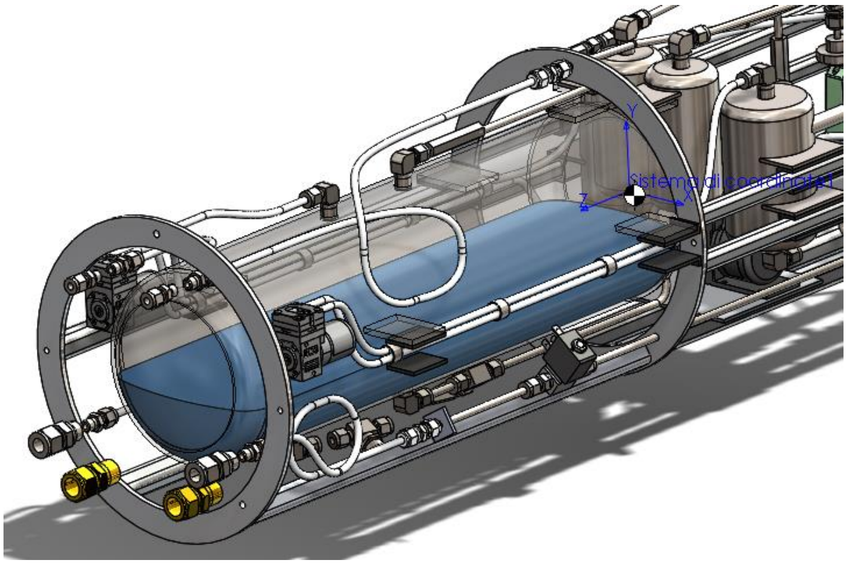

Figure 5.15 - initial state of the system

Table 5.11

	weight	**Center of gravity location**		
KOH	3.9. kg	**X**	**Y**	**Z**
Water	4.7 kg	+0.45 mm	-5.35 mm	-6.61 mm
Entire power bank	84.54 kg			

- *Horizontal position: tank at medium capacity.*

Analysis with a liquid volume of 7L and molar concentration of 11M.

Table 5.12

	Weight [kg]	**Center of gravity location [mm]**

KOH + H_2O	10.91	**X**	**Y**	**Z**
Entire power bank	86.9	0	+2.95	-6.45

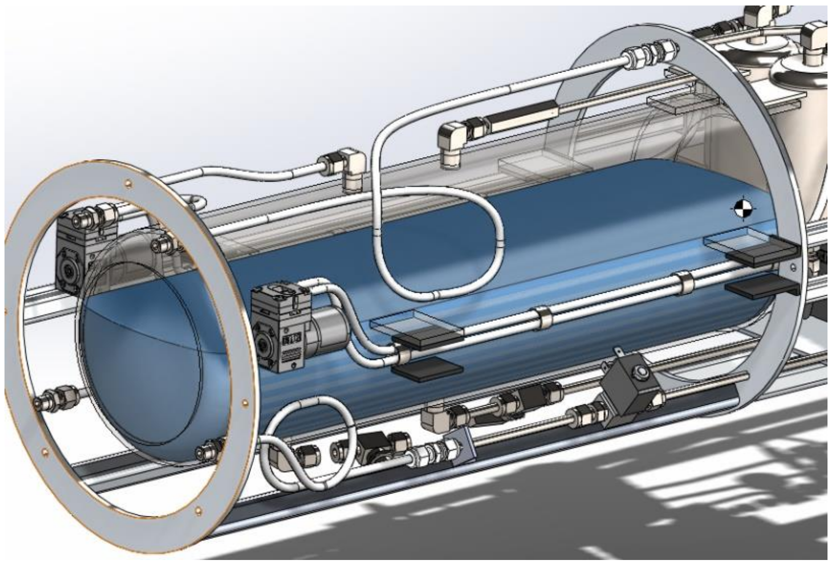

Figure 5.16 - intermediate capacity of the tank

- *Horizontal position: tank at full capacity.*

  Analysis with a liquid volume of 10L and molar concentration of 7M. In this particular case is also analyzed the effect of having water stored only on one of the separation tanks.

Table 5.13

	Weight [kg]	**Center of gravity location [mm]**		
KOH + H_2O	13.86	**X**	**Y**	**Z**
Entire power bank	89.8	1.2	1	3

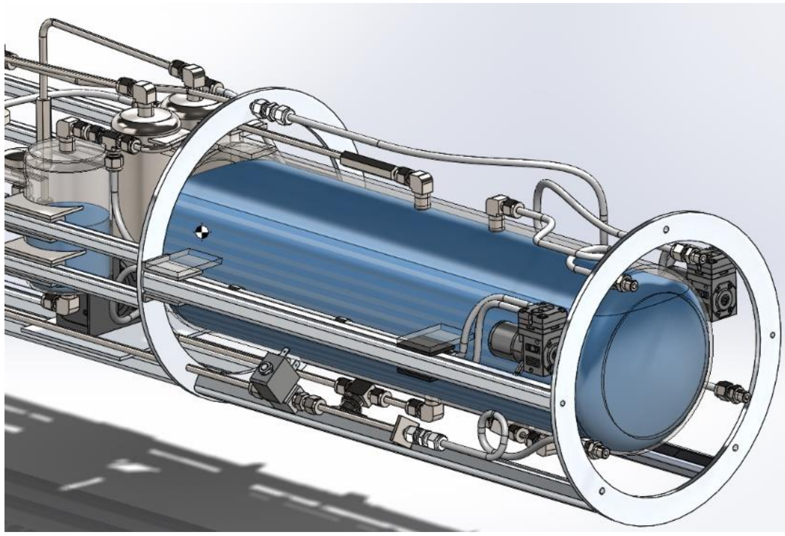

Figure 5.17 - tank at full capacity

- *45° tilted position: tank at initial capacity.*

  As explained before this is the case in which the center of mass suffers the biggest displacement.

  Is analyzed the case of upwards and downwards direction.

Table 5.14

Downwards				
	Weight [kg]	**Center of gravity location [mm]**		
KOH + H_2O	8.56	**X**	**Y**	**Z**
Entire power bank	84.54	0	0	-21.66
Upwards				
	Weight [kg]	**Center of gravity location [mm]**		
KOH + H_2O	8.56	**X**	**Y**	**Z**
Entire power bank	84.54	0	0	-30.16

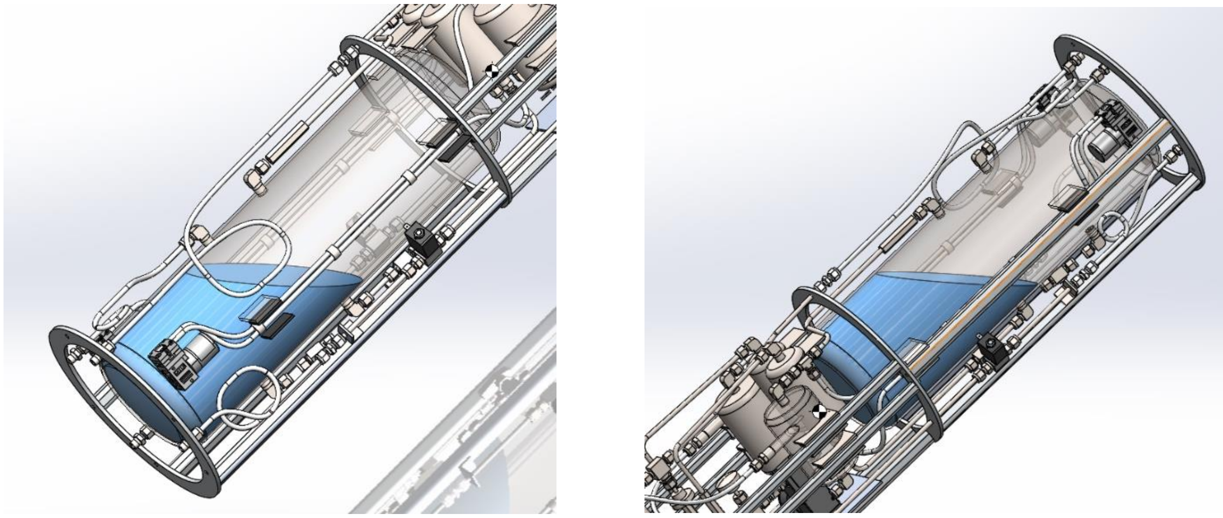

a). downwards *b).upwards*

Figure 5.18 - Downwards and upwards direction.

<u>Notes</u>

- The weight taken for the requirement of neutral buoyancy is the initial weight because when the operation begins, mass is going into the system from the external tanks, and these tanks were out of the analysis.
- is important to remark that as the cylinder gets filled, its center of mass moves up, and at full capacity, it is located approximately in the geometrical center, thus during the filling process the center of mass of the group KOH tank and liquid displaces in a limited range along the Y-axis.

Can be concluded that the center of mass moves in an axial range of 45 mm, vertical range of 6 mm, and a negligible movement in the X-axis other two axes. As the maximum displacement is not that high, and the AUV will not present considerably abrupt movements, for now, the displacement of the barycenter will be taken as a feature to have into account in the control system design, as future improvements can be analyzed the implementation of transversal divider baffles into the electrolyte tank to have a more controlled displacement of the liquid.

6. Results

The results of the preliminary design for the power bank system are summarized in Table 6.1, where are shown the main specifications. Figure 6.1 shows the global dimensions of the power bank and the stack. The power and voltage requirements were achieved, as well as the neutral buoyancy and a balanced location of the barycenter, all this assuring the sealing of the stack which is a critical aspect as it was discussed.

Table 6.1 - Main parameters of the system.

Parameter	**Value**
Operational depth	800 m
Power output	300W
Operating voltage per cell	0.8V
Number of cells	15
Total voltage	12V
Operation temperature	60-70°C
Operation pressure	1 bar
Electrode area	201.06 cm^2
Electrode diameter	16 cm
Hydrogen stored	0.625 kg @200bar
Autonomy	1.6 days
Cell Efficiency	58.9%
Energy generated	11.52 kWh (41.47MJ)
Maximum barycenter displacement	45 mm
Type of seals	O-rings

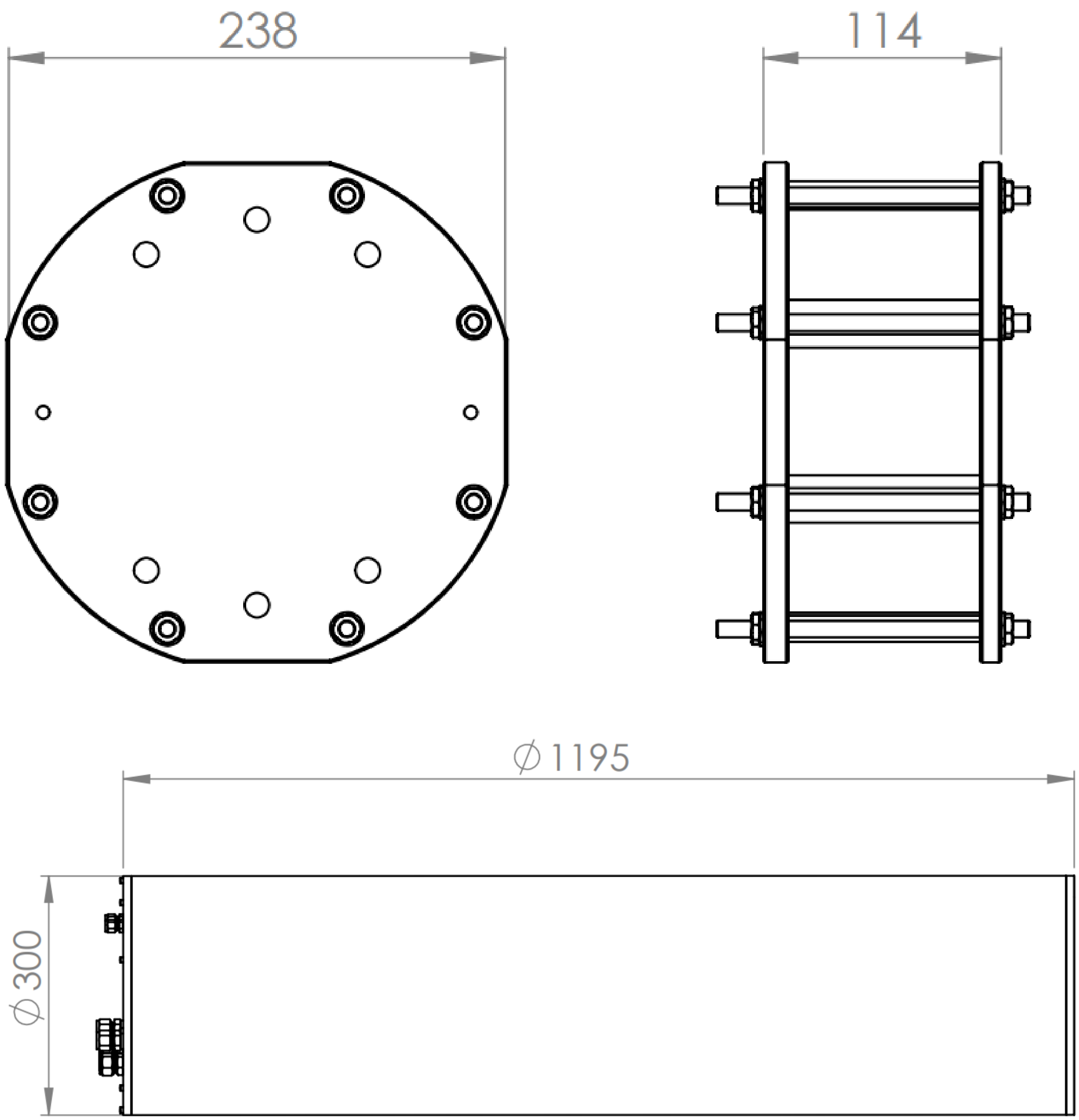

Figure 6.1 – Final dimensions stack and housing.

The main motivation to store the energy in hydrogen for this application is the remarkable specific energy that the hydrogen has. From reference (6) are taken the energy and power density for Li-ion batteries and Hydrogen, Table 6.2 - Energy and power density for Li-ion batteries and hydrogen found in the state of art.Table 6.2 shows that hydrogen by itself can store approximately

140 times more energy per kilogram than the Li-ion batteries, this is an important feature given that the weight in the AUV is limited to fulfill the neutral buoyancy requirement.

Table 6.2 - Energy and power density for Li-ion batteries and hydrogen found in the state of art.

	Lithium-ion Battery	**Hydrogen**
Energy density [kWh/L]	0.25 – 0.69 (0.9-2.43 MJ/L)	0.53 (1.91MJ/L) @200bar
Specific energy [kWh/kg]	0.1 – 0.26 (0.36-0.875 MJ/kg)	33.3 (120 MJ/kg)

From the energy consumption and weight of the system, was obtained the specific energy after the energy losses Table 6.3 this value confirms the theoretical efficiency found, taking as a reference the specific energy given in the state of the art.

Table 6.3 - Specific energy after losses.

	System
Specific energy [kWh/kg]	18.43 (66.3 MJ/kg)

To carry out a fair comparison between using Li-ion batteries or hydrogen must be used the entire system, i.e. besides the elements to store the hydrogen, also the system to convert the energy stored in the hydrogen must be considered, Table 6.4 shows the specific energy after considering the weight of the fuel cell system. This result indicates that for the specified conditions for the hydrogen (pressure and mass stored) and the weight of the components of the fuel cell, on average the specific energy and energy density of both systems are around the same value.

Table 6.4 - Energy density and specific power.

	Power bank system
Volume [L]	84.5
Weight [kg]	84.5
Energy density [kWh/L]	0.136

Specific energy [kWh/kg]	0.136 (0.49 MJ/kg)
Specific power [W/kg]	3.5

This means that up to this point, both systems would have comparable weights and volumes, but is important to remark that the fuel cell design is highly flexible, i.e. additional fuel cells could be assembled, also it could be added more tanks for hydrogen, the pressure of storage could be rised, and the materials can be highly optimized since many components are made of stainless steel, features that would cause a positive impact on the specific energy and energy density. Note that the specific energy was not the only parameter taken into account to select hydrogen storage, many other features affect the selection, for instance self discharge rate, recharging time, round trip efficienc, etc.

As a preliminary design the outcomes are positive because it shows good features in relation to Li-ion batteries, this demonstrates the feasibility of applying fuel cell technology to Autonomous Underwater Vehicles. Currently, the project is in the construction and testing phase, where a mono cell was constructed and is being tested to verify the hypothesis taken during the conceptual design. In Figure 6.2 to 6.7 are shown the modelled stack and the power bank system.

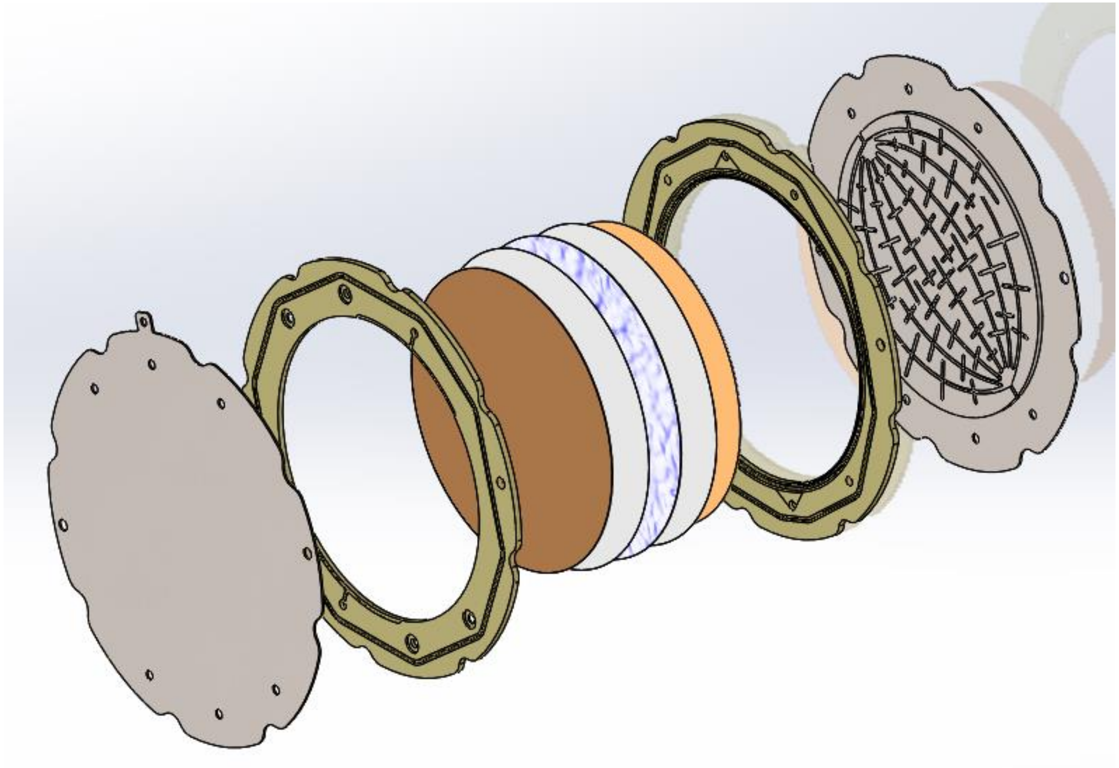

Figure 6.2 - modelled mono cell

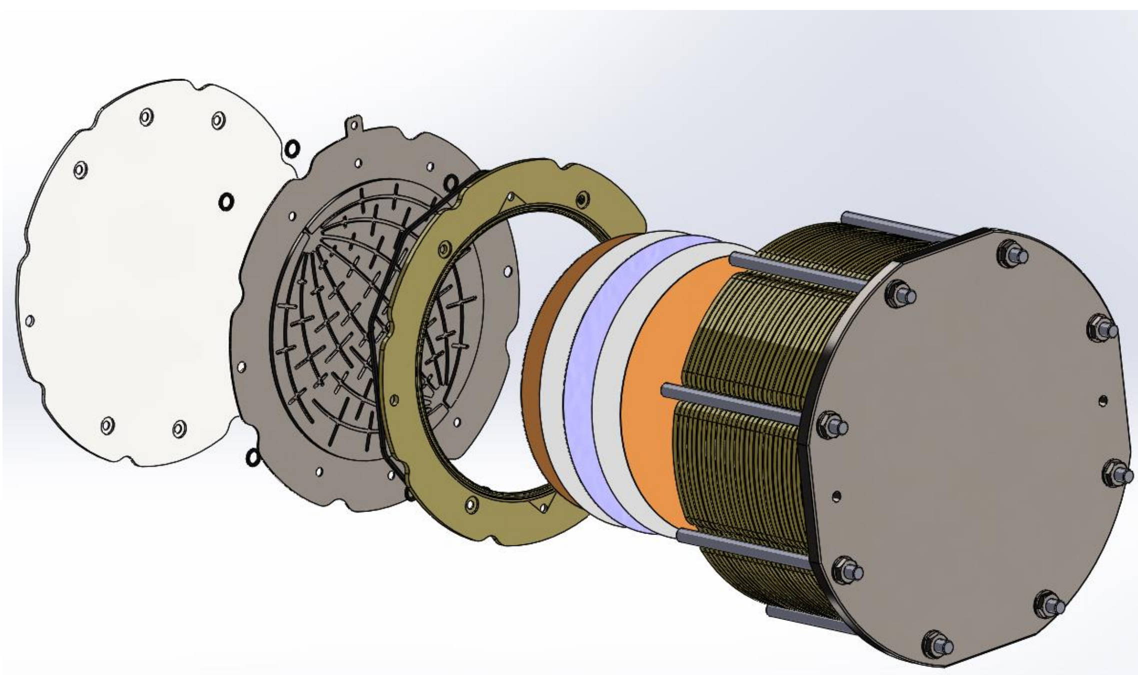

Figure 6.3 - Stack of cells

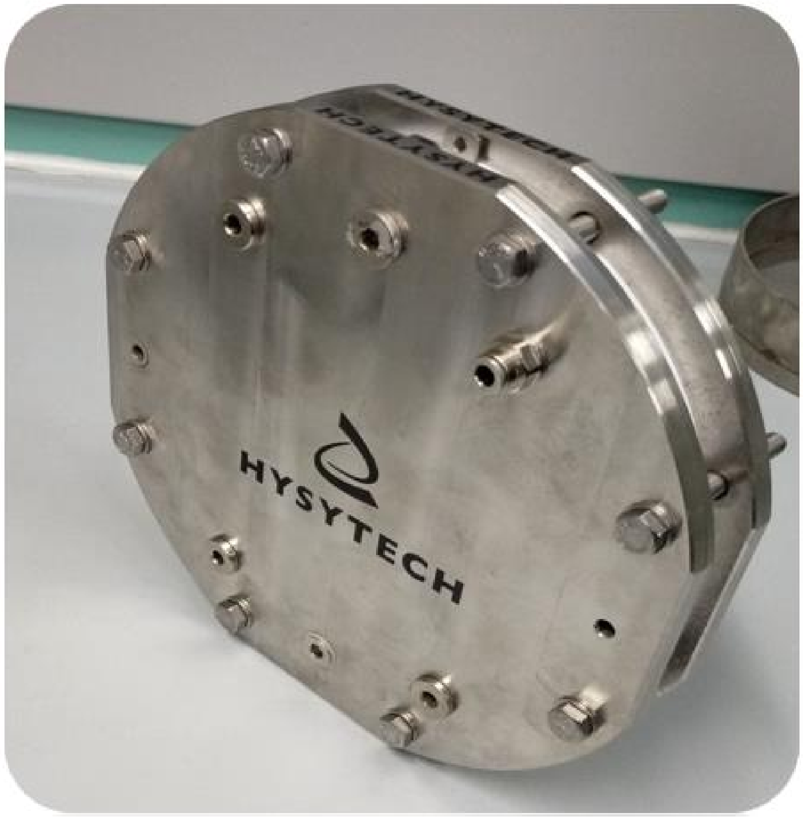

Figure 6.4 - Manufactured mono cell.

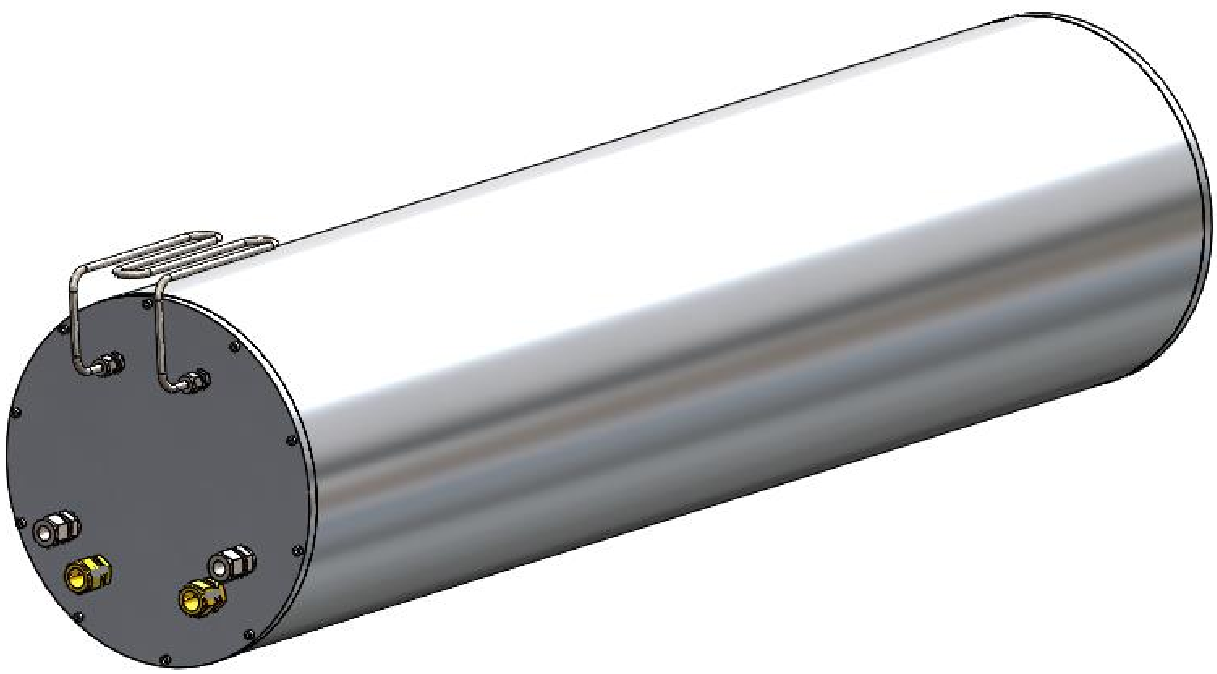

Figure 6.5- Power bank system

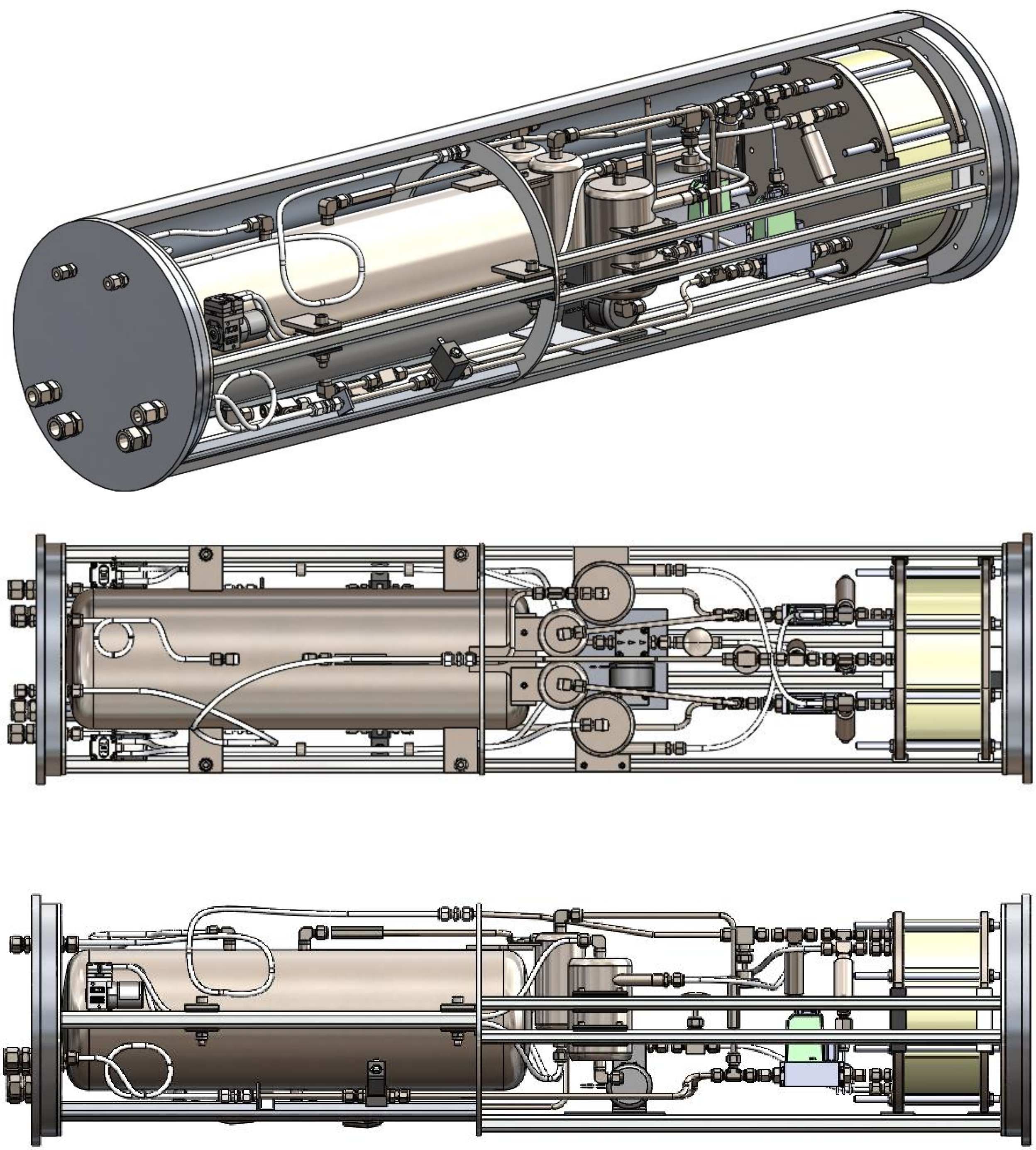

Figure 6.6 - Power bank system

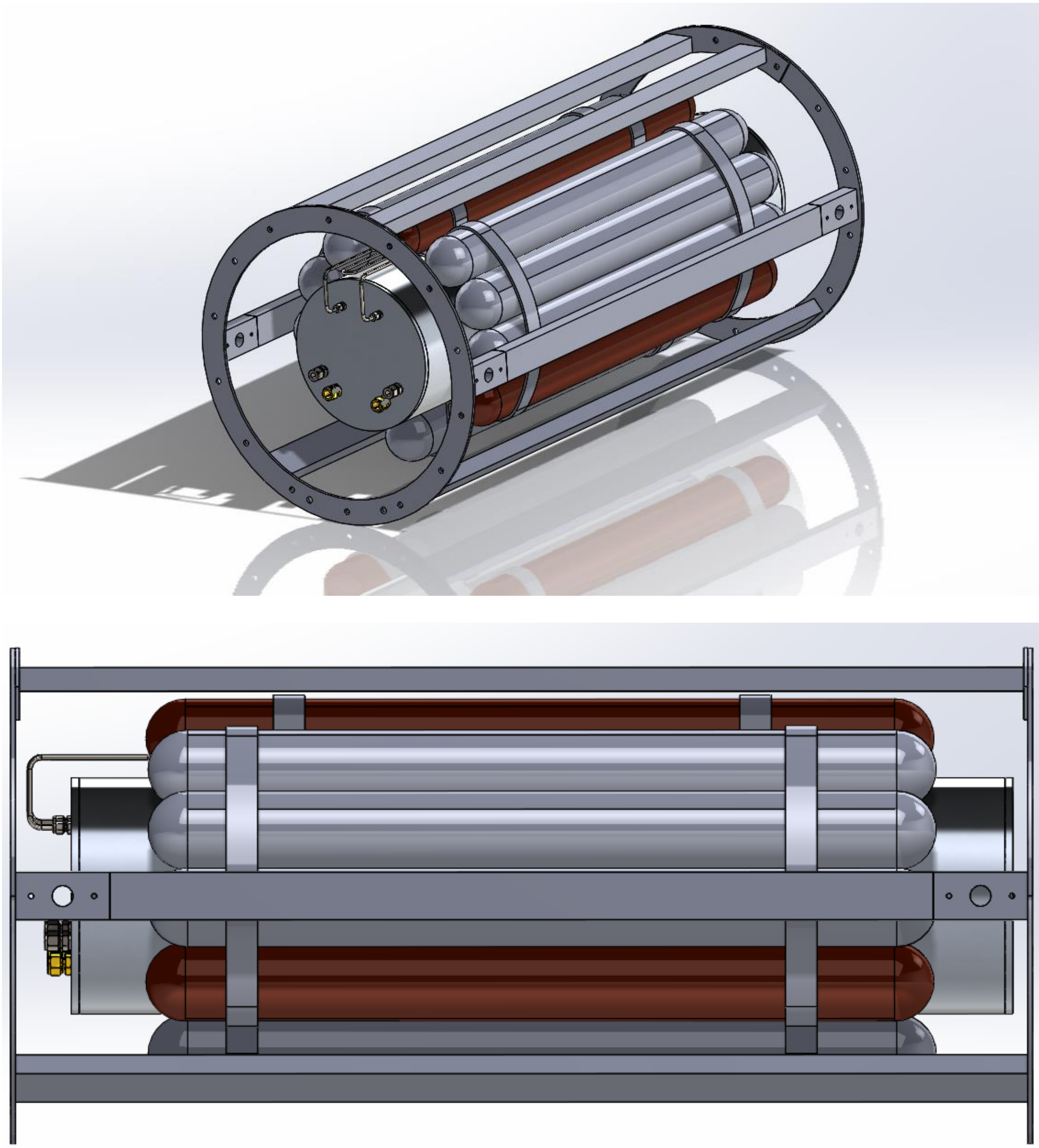

Figure 6.7 – Power system with hydrogen storage system

7. Conclusions

A fuel cell system was designed as a power bank for an autonomous underwater vehicle, dividing the process into three stages: stack's design, power bank system configuration design, structural analysis, and finally, neutral buoyancy verification.

Assuming that all the components were correctly selected, the most sensitive aspect for the proper performance of the stack of cells is the sealing element selected, since leakages between chambers inhibit the functioning and also have a high impact on the fuel cell efficiency. Thus these elements require special attention during the design.

The challenge of the extraction process for the heat generated inside the cells was satisfactorily figured out but is important to remark that variations in the number of cells or rise in the amount of hydrogen used may impact the performance of the proposed device, thus the heat exchanger must be adjusted after tests.

The selected materials and dimensions during the structural analysis, ensure the capability of the system to undergo the high pressures and the demanding sea conditions. Even though a combination of aluminum and stainless steel is encountered inside the system to reduce costs, in future developments is recommended to use only aluminum in combination with some polymers to obtain a lighter system and avoid corrosion problems, for now, isolating materials are used.

The neutral buoyancy was achieved and also the barycenter was kept around the central point of the system, this guarantees that the stability of the system is not going to be affected during operation.

The autonomy of the power bank shows the feasibility of the project, where the results are quite optimistic to be the preliminary design, since many improvements can be done in each stage of the design process, such as increasing the number of cells, the employment of lighter materials for the components in the power bank, changes in the amount of hydrogen stored and its pressure.

All the hypotheses that were taken to carry out the preliminary design, will be tested during the performance test for the constructed mono cell, from that, adjustments and further improvement decisions can be proposed.

8. References

1. Seabed 2030. seabed2030. [En línea] 2020. https://seabed2030.org/.

2. https://enduruns.eu/. Enduruns Project. [En línea] 2020. https://enduruns.eu/.

3. *ENDURUNS: An Integrated and Flexible Approach for Seabed Survey Through Autonomous Mobile Vehicles*. M. Simone, G. Nicola, G. Shashank, S. Benjamin, O. Ennio, F. Pedro. et al. 2020, Journal of Marine Science and Engineering.

4. Larminie, J. Dicks, A. *Fuel Cell Systems Explained*. s.l. : Wiley, 2003.

5. Ralph H. Petrucci, F Geoffrey Herring, Jeffry D. Madura, Carey Bissonnette. *General Chemistry: Principles and Modern Applications, 11th edition*. s.l. : Pearson , 2017.

6. O'Hayre, R. Cha, S.W. Colella, W.G. Prinz, F.B. *Fuel Cell Fundamentals*. s.l. : Wiley, 2016.

7. Spiegel, C. Polarization Curves. *Fuel Cell Store*. [En línea] 2017. https://www.fuelcellstore.com/polarization-curves.

8. Incropera, F. P., & DeWitt, D. P. *Fundamentals of heat and mass transfer*. New York : J. Wiley., 2002.

9. Cengel, Y. A., & Ghajar, A. J. *Heat and mass transfer: Fundamentals and applications (5th ed.)*. s.l. : McGraw-Hill Professional.

10. *O-ring Basic Catalogue*. Angst+Pfister.

11. *O-ring Handbook*. Parker Hannfin,. 2015.

12. Degarmo, E.P. Black, J.T. Kosher, R.A. *Materials and Processes in Manufacturing*. *9th Edition*. s.l. : Wiley, Hoboken.

13. Marco Rubber and Plastics. O-Rind design considerations. *Marco Rubber & Plastics*. [En línea] 2021. https://www.marcorubber.com/o-ring-groove-design-considerations.htm.

14. *Systematic calculation of high duty bolted joints*. DIN Standards - VDI 2230. 2003. ICS 21.060.10.

15. Spiegel, C. The Effect of Clamping Pressure on Fuel Cell Performance. *Fuel Cell Store*. [En

línea] 2019. https://www.fuelcellstore.com/blog-section/effects-of-clamping-pressure-fuel-cell-performance.

16. Cengel, Y. Cimbala, J. *Fluids Mechanics Fundamentals and Applications.* s.l. : McGraw-Hill, 2006.

17. Young, W., & Budynas, R. *Roark's formulas for stress and strain, 7.* s.l. : McGraw-Hill, 2002.

18. MatWeb. MatWeb data sheet. *MatWeb Property Data.* [En línea] 2021.

9. Acknowledgments

During the development of this thesis, I have received great support from the people of the company Hysytech. First I would like to thank Sorani, who was the first person in the company which I had contact with and always was very kind and willing to help. I also want to thank Corrado, my advisor in Hysytech, from which I have learned a lot so far and has helped me immensely to finish my thesis, thank you for your willingness and patience to answer my thousands of daily questions. Thank you, Stefano, the Process Engineer that I work with on the project, for your availability to solve any doubt and help out. I would also like to thank my academic advisor Alessandro Monteverde for his time and cooperation.

Finally, I want to thank Martha Cordoba, my mom. Thank you for your unconditional support, the person that I've become has been thanks to you, I couldn't have done it without you, this achievement is of both of us.